

Molecular Characterisation of Radiation-Induced Human HPRT Mutant Clones

Dissertation

zur Erlangung des Grades

eines Doktors der Naturwissenschaften (Dr. rer. nat.)

der Medizinischen Fakultät

Der UNIVERSITÄT DES SAARLANDES

vorgelegt von

Karumpullige Udaya Thilaka Gunasekara

Homburg

2007

Der Dekan:

Prof. M.D. Menger

Die Berichterstatter:

Prof. M. Löbrich

Prof. M. Montenarh

Erklärung

Ich erkläre hiermit an Eides statt, dass ich die vorliegende Arbeit ohne unzulässige Hilfe Dritter und ohne Benutzung anderer als der angegebenen Hilfsmittel angefertigt habe. Die aus anderen Quellen direkt oder indirekt übernommenen Daten und Konzepte sind unter Angabe der Quelle gekennzeichnet.


Weitere Personen waren an der inhaltlich- materiellen Erstellung der vorliegenden Arbeit nicht beteiligt. Insbesondere habe ich nicht die entgeltliche Hilfe von Vermittlungs- bzw. Beratungsdiensten (Promotionsberater /innen oder anderer Personen) in Anspruch genommen. Außer den Angegebenen hat niemand von mir unmittelbar oder mittelbar geldwerte Leistungen für Arbeiten erhalten, die im Zusammenhang mit dem Inhalt der vorgelegten Dissertation stehen.

Die Arbeit wurde bisher weder im Inland noch im Ausland in gleicher oder ähnlicher Form in einem anderen Verfahren zur Erlangung des Doktorgrades einer anderen Prüfungsbehörde vorgelegt.

Ich versichere an Eides statt, dass ich nach bestem Wissen die Wahrheit gesagt und nichts verschwiegen habe.

Vor Aufnahme der vorstehenden Versicherung an Eides Statt wurde ich über die Bedeutung einer eidesstattlichen Versicherung und die strafrechtlichen Folgen einer unrichtigen oder unvollständigen eidesstattlichen Versicherung belehrt.

Mittwoch, 4. April 2007

A handwritten signature in black ink, consisting of a stylized first letter followed by a series of loops and a horizontal line at the end.

.....
Unterschrift der /des Promovierenden

Contents

List of Abbreviations.....	iv
List of Figures	vi
List of Tables	vii
1 Summary.....	1
Zusammenfassung.....	3
2 Introduction.....	6
2.1 Ionizing Radiation.....	6
2.1.1 X-rays and γ -rays.....	6
2.2 Radiation-Induced DNA Lesions and Double Strand-Breaks (DSBs).....	7
2.2.1 DNA DSBs and repair mechanisms.....	10
2.2.1.1 Homologous recombination (HR).....	10
2.2.1.2 Non-homologous end-joining (NHEJ).....	12
2.2.2 Cell cycle and DNA damage.....	15
2.3 Radiation-Induced Mutagenesis and Cancer	17
2.3.1 Mutations and classification	18
2.3.1.1 Small-scale mutations.....	19
2.3.1.2 Large-scale mutations	21
2.4 Mutagenesis Analysis.....	23
2.4.1 Hypoxanthine-guanine phosphoribosyl transferase (HPGRT/HPRT)	23
2.4.2 Adenine phosphoribosyl transferase (APRT).....	25
2.5 Scope of this thesis.....	26
3 Materials and Methods.....	28
3.1 Primary Cell Culture.....	28
3.1.1 Human bladder carcinoma cell line - MGH-U1.....	28
3.1.2 Immortalised human primary fibroblasts cell line - 82-6 hTERT.....	28
3.2 Cell Irradiation	29
3.2.1 Cell irradiation for cell survival colony forming assay.....	29
3.2.1.1 MGH-U1 cells and cell survival colony assay.....	29
3.2.1.2 Immortalised human fibroblasts and cell survival colony assay.....	31
3.2.2 Acute cell irradiation for mutation induction	32
3.2.2.1 Acute dose cell irradiation and mutation induction in wortmannin-treated cells.....	32
3.2.3 Mutation induction following dose fractionation.....	33

3.3	Mutation Selection.....	34
3.3.1	Mutation selection following acute dose irradiation	34
3.3.1.1	Isolation of radiation-induced 6-thioguanine-resistant (6-TG ^r) mutant sub clones	34
3.3.1.2	Isolation of spontaneous mutant sub clones.....	35
3.3.1.3	Expansion of HPRT-deficient-mutant sub clones.....	35
3.3.2	Mutation selection following dose fractionation.....	36
3.3.3	Mutation frequency and independent mutation estimate.....	36
3.4	Molecular Characterisation of HPRT Mutant Clones.....	37
3.4.1	Genomic DNA embedded agarose plugs and cell lysates.....	37
3.4.1.1	Restriction digestion.....	38
3.4.1.2	Pulse field gel electrophoresis (PFGE).....	38
3.4.1.3	DNA transfer /Alkaline vacuum blotting.....	39
3.4.1.4	Probes and radioactive ³² P-labelling.....	40
3.4.1.5	Southern hybridisation.....	41
3.4.2	Exon-deletion screening at HPRT gene locus.....	42
3.4.2.1	Genomic DNA extraction.....	42
3.4.2.2	Multiplex polymerase chain reaction (M-PCR).....	43
3.4.2.3	Uniplex /Standard polymerase chain reaction (Single-PCR).....	46
3.4.2.4	Agarose gel electrophoresis.....	47
3.4.3	RNA isolation and analysis of HPRT-mRNA-transcripts.....	48
3.4.3.1	Total RNA isolation.....	48
3.4.3.2	Reverse transcriptase polymerase chain reaction (RT-PCR).....	49
3.4.4	DNA sequencing of cDNA products of mutant clones.....	51
3.5	Categories of Mutations.....	51
3.6	Fluorescence <i>in situ</i> Hybridisation (FISH).....	52
4	Results.....	53
4.1	Human Bladder Carcinoma Cells - MGH-U1.....	53
4.1.1	Cell survival colony-forming assay.....	53
4.1.2	Isolation of independent HPRT mutant clones	54
4.1.3	<i>NotI</i> digested restriction fragment analysis.....	56
4.1.4	Multiplex-PCR-based HPRT exon-deletion analysis.....	58
4.1.5	Cytogenetic screening using fluorescent <i>in situ</i> hybridisation (FISH).....	60
4.2	Acute Dose Irradiation and Immortalised-Human Primary Fibroblasts (82-6 hTERT Cells).....	61
4.2.1	Cell survival and HPRT mutation frequency.....	61
4.2.2	Isolation of independent HPRT mutant clones.....	62
4.2.3	<i>NotI</i> cleaved restriction fragment analysis of HPRT mutation.....	64
4.2.3.1	Detailed analysis of mutant clones with double-restriction bands.....	66
4.2.4	Multiplex-PCR-based HPRT exon-deletion analysis.....	67
4.2.4.1	Break point mapping of two selected HPRT mutant clones.....	71
4.2.5	mRNA isolation and RT-PCR.....	73
4.2.6	DNA sequencing.....	75
4.2.7	Cytogenetic screening using fluorescent <i>in situ</i> hybridisation (FISH).....	78

CONTENTS

4.3	Fractionated Irradiation /Mutation Induction in hTERT-Immortalised Primary Fibroblasts.....	81
4.3.1	Surviving fractions & mutation frequencies of fractionated X-irradiated cells.....	81
4.3.2	Independence of spontaneous /X-ray-induced mutant clones.....	83
4.3.3	<i>NotI</i> digested restriction fragment analysis.....	84
4.3.4	RT-PCR-based HPRT mRNA analysis.....	89
4.3.5	Multiplex PCR-based HPRT exon-deletion analysis.....	90
5	Discussion.....	94
5.1	Molecular Mechanisms in HPRT Gene Mutations.....	94
5.2	Acute Dose Irradiations in MGH-U1 Cells.....	98
5.2.1	6-Gy X-ray-induced mutant clones.....	98
5.2.2	2-Gy + wortmannin (WM) mutant clones.....	100
5.2.3	Spontaneous mutant clones.....	102
5.3	Acute Dose Irradiation in hTERT-Immortalised Primary Fibroblasts.....	103
5.3.1	X-ray-induced mutant clones.....	104
5.3.2	Spontaneous mutant clones.....	109
5.4	Fractionated Irradiation in hTERT-Immortalised Fibroblasts.....	110
5.4.1	Dose fractionation vs. acute dose mutant clones.....	110
6	References.....	113
7	Acknowledgements.....	134
8	Appendix.....	135

List of Abbreviations

bp	basepair
d	day
DAPI	4'-6-Diamidino-2-phenylindole (DAPI)
ddH ₂ O	doubled distilled water
DMEM	dulbecco's modified eagle's medium
DMSO	dimethylsulfoxide
DNA	deoxyribonucleic acid
DNase	deoxyribonuclease
dNTP	deoxyribonucleoside triphosphate
EDTA	ethylene-diaminetetraacetic acid
<i>et al.</i>	<i>et altera</i>
FCS	fetal calf serum
FISH	fluorescence <i>in situ</i> hybridisation
g	gram
h	hour
HEPES	4-(2-Hydroxyethyl)-piperazin-1-ethansufonic acid
HR	homologous recombination
IR	Ionizing Radiation
kbp	kilobase pairs
kDa	kilodalton
kV	kilovolt
l	litre
LOH	loss of heterozygosity
M	molar
μM	micromolar
mA	milliampere
Mbp	megabase pairs
MEM	modified eagle medium
min	minute
mM	millimolar
M-PCR	multiplex polymerase chain reaction

LIST OF ABBREVIATIONS

NHEJ	non-homologous end-joining
<i>NotI</i>	<i>Nocardia</i> otitidis
PBS	phosphate-buffered saline
PE	plating efficiency
PFGE	pulse field gel electrophoresis
pH	<i>potentium hydrogeni</i>
rpm	rotations per minute
RT	room temperature /reverse-transcription
RT-PCR	reverse-transcriptase polymerase chain reaction
6-TG	6-thioguanine
SKY	spectral karyotyping
SSA	single-strand annealing
SSC	standard saline citrate
Tris	tris-(hydroxymethyl)aminoethane
U	unit (enzymatic activity)
V(D)J	variable diversity joining
Vol	volume
w/v	weight per volume
w/w	weight per weight
v/v	volume per volume

List of Figures

Figure 2.1	Schematic diagram of the major repair pathways in mammals.....	11
Figure 3.1	Representative diagram for cell survival colony forming assay.....	31
Figure 3.2	Gene bank sequence of the human HPRT cDNA (NM_000194) showing the locations of the primers for RT-PCR.....	50
Figure 4.1	Cell survival of MGH-U1 tumour cells as a function of dose of X-rays in the presence or absence of 20 μ M wortmannin (WM).....	53
Figure 4.2	Schematic diagram of human HPRT gene locus viewing binding site and the sizes of exons and the PCR amplification products.....	56
Figure 4.3	Representative picture of restriction fragment migration patterns of 12 HPRT mutant clones in MGH-U1 cells.....	57
Figure 4.4	Multiplex-PCR based exon-deletion screening HPRT mutant clones in human bladder carcinoma (MGH-U1) cells.....	58
Figure 4.5	Examination of cytogenetically visible aberrations of HPRT mutant clones in human bladder carcinoma (MGH-U1) cells.....	60
Figure 4.6	Cell survival of hTERT-immortalised primary fibroblasts (82-6 hTERT) as a function of increasing dose of X-rays.....	62
Figure 4.7	Representative diagram of <i>NotI</i> digested banding patterns of 11 x HPRT deficient mutant clones in 82-6 hTERT cells.....	64
Figure 4.8	Detailed fragment analysis of mutant clones 6/6dII and 6/11d.....	67
Figure 4.9	Mutation patterns of 5 x spontaneous, 11 x 2-Gy X-ray-induced and 14 x 6-Gy X-ray-induced mutant clones.....	70
Figure 4.10	Detailed analysis of genomic DNA of HPRT mutant clone 6/7aI	71
Figure 4.11	Detailed analysis of genomic DNA of mutant clone 2/10d.....	72
Figure 4.12	PCR amplification of genomic DNA from mutant clone (6/10e) that was missing the entire exon 8 in complementary DNA and identification of the deletion.....	77
Figure 4.13	Fluorescence <i>in situ</i> hybridisation analysis of HPRT mutant clones in hTERT-immortalised fibroblasts.....	79
Figure 4.14	Survival data for fractionated X-irradiated experiments.....	83
Figure 4.15	Restriction fragment analysis of 10 x 0.6-Gy human HPRT mutant clones.....	87
Figure 4.16	Agarose gel electrophoretic UV-picture of multiplex PCR and reverse transcriptase PCR analyses of HPRT mutant clones in hTERT-immortalised-primary fibroblasts after exposure to fractionated dose 0.6-Gy of X-rays.....	91
Figure 4.17	Mutation patterns of 8 x spontaneous, 6 x 0.6-Gy fractionated dose, 13 x 2-Gy acute dose and 17 x 6-Gy acute dose of X-ray-induced HPRT mutant clones that were analysed by hybridisation assay and M-PCR....	93

List of Tables

Table 3.1	Primers (including the primers for exon 1) used for M-PCR to amplify targeted sequences at the human HPRT gene locus.....	44
Table 3.2	Primers used for single-PCRs to amplify desired sequences at the human HPRT gene locus of three selected HPRT mutant clones.....	47
Table 4.1	Mutation frequencies of 6-TG ^r HPRT MGH-U1 mutant clones.....	55
Table 4.2	Comparison of spontaneous and X-ray-induced HPRT mutant clones in human MGH-U1 cells.....	59
Table 4.3	Mutation frequencies of 6-TG ^r HPRT 82-6 hTERT mutant clones depending on acute X-ray doses employed.....	61
Table 4.4	Background correction of the mutant clones considering mutant fraction arising spontaneously.....	66
Table 4.5	Comparison of spontaneous and X-ray-induced HPRT mutant clones in human hTERT-immortalised fibroblasts.....	69
Table 4.6	Mutation frequencies of 6-TG ^r HPRT 82-6 hTERT-mutant clones depending on acute and fractionated X-ray doses employed.....	82
Table 4.7	Patterns of <i>NotI</i> digested fragments of isolated HPRT mutant clones from mutation induction Experiment I.....	86
Table 4.8	Patterns of <i>NotI</i> digested fragments on Southern blots in isolated HPRT mutant clones from mutation induction Experiment II	88
Table 4.9	Summary of RT-PCR analyses of both spontaneous and X-ray-induced HPRT mutant clones in hTERT-immortalised human fibroblasts.....	89
Table 4.10	Summary of M-PCR analyses of both spontaneous and X-ray-induced HPRT mutant clones in hTERT-immortalised human fibroblasts.....	90
Table 4.11	Comparison of spontaneous and X-ray-induced HPRT mutant clones in hTERT-immortalised fibroblasts (82-6 hTERT cells) following fractionated irradiations.....	92

1 Summary

The objective of this work was to investigate radiation-induced mutagenesis in human cells, thus representing the response of cells in the organism as a whole. The current molecular characterisation was initialised with a well-established human malignant cell line: MGH-U1. The complete radiation-induced mutation study was conducted with hTERT-immortalised primary fibroblasts with karyotypically stable diploid characteristics. Mutation selection successfully made use of the ability of HPRT deficient cells to remain resistant to a drug containing in culture medium. Molecular characterisation was based on a previously introduced hybridisation assay. In addition, to further characterise the aberrations, mutant clones were examined in parallel by multiplex PCR, RT-PCR and chromosome painting based on a 3-dye FISH. Hybridisation assay was introduced primarily to evaluate DSB repair fidelities following IR. In this study, the incorrectly rejoined DSBs of clonal cell populations are represented by aberrant restriction bands on the Southern blots whereas in DSB repair evaluations this is observed as a smear around the targeted bands. Restriction fragment alterations of 2 Mbp *NotI* fragments of mutant DNA in both X-ray-induced and untreated HPRT clones were compared.

In the absence of a NHEJ repair pathway, thought to be the predominant molecular repair mechanism for higher eukaryotes, 2-Gy X-ray-induced mutant clones derived from NHEJ deficient MGH-U1 cells revealed that the mutagenicity at the HPRT gene locus was significantly decreased in comparison to cells proficient in the repair pathway at equitoxic doses of 6-Gy of X-rays. This suggests that an alternative repair pathway may act and result in the reduction of mutation frequency in wortmannin pre-treated cells. Such alternative mechanisms can be suppressed in NHEJ proficient cells.

78 radiation-induced and 47 spontaneous HPRT mutant clones of hTERT-immortalised fibroblasts were isolated and genetic alterations at the HPRT locus were studied by hybridisation assay. The results are consistent with those obtained by 22 radiation-induced and 26 spontaneous MGH-U1 mutant clones. The majority of spontaneously arising mutant clones are a result of point mutations or small deletions in the coding segments of the gene. These small-scale mutations include base pair substitution, for example: a transversion from A to C (A: T \rightarrow C: G) as found in exon 9; a transition from C to T (C: G \rightarrow T: A) in exon 6; a mutation causing a splicing error due to a transversion from T to G (T:A \rightarrow G:C) found in intronic sequences, and 13 base pairs upstream from exon 8. Small-scale mutations were nearly 8% (2/26) and 94% (44/47) for spontaneously arising mutant clones in MGH-U1 cells

and hTERT-immortalised cells respectively. These small-scale mutations decreased as the dose of X-rays used for mutation induction was increased, thus indicating a dose dependence. The respective percentages of small-scale mutations for 2 and 6-Gy were 29% (7/24) and 14% (6/44), respectively. Deletions spanning the entire HPRT gene and the adjacent regions within at least 200 kbp at the telomeric end of the gene (16 and 38% for 2 and 6-Gy mutant clones respectively) increased as the acute dose of X-rays increased.

Consistent with previous reports, the partial deletions at the HPRT gene of X-ray-induced mutant clones declined as the dose increased. Such deletions were 25% (6/24) and 10% (3/31) for 2 and 6-Gy mutant clones, respectively. The hybridisation assay revealed that a substantial proportion of WT pattern mutant clones were the result of a genomic rearrangement. 71% for X-ray-induced WT mutants and 38% of the total number of radiation-induced mutant clones. Had only multiplex PCR been employed for molecular characterisation, a large fraction of mutant clones might have mixed with WT mutant clones resulting in point mutations or small deletions in the coding regions. The results of RT-PCR revealed that mutant clones failed to give relevant amplification products due to the scattering of HPRT exons by genomic rearrangements which occur in either intronic or regulatory regions of the gene. Therefore, only mutant clones with unaltered *NotI* restriction fragment retained RT-PCR products whereas mutant clones making up a larger proportion failed to do so. Surprisingly, a predominant proportion of these rearrangements are intra-genomic chromosomal exchanges (83% and 94% of hTERT clones and MGH-U1 clones, respectively) rather than inter-chromosomal, as keeping with the cytogenetic investigations performed in a representative number of mutant clones. Mutation induction experiments based on dose fractionation showed significantly lower HPRT mutation frequencies (at least a 7-fold reduction in mutation frequency for dose point 6-Gy) in comparison to their corresponding acute irradiations. Cell survival noticeably increased at fractionated irradiations.

In conclusion, hybridisation assay in combination with RT-PCR method yielded a significant higher number of mutation patterns than multiplex PCR exon screening alone, because regions of 2 Mbp or more were examined. RT-PCR revealed that exclusively mutant clones with unaltered *NotI* restriction fragments retained a corresponding HPRT RT-PCR product. The remaining mutant clones were the result of genomic rearrangements occurring in the intronic or in the regulatory region of the HPRT gene and therefore failed to give such a product.

Zusammenfassung

(Molekulare Charakterisierung der strahleninduzierten humanen HPRT Mutanten Klonen)

Das Ziel dieser Arbeit war die Untersuchung der strahleninduzierten Mutagenese in menschlichen Zelllinien, stellvertretend für die Reaktion der Zellen im Organismus als Ganzem. Die vorliegende molekulare Charakterisierung wurde mit einer gut etablierten, malignen, menschlichen Zelllinie, MGH-U1, initialisiert. Die weiterführende strahleninduzierte Mutationsstudie wurde mit hTERT-immortalisierten primären Fibroblasten mit karyotypisch stabilen diploiden Eigenschaften durchgeführt. Die Selektion der Mutanten wurde erfolgreich durchgeführt unter Ausnutzung der Fähigkeit HPRT-defizienter Zellen, in einem *in vitro*-Kulturmedium mit einer bestimmten Substanz zu überleben. Die molekulare Charakterisierung basierte auf einem zuvor eingeführten Hybridisierungsverfahren. Um die nach der ionisierenden Bestrahlung erhaltenen Mutationen zu vergleichen, wurden die Mutanten-Klone parallel mittels Multiplex-PCR, RT-PCR und Chromosomenanfärbung durch eine 3-Farbe-FISH-Analyse untersucht. Das Hybridisierungsverfahren war ursprünglich etabliert worden, um die Genauigkeit der DSB-Reparatur im Anschluss an eine Bestrahlung zu evaluieren. In der vorliegenden Studie wurden die fehlreparierten DSB von klonalen Zellpopulationen durch aberrante Restriktionsbanden auf den ‚Southern Blots‘ dargestellt, während in den, früheren DSB-Reparatur-Studien diese als eine Verschmierung um die Zielbanden beobachtet wurden. Restriktionsfragment-Veränderungen eines 2 Mbp *NotI*-Fragments von Mutanten-DNA sowohl in röntgenstrahleninduzierten als auch in spontanen HPRT-Mutanten wurden verglichen.

Bei Fehlen des NHEJ-Reparatur-Mechanismus, der für den vorherrschenden molekularen Reparatur-Mechanismus höherer Eukaryoten gehalten wird, zeigten 2-Gy-röntgenstrahleninduzierte Mutantenklone, die von NHEJ-defizienten MGH-U1-Zellen erhalten wurden, dass die Mutagenität am HPRT-Genlocus signifikant verringert war im Vergleich mit Zellen mit einem funktionierenden NHEJ-Reparatur-Mechanismus bei equitoxischen Dosen von 6-Gy Röntgenstrahlen. Dies lässt vermuten, dass ein alternativer Reparatur-Mechanismus die Reduktion der Mutationsfrequenz in mit Wortmannin vorbehandelten Zellen überzeugend erklären kann, da solche Mechanismen bei Funktionieren des NHEJ unterdrückt werden können.

78 strahleninduzierte und 47 spontane HPRT-Mutanten-Klone wurden aus hTERT immortalisierten Fibroblasten isoliert und genetische Veränderungen am HPRT-Genlocus mit einem Hybridisierungsverfahren untersucht. Die erhaltenen Ergebnisse sind in Übereinstimmung

mit denjenigen, die mit 22 strahleninduzierten und 26 spontanen MGH-U1 Mutanten-Klonen erhalten wurden. Eine Ausnahme ist die Vielzahl spontan entstandener Mutanten-Klone, die das Resultat von Punktmutationen oder kleinen Deletionen in den codierenden Gensegmenten sind. Diese kleinen Mutationen beinhalten Basenpaar-Substitutionen, z.B.: eine Transversion von A zu C (A: T \rightarrow C: G) wie in Exon 9 festgestellt; eine Transition von C zu T (C: G \rightarrow T: A) wie in Exon 6 festgestellt; eine Mutation, die einen ‚Splicing‘- Fehler verursacht infolge einer Transversion von T zu G (T: A \rightarrow G: C) wie in intronischen Sequenzen und 13 Basenpaare oberhalb von Exon 8 festgestellt. Kleine Mutationen beliefen sich auf fast 8% (2/26) und 94% (44/47) der spontan entstandenen Mutanten-Klone in MGH-U1-Zellen und hTERT-immortalisierten Zellen. Diese Tendenzen nahmen allerdings mit der Steigerung der zur Mutationsinduktion verwendeten Röntgenstrahlendosis ab, und wiesen damit auf eine Dosis-Abhängigkeit hin. Dagegen nahmen die Deletionen, die das komplette HPRT-Gen und die angrenzenden Regionen innerhalb von mindestens 200 kbp am telomerischen Ende des Gens umfassten, mit Steigerung der akuten Röntgenstrahlendosis zu (16% und 38% für die mit 2-Gy bzw. 6-Gy bestrahlten Mutanten-Klone). Die jeweiligen Prozentsätze für die kleinen Mutationen bei 2-Gy und 6-Gy waren 29% (7/24) bzw. 14% (6/44).

In Übereinstimmung mit früheren Studien nahmen die Partialdeletionen am HPRT-Gen der mit Röntgenstrahlen induzierten Mutanten-Klone mit Steigerung der Strahlendosis ab. Diese Deletionen beliefen sich auf 25% (6/24) und 10% (3/31) für die 2-Gy- und 6-Gy-Mutanten-Klone. Das Hybridisierungsverfahren ergab, dass ein beträchtlicher Anteil der Mutanten-Klone mit WT-Muster das Resultat von genomischen Rearrangements war. Insgesamt ergab sich ein Anteil von 71% für die röntgenstrahleninduzierten WT-Mutanten und von 38% für die Gesamtzahl der strahleninduzierten Mutanten-Klone. Wäre nur Multiplex-PCR für die molekulare Charakterisierung verwendet worden, so wäre möglicherweise ein großer Teil der WT-Mutanten-Klone, die aus Punktmutationen oder kleinen Deletionen in den codierenden Regionen resultierten, falsch klassifiziert worden. Die Ergebnisse der RT-PCR offenbarten, dass Mutanten-Klone keine relevanten Amplifizierungsprodukte liefern konnten, da die HPRT-Exons infolge genomischer Rearrangements, die entweder in intronischen oder in regulatorischen Genregionen auftraten, anders angeordnet waren. Daher ergaben nur Mutanten-Klone mit unverändertem *NotI*-Restriktionsfragment RT-PCR-Produkte, während ein größerer Teil der Mutanten-Klone keine ergab. Überraschenderweise sind der überwiegende Anteil dieser Rearrangements intrachromosomale Austausche (83% bzw. 94% bei den hTERT-Klonen bzw. MGH-U1-Klonen) und nicht interchromosomale, wie bei den zytogenetischen Untersuchungen einer

repräsentativen Anzahl von Mutanten-Klonen festgestellt wurde. Mutationsinduktionsexperimente mit Fraktionierung der Bestrahlungsdosis zeigten signifikant geringere HPRT-Mutationsfrequenzen (mindestens eine 7-fache Reduktion der Mutationsfrequenz für die Dosis 6-Gy) im Vergleich mit den entsprechenden akuten Bestrahlungen. Die Überlebensfähigkeit der Zellen nahm bei fraktionierten Bestrahlungen deutlich zu.

Zusammenfassend lässt sich sagen, dass das Hybridisierungsverfahren in Kombination mit RT-PCR eine signifikant größere Zahl von Mutationsmustern ergab als Exon-Screening alleine, da eine Region von 2 Mbp oder mehr betrachtet wurde. RT-PCR zeigte dass nur Mutanten-Klone mit unverändertem *NotI*-Restriktionsfragment ein entsprechendes HPRT-RT-PCR-Produkt ergaben. Die restlichen Mutanten-Klone waren das Resultat von genomischen Rearrangements, die in der intronischen oder in der regulatorischen Region des HPRT-Gens auftraten, weshalb diese kein RT-PCR-Produkt liefern können.

2 Introduction

2.1 Ionizing Radiation

There is one particular idiosyncrasy of ionizing radiation (IR) inherent within radiation itself which makes its subsistence as a carcinogen outstanding, and shows how it greatly differs in its physical make-up when compared with other exogenous agents such as chemical toxicants, or other physical carcinogens, which are, on the whole, tissue specific in their action (Hall 2000; Schecker & Reynolds 1995). Not being hampered by the usual cellular walls that chemical agents produce, radiation has the power to deposit energy randomly within the biological material it so aptly penetrates (Nias 1998). Even though all the cells of the human body are, in such an event, likely to suffer damage through IR, the damage consistency is relative to the physical parameters that determine the dose of radiation which those particular cells, or tissue, actually receive. In recent years, cellular systems have been developed in order to be able to study better the malignant transformation of an individual cell *in vitro* (Liber et al. 1989). Conclusions resulting from these studies have confirmed several of the corroborative factors derived from the *in vivo* experiments (Pfeiffer et al. 2004). Despite the fact that the overall characteristics of radiation-induced cancer *in vivo* and the basic aspects of cellular transformation *in vitro* had already been quite clearly identified by the 1980s, only a limited quota of research has been undertaken in this specific field since then. In fact, IR has become a widely used tool for studying cellular and molecular responses to DNA damage, as these serve to enhance better understanding of the mutations and carcinogenic transformation of the cells. IR includes, sparsely ionizing events resulting from X-rays and γ -rays (electromagnetic) and densely ionizing events induced by α -particles, neutrons and atomic nuclei such as helium, carbon or argon (particulate), which can be accelerated in nuclear physics machines (Hall 2000).

2.1.1 X-rays and γ -rays

X- and γ -rays belong to electromagnetic radiations. X-rays are the rays most familiar to human beings and are being used widely in medical diagnosis and also for the treatment of cancer. They are also used industrially for testing the quality of welds and other materials. A conventional X-ray machine contains a sealed tube in which electrons are accelerated towards a metal target; when the electrons hit the metal with sufficient energy then X-rays are produced. The wavelength of the X-rays depends not only on the energy of the electrons but

also on the atomic number of the metal target. The X-ray photons thereby produced have a wavelength that is characteristic of the interaction of those two factors. For example, an X-ray tube operating at 100 keV energy and using a tungsten target will produce radiation with a wavelength of 10^{-2} nm. Though there will be a range of energies produced by such an X-ray tube only the peak energy is the one that is usually quoted; here, in this case, it is 100 keV. These would be grouped as soft X-rays that would not pass through very far into biological material. For diagnostic purposes, the photon energies of 12.4 keV-124 keV with corresponding wavelengths of 0.1-0.01 nm are customarily used (Hall et al. 1988).

When possessing higher energies, γ -rays are emitted by radio-active isotopes such as ^{60}Co . Resulting from discrete nuclear disintegrations, γ -rays to be motivated by one single energy. When comparing X-rays with γ -rays, both, in most instances, reveal similar characteristics when interacting with matter (Hall 2000). Results based on gamma induced mutant clones support that the majority of radiation-induced mutations at the HPRT gene locus are large deletions (Morris et al. 1993; Park et al. 1995).

The mode of interaction when dealing with X-ray energies of less than 0.5 MeV is *photoelectric effect*. This is when a photon is completely absorbed by the target atom and emits an electron which produces radiation. At higher energies between 0.5 MeV and 5 MeV *Compton scattering* is shown to be predominant. On the recoil during this process, the incidentally formed photon collides with an orbital electron; a so-called recoil electron is produced, and so the dispersed photon departs with reduced energy. Much dependant upon its energy level, this scattered photon may then be interpolated among additional target atoms by further *Compton scattering* or by recurrent photoelectric interaction. In both processes, an electron is ejected from the target atom, leaving it in an unstable condition. Raising an electron in an atom, or molecule, to a higher energy level without ejection of the electron is called: *excitation* (Hall 2000).

2.2 Radiation-Induced DNA Lesions and Double Strand-Breaks (DSBs)

IR induces a set of lesions in DNA (Steel 1996), including base damage, single-strand breaks (SSBs) and DSBs, hydrogen bond breakage between chains, damage to the phosphodiester backbone and cross linking within helical orders to another DNA molecule or to protein. DNA DSBs are generally thought to be the most critical lesions in radiation-induced killing of cells (Badie et al. 1995; Collis et al. 2005), and cells deficient in DSB repair are killed at a higher rate (Hashimoto et al. 2003). In general, while exogenous DSBs are induced by IR, or radiomimetic-drugs, such as bleomycin, or etoposide, endogenous DSBs arise as byproducts in

DNA metabolism, oxidative damage and V(D)J recombination, and meiotic cellular events. It is estimated that the DSBs which arose spontaneously may be as high as 50 breaks per cell cycle (Vilenchik & Knudson 2003). For example, DSBs can be detected when replication forks arrest (Ohashi et al. 2005), and collapse, a process that is thought to occur frequently during the DNA synthesis (S-phase) of cell cycle. Data from Goodhead (1994) revealed the damage produced in a mammalian cell nucleus by 1 Gy of low linear energy transfer (LET) radiation: 100 000 x ionizations in cell nucleus; 2000 ionizations directly in DNA; 1000 x DNA SSBs and 40 x DSBs. Such a dose will produce a large number of ionizations in the nucleus but far fewer DNA lesions, such as sugar or base damage, DNA-DNA and DNA-protein cross links, DNA single-or DSBs and chromosome aberrations. In brief, only 40 DSBs are produced per Gy per cell; by approximation, only 1 DSB per chromosome (Nias 1998).

It has been shown that single DSBs that are not repaired can be lethal (Bennett et al. 1996), as well as misrepaired (Pastwa & Blasiak 2003). Further, misrepaired DSBs can lead to chromosome aberrations (Bailey et al. 2004; Lobrich et al. 2000; Natarajan et al. 1994), other mutations, or cell death (Collis et al. 2005; Khanna & Jackson 2001). In particular, misjoining of the exchanged ends of two such breaks on different chromosomes may account for many, if not most, of the reciprocal translocations and dicentric chromosomes induced by the above mentioned agents (Galloway 1994; Preston 1990). It is shown that, following treatment with radiation, or radiomimetic-drugs, a subpopulation of the progeny cells acquire a persistent global chromosomal instability and continue to accumulate additional chromosome alterations many generations after the treatment (Kadhim et al. 1995). Although the mechanism for this delayed effect is not well-known, it is generally accepted that the effect cannot be due to the residual radiation-induced damage, because such damage, even if not repaired, would be less in numbers by dilution as the cells divide further. Thus, the putative indirect genomic effects raise the question of whether even the early chromosome changes that occur in the first few generations after treatment might be due to an induced global chromosome instability, rather than to the misrepair of DSBs (Foray et al. 1999). However, it is observed that if DSB-repair functions are inhibited in cells then a higher rate of cell killing is the consequence. This was demonstrated clearly in studies of radiosensitive DSB repair-deficient mutants such as murine cells from severe combined immune deficiency (SCID) (Biedermann et al. 1991; Hendrickson et al. 1991). Many cancer therapies exploit the lethality of DNA DSBs (McMillan et al. 2001) by chemically or physically inflicting this type of damage on cancer cells (Jackson 2002; Lobrich et al. 2005).

In terms of radiation-induced cell killings, there are two distinct mechanisms. The first is apoptosis, also called programmed cell death (Wang et al. 1996). Cells undergoing apoptosis as an immediate consequence of radiation damage usually die in interphase within a few hours of irradiation (Peng et al. 2002; Takata et al. 1998). Apoptotic cell death occurs in a few cell types, including small lymphocytes, type A spermatogonia and oocytes, following relatively low doses of radiation (Nitta & Hoshi 2003; Vilenchik & Knudson 2000). Moreover, apoptosis could also be a significant cause of death in a large number of cell types exposed to higher radiation doses (Mendrysa et al. 2003), including those of hematopoietic or lymphoid origin (Griffiths et al. 1997; Mendrysa et al. 2003), as well as some malignant cells (Preisler et al. 1996; Young et al. 2003). The second mechanism for cell killing after cells' exposure to radiation is radiation-induced reproductive failure. It has been shown that radiation in sufficient doses can inhibit mitosis (Jayanth et al. 1994) and the inhibition of cell proliferation is believed to be the mechanism by which radiation kills most cells. The nature and kinetics of the cytotoxic effects of radiation in mammalian cells were described by several authors previously (Amundson et al. 1996; Crompton et al. 2002; Liber et al. 1983).

In *in vitro* analyses, there are several methods that are currently being employed to detect double strand DNA breaks. One of the earlier invented methods is comet assay, which is a sensitive rapid method for detecting DSBs in individual cells. In the examination of DSBs, cells are embedded in agarose. Following exposure to an electric field, broken DNA can be monitored as a tail or a comet (Rapp & Greulich 2004). FAR (fraction activity released) (Rydberg et al. 1994) and hybridisation assay with single-copy probes have been frequently used as a measure for DSB rejoining in a certain genomic region (Lobrich et al. 1996; Lobrich et al. 2000; Rothkamm & Lobrich 1999). Apart from the above two methods, enumeration of γ -H2AX foci (due to phosphorylation of a histone) can also be used to measure the induction and DSB repair incubation of both human and murine cells (Rogakou et al. 1998). The latter method was even used to analyse DSBs following doses as low as 1 mGy to 2 Gy (Rothkamm & Lobrich 2003). Furthermore, very recent studies *in vivo* revealed that γ -H2AX foci (Lobrich et al. 2005), can also serve as a biologically relevant bio indicator for a cell's exposure to low levels of ionizing radiation.

2.2.1 DNA DSBs and Repair Mechanisms

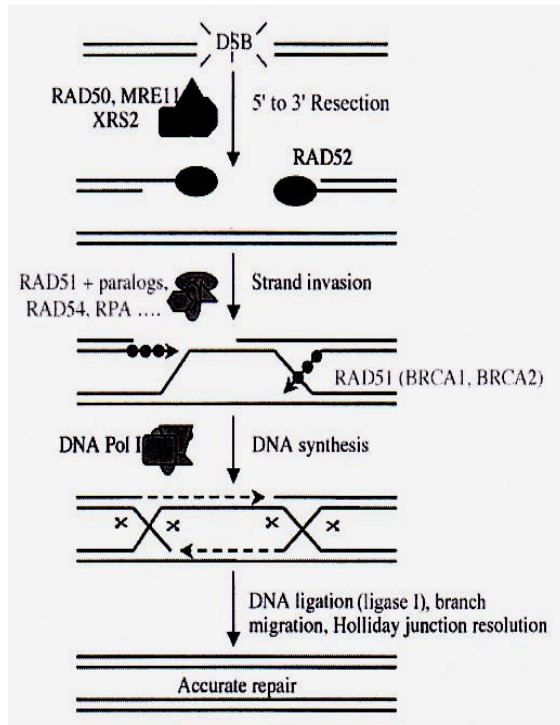
Eukaryotes have at least two major pathways for the repair of DSBs: Homologous Recombination (HR) and Non-homologous end-joining (NHEJ) (Jackson 2002; Karanjawala et al. 2002). These two major repair mechanisms differ in their requirement for a homologous template DNA and in the fidelity of DSB repair. While HR ensures accurate DSB repair, NHEJ does not (Pfeiffer et al. 2004). The relative contribution of these two main pathways is likely to differ depending on cell cycle phase. In mammalian cells, NHEJ is the main repair pathway, operating in all phases of the cell cycle. In contrast, HR is most efficient in the S and G₂- cell cycle phases because of the access of sister chromatids as repair templates (Anderson & Eliason 1986).

2.2.1.1 Homologous Recombination

Particular repair pathway in lower eukaryotes such as *S.cerevisiae*, is functioned by the products of the RAD52 group: RAD50, RAD51, RAD52, RAD54, RAD55, RAD57, RAD59, MRE11 and XRS2 (Carney et al. 1998; Thacker 2005). Although functional mammalian counterparts exist, there are some important differences between the two systems. RAD51p of *S.cerevisiae*, which takes part in DNA strand-exchange, is non-essential, whereas homozygous loss of RAD51 in mice results in early embryonic cell lethality (Donoho et al. 2003). Furthermore, mammalian homologues exist for all of the known HR factors in *S.cerevisiae*, but detailed enzymatic machinery is seen to be considerably more complex in higher eukaryotes. The existence of several RAD51 paralogues (they diverged due to a gene duplication within a species), such as RAD51B, C and D, and the other counter proteins with relatively impaired homology to the catalytic domain of RAD51, such as XRCC2 and XRCC3 (Pluth et al. 2001; Wood et al. 2001) supports the latter hypothesis. And loss of RAD51 in a chicken B-lymphocyte cell line (DT-40) leads to chromosomal breaks (Yamamoto et al. 2005), indicating that chromosomal stability in cells that have not been deliberately treated with genotoxic agents requires a RAD51-dependent recombinational-repair pathway.

This homologous recombination pathway in yeast, has, in the meantime, been more thoroughly studied (Brendel et al. 2003; Harvey et al. 2005). To begin the homologous recombination in yeast, one could consider the nucleolytic resection of DNA DSBs in the 5' to 3' direction to be the first step (Figure 2.1a). The efficiency of this reaction *in vivo* is guaranteed and most likely involves a complex containing RAD50p, MRE11p and XRS2p

a) Homologous Recombination



b) Non-homologous End-joining

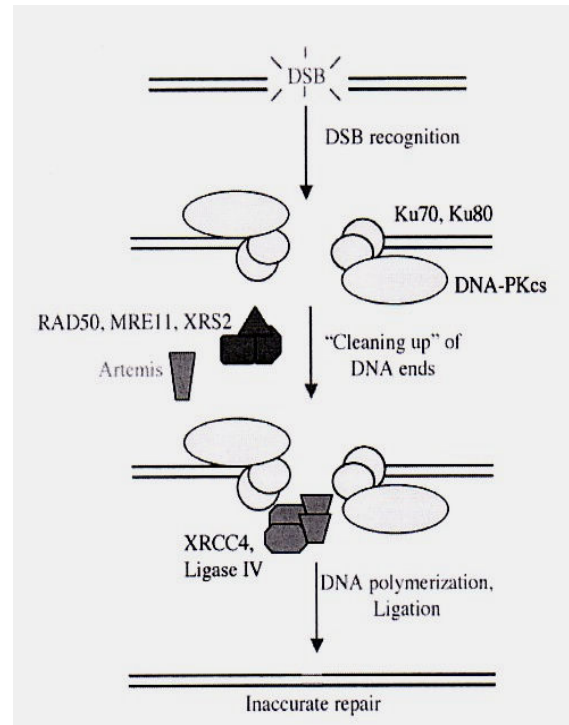


Figure 2.1. Schematic diagram of the major repair pathways in mammals: a) an outline of the homologous recombination-pathway indicating the participation of the variously designated proteins b) Non-homologous end-joining pathway representing its *respective* proteins (From Jackson 2002).

(the human counterpart is NBS1). RAD51p then binds the resulting 3' single-strand DNA-tails in a process that is influenced by a range of other proteins, including replication protein A (RPA) (Zou & Elledge 2003; Zou et al. 2003), RAD52p and RAD54p. Of prime importance is, that human RAD52 is shown to bind to DNA DSBs preferentially (Scully & Xie 2005), leading to the proposal that Ku, in competition with this complex, to attain DNA ends may determine which of the two DSB repair-pathways should be employed (Van Dyck et al. 1999). In such a case, the RAD51p nucleoprotein filament would then interact with an undamaged DNA molecule, and, when locating a homologous region, would create a RAD51p strand-exchange. This strand is then extended by DNA polymerase that copies information from the undamaged partner. After migration of crossovers (Holliday junctions) they are resolved by cleavage and ligation. An exception to this could be a region of direct repeats. In such a case, a sub pathway of HR, single strand-annealing (SSA) repairs the breaks. SSA results in the loss of one of the two direct repeats and also the intervening DNA (Essers et al. 2002; Takata et al. 1998).

Recent reports on HR and the breast cancer susceptibility proteins, BRCA1 and BRCA2, for which no homologues in yeast have been found, have shown close links between

HR and BRCA (Foray et al. 2003; Gatei et al. 2000). As reviewed by several authors (Khanna & Jackson 2001; Merel et al. 2002), particularly the loss of function of one of the breast cancer proteins in mammalian cells causes a marked reduction in the efficiency of accurate homology-dependent DNA repair (Snouwaert et al. 1999). Although HR is well-known as an error free DNA repair mechanism at least theoretically, a mutation of BRCA2 is believed to stimulate error-prone homology directed repair of DNA DSBs (Griffin & Thacker 2004; Tutt et al. 2001). In any case, detailed information about the way these effects interact is yet to be elucidated, despite the fact, that they may reflect the affinity to BRCA1 and BRCA2 to RAD51 (Amundson & Chen 1996; Chen et al. 1999).

2.2.1.2 Non-homologous End-Joining (NHEJ)

Non-homologous end-joining (NHEJ) - the main pathway (Jeggo & Lobrich 2005; Richardson & Jasin 2000) for repairing double-strand-DNA breaks - functions throughout the mammalian cell cycle (Karanjawala et al. 2003; Lieber et al. 2003) (Figure 2.1b). NHEJ involves the following proteins: DNA ligase IV, XRCC4, DNA-dependent protein kinase (DNA-PK), RAD50, MRE11, NBS1 and a novel factor, known as *Artemis* (Collis et al. 2005; Jeggo & Lobrich 2005). These components also play a major role in ‘*variable diversity joining recombination*’ (V(D)J recombination) in generating a wide variety of antigen-specific molecules, the immunoglobulins and T- cell receptors (Dai et al. 2003). The genomes of multicellular eukaryotes, unlike yeast, contain a substantial fraction of repetitive DNA. Therefore, when a break occurs in the genome, homology is rendered useless. This is because breaks in the genome are 40% repetitive and homology tries to repair DSBs with homologous recombination (Platzter et al. 1997). A homologous crossover event arising during DSB repair could thus result in a chromosomal translocation. Therefore, homologous recombination could be far too slow and dangerous in organisms involving genomes that have a substantial fraction of repetitive DNA. This might be the primary reason for the distribution of those major repair pathways in lower and higher eukaryotes (El-Khamisy et al. 2005).

The principal enzyme in the NHEJ-pathway (Collis et al. 2005; Rothkamm et al. 2001) is the DNA-dependent protein kinase (DNA-PK) which consists of the DNA end-binding heterodimer Ku70 and Ku80, and the DNA-dependent protein kinase catalytic subunit (DNA-PKcs) (Jeggo 1998; Meek et al. 2004; Rothkamm et al. 2001). The function of the enzyme is thought to serve in the regulation of the NHEJ-mechanism, in which the further enzymes are activated (Hendrickson et al. 1991; Jeggo & Lobrich 2005; Koch et al. 2004). This particular holoenzyme is an abundant serine-threonine protein kinase (Hammarsten & Chu 1998), which

lodges within the nucleus of human cells where its general function is to produce phosphorylated serine and threonine residues in specific proteins bound to DNA. It also plays a key role in the repair of those double-strand breaks which are created by IR or by V(D)J recombination (Dai et al. 2003; Yoshioka et al. 2001).

In vertebrates, Ku's function is to serve as the DNA targeting subunit of the DNA-dependent protein kinase (Meek et al. 2004; Rooney et al. 2005). In NHEJ, Ku forms an open ring-type structure that can be threaded onto a DNA-end. One side of the ring forms a cradle that has a protection device for one surface of the DNA double helix, whereas the other side is much more open, maybe to allow the remaining NHEJ factors to access the DSB (Jackson 2002). In normal cells, Ku is thought to be about fivefold more abundant than DNA-PKcs (Anderson & Carter 1996) and its binding to DNA is thought to be tighter (Meek et al. 2004; Pastwa & Blasiak 2003). Studies indicate that the association of Ku and DNA-PKcs cannot be observed in the absence of a DNA terminus (Lieber et al. 1997; Yaneva et al. 1997).

DNA-PKcs is encoded by an open reading frame of 4096 amino acids, with a predicted molecular weight of 465.482 kDa (Hartley et al. 1995). The C-terminal region of DNA-PKcs has homology to catalytic domains of proteins of the phosphatidylinositol-3 kinase-like-kinase (PIKK) family (Canman & Lim 1998; Hartley et al. 1995; Stiff et al. 2005) to which also the significant signal transducers of the DNA damage response, ataxia-telangiectasia (ATM) and ATM-Rad3-related (ATR) genes belong. This PKcs enzyme is unique in that it requires a DNA-end to become active (Collis et al. 2005; Thacker & Zdzienicka 2004). Furthermore, DNA-PKcs activity is stimulated by Ku when the DNA is longer than 26 bp; otherwise Ku prevents the DNA PKcs from progressing (Hammarsten & Chu 1998). The severe combined immune deficiency (SCID) mouse, which is the most seriously inherited immunological deficit, has a mutation in the DNA-PKcs gene causing truncation of terminal 83 amino acids in the kinase domain (An et al. 2005; Niimi et al. 2005) which leads inevitably to hypersensitivity in IR (Biedermann et al. 1991; Hendrickson et al. 1991), and to a defect in V(D)J recombination characterized by undetectable coding-joints alongside relatively normal signal-joints (Dai et al. 2003; Finette et al. 1996). As previously mentioned, since DNA-PKcs gene product has a homology to PIKK family, studies examining the radiation sensitivity using selective inhibitors of PI-3 kinase have recently been reported (Price & Youmell 1996; Rosenzweig et al. 1997). In such investigations, relatively high concentrations of wortmannin (20 μ M) (Kinashi et al. 2003; Okayasu et al. 1998; Sasaki et al. 2002) or LY294002 (50 μ M) (Brunn et al. 1996; Rosenzweig et al. 1997; Stiff et al. 2004) have been used to radiosensitize the cells of various human and murine cells *in vitro*.

Wortmannin inhibits PI-3 kinase, an important enzyme involved in intracellular signalling, through covalent binding to the C-terminal region of the catalytic subunit (Wymann et al. 1996). Moreover, it has been shown that wortmannin has a greater effect on the survival of G1-phase cells than of S/G2- phase cells after irradiation and suggested that the particular fungal metabolite as a drug might be more effective in normal cells compared to malignant cells, a result that would be more helpful in radiation therapy according to Chernikova et al. (2001).

The novel candidate of NHEJ is the so-called *Artemis* gene, and was identified on the basis of its mutation in patients with SCID (Moshous et al. 2001). Though the function of the *Artemis* gene was not known at the beginning, it has now been revealed that *Artemis* and DNA-PKcs form a physical complex both *in vitro* and *in vivo*, and DNA-PKcs can phosphorylate *Artemis* (Dai et al. 2003; Ma & Lieber 2002). Also cells from *Artemis-null* patients have shown a failure in the formation of signal joints but not in V(D)J recombination, that are indistinguishable from DNA-PKcs-null mice (Moshous et al. 2003). The *Artemis-DNA-PKcs* complex acts as an endonuclease at both 5'overhangs and 3'overhangs. Mutations of *Artemis* in its β -lactamase fold abolish endonuclease activity, which indicates that this region might be at least partly responsible for the extent of nuclease activity (Lieber et al. 2003). Further, the *Artemis-PKcs* complex is also very efficient at opening DNA hairpins (Karanjawala et al. 2002). *Artemis* deficient cells have exhibited radiation sensitivity and defective V(D)J recombination, implicating *Artemis* function in the NHEJ pathway (Jeggo & Lobrich 2005; Riballo et al. 2004). And in the mean time, a syndrome called Omenn has been found to be related with *Artemis* gene mutations (Ege et al. 2005). Cells taken from athabascan-speaking native american SCID patients have recently shown significantly elevated sensitivity to IR but only a subtle change in DSB repair in contrast to the severe DSB repair defect of NHEJ-deficient cells (Wang et al. 2005) (This repair defect has been extensively studied by our group !!!).

DNA Ligase IV takes part in the formation of DNA strand-joining events via the NHEJ pathway and functions in a stringent complex with the protein XRCC4 (Grawunder et al. 1997; Li et al. 1995). Ligase IV's responsibility for collocating DSBs were observed in *S.cerevisiae* (Wilson et al. 1997). Similarly, the DNA Ligase IV in mammalian cells was understood as the ligase for DSB repair on the basis of its physical association with XRCC4. This complex was shown in radiation-sensitivity studies to be most vital for NHEJ (Grawunder et al. 1997). Recently, a syndrome called LIG4, under the guise of hypomorphic

mutations in DNA Ligase IV, has been found in some human patients (Karanjawala et al. 2002; Rothkamm et al. 2001).

The size of the XRCC4-gene product is a protein of about 38 kDa in humans, whose precise role in NHEJ is still unknown (Koch et al. 2004; Li et al. 1995). However, consistent with a previous report (Teo & Jackson 2000), biochemical studies in the mammalian system have shown that Ku can load the XRCC4-ligase IV complex onto DNA ends and affect the DNA-end-ligation (Grawunder et al. 1997; Li et al. 1995).

The MRE11/RAD50/NBS1 complex found in humans has been implicated in supplying the exonuclease activity involved in the NHEJ, but other reports recently suggested that this complex may function primarily in HR repair, with secondary roles in NHEJ and damage events (Lee & Paull 2005). A functional homologue of XRS-2 in human, p95 (NBS1) is found to be mutated in the Nijmegen breakage syndrome (NBS) which is recognized as a human cancer predisposition and radiation sensitivity syndrome (Carney et al. 1998; Varon et al. 1998) as has been the case for ataxia-telangiectasia (A-T) patients. Mutations in ATM (ataxia-telangiectasia mutated) gene which is the central signal transducer of DNA damage response (Lobrich & Jeggo 2005), lead to A-T, and cells from these patients were hypersensitive to DSBs (Shiloh 2003). A-T and NBS are generally characterised by chromosome instability especially involving chromosome 7 and 14 (Stiff et al. 2005). NBS has therefore been described as an Ataxia-telangiectasia-like disorder (ATLD) (Varon et al. 1998). Patients with ATLD, however, showed a mild A-T phenotype with no microcephaly or developmental delay (Stewart et al. 1999). Further, hypomorphic mutations in hMRE11 gene (Stewart et al. 1999), but not in ATM gene, were observed in ATLD-patients recently suggesting that ATM and the human MRN protein complex seem to act in the same DNA damage response pathway and there is a link between human MRE11 and the complex pathology of A-T. Furthermore, other studies have provided that the ATM gene is nonessential in mice and humans, while NBS1 and MRE11-defective in mice are embryonically lethal (Stiff et al. 2005; Yamaguchi-Iwai et al. 1999).

2.2.2. Cell Cycle and DNA Damage

Exogenous DNA damaging agents such as ionizing radiation (IR) influence the transcription of many genes in mammalian cells (Allen et al. 2003). Several early-response genes are transcribed at high levels shortly after exposure to IR (Amundson et al. 2002; Lowe et al. 1993b). Some of these early-response genes encode transcription factors that direct the cellular responses to IR, including cell cycle arrest, induction of DNA repair, and apoptosis.

The well-known tumour suppressor p53 gene is among the early-response genes. After DNA damage, p53 functions in the induction pathway of cell cycle arrest (Caspari 2000; Kastan et al. 1991) and the induction of apoptosis (Goi et al. 1997; Lowe et al. 1993a). The activation of p53 gene is known to depend on the ATM kinase gene (Caspari 2000). However, the precise mechanisms by which the p53 gene regulates DNA repair, genomic stability and mutagenesis remain to be further elucidated (Jeggo 1998), although many biochemical functions of the p53 were identified (Agrawal et al. 1998). In addition, the ATM-gene is the apex of a signalling cascade that responds to the most significant damage to DNA, and is the key to co-ordinating all resulting cellular responses (Khanna et al. 2001; Shiloh 2003). ATM is activated following cell exposure to irradiations (Bakkenist & Kastan 2003; Pandita et al. 2000) and phosphorylates proteins involving in cell cycle checkpoint mechanisms and DNA repair. It was suggested, that ATM is activated by intermolecular autophosphorylation on Ser1981 (Bakkenist & Kastan 2003; Riballo et al. 2004).

Although checkpoints can easily be demonstrated in cell culture systems, the occurrence and role they play *in vivo* seem to be less clear (Liang et al. 2002; Shao et al. 2000). However, since proteins involving in DNA damage responses activate checkpoint proteins, they are indispensable in preventing carcinogenesis (Slupphaug et al. 2003). This is the reason why cells derived from A-T-patients show defective cell-cycle checkpoints after DNA damage (Kuhne et al. 2004; Mondello et al. 2001; Riballo et al. 2004) and also why a high incidence of chromosomal translocations and frequent malignancies in lymphoid cells is evident (Thacker 2005). Therefore, the defective cell-cycle checkpoints found in A-T-cells after DNA damage represent the defective phosphorylation of ATM-substrates (Shiloh 2003). Apart from that, A-T-patients display clinical radiation sensitivity (Morrison et al. 2000), immunodeficiency (Riballo et al. 2004) and also show higher risk of cancer induction (Chun & Gatti 2004). In addition, recent studies revealed that null mutations in ATR gene which is also a signal transducer in DNA damage (Foray et al. 2003; Helt et al. 2005), are lethal (de Klein et al. 2000), but the mutants, having been sensitised to all forms of DNA damage, were therefore seen to affect the intra-S and G2/M checkpoint responses (Cliby et al. 1998; Nghiem et al. 2001). Further, it has been suggested that replication protein A (RPA) bound to single-strand DNA is a requisite for the recruitment of ATR to sites of DNA damage (Zou & Elledge 2003). Recently, O'Driscoll et al. (2003) identified a hypomorphic mutation in the ATR gene in two related Seckel syndrome patients. ATR-Seckel patients had characteristics that overlap with NBS, namely pronounced microcephaly, developmental delay and distinct facial features (Goodship et al. 2000; O'Driscoll et al. 2003). Nevertheless, while ATM responds to the

presence of DNA DSBs, ATR appears to be activated by ssDNA, arising at stalled replication forks, or an unexpected reaction generated during processing of bulky lesions (Zou & Elledge 2003).

2.3 Radiation-Induced Mutagenesis and Cancer

Irrespective of the fact that the mutagenic effect of ionizing radiation was first known after Hermann Müller performed his classic experiments with *Drosophila* in 1927 (Nissani & Carlson 1975), it is only later that information has focussed on the molecular nature of mutations in mammalian cells. Previous molecular studies with the X-linked HPRT gene have already shown that radiation could induce both small-scale mutations and large-scale mutations such as deletions (Jackson 2002) with the latter sometimes including the entire gene (Bao et al. 1995). The impact of radiation-induced deletions at a hemizygous gene locus that can give rise to a survivable cell is, in most cases, limited. This is due to the presence of adjacent essential genes where mutation can not be induced by homologous recombinational events. Alternatively, studies in which autosomal loci were implemented for the study of mutational events have yielded large-scale events involving loss of heterozygosity (LOH) as the most frequent genetic changes (Amundson et al. 1992; Hutchinson 1995; Miles et al. 1990). LOH is, by nature, frequently extended to both proximal and distal sites from the aimed gene (Li et al. 1992). One therefore takes it for granted that LOH is often the result of a simple deletion and it has been revealed that some cases are, inadvertently, the consequence of recombinational events (Wiese et al. 2001).

Apart from the mutations occurring directly after the cells' exposure to radiation, the observance of mutagenesis of cells that were not, themselves, irradiated, but were neighbouring cells of those actually traversed by an alpha particle has been reported. In the literature, the latter case has been termed as a 'bystander' effect (Nagasawa et al. 2003). Furthermore, it has been common knowledge for a long time, that ionizing radiation can develop into an universal carcinogen, in that it can induce cancer in most tissues of most species, regardless of age, whether adult, child or even foetus. These cancers induced by radiation appear to be of a similar histological type, as they occur spontaneously, and in most cases, their type, an actual virulence, endemic in such typical growths, is likely to vary quite a lot. Later on, in experimental stages, it became quite clear that radiation-induced carcinogenesis could, no doubt, be influenced by a variety of non-carcinogenic secondary factors (Heidenreich & Paretzke 2004; Trosko 1996). The genetic changes that radiation can induce include a wide variety of stable chromosomal aberrations, including deletions and

reciprocal translocations. It is, therefore, tempting to speculate that these aberrations may play quite a fundamental role in the complex process of radiation carcinogenesis. While radiation-induced cancers are reported to contain multiple unbalanced chromosomal rearrangements, few have shown specific translocations, or deletions, as those obviously related to the activation of notable oncogenes, or tumour suppressor genes (Applegate et al. 1992; Van Steeg et al. 2000).

Notwithstanding, evidence shows that certain types of cancers, normally discovered to be extremely virulent, not only in irradiated but also in non-irradiated populations, make it difficult for anyone to deduce with any degree of certainty whether any given type of cancer is, in fact, due to either a given magnitude of radiation-exposure, or, adversely; the consequence of a large number of other factors (Schecker & Reynolds 1995; Van Steeg et al. 2000). Similarly, despite the fact that a great deal of data still remain inadequate, it is a fact that radiation does indeed initiate malignancies and one is also forced to admit that spontaneously induced malignancies are caused by other carcinogens. Following up on this, it has also been difficult to determine the manner in which genetic changes occur, since a normal cell becoming transformed into a cancerous one is an involved and intricate process that requires multiple mutational changes accumulated in an enigmatic and complex manner over a period of many years (Hall 2000).

2.3.1 Mutations and Classification

Any heritable change which takes place in a gene is called a mutation. Although mutations take place spontaneously, aside from radiation, they can also be induced by a variety of other chemical agents that damage nucleotides, or that produce breaks in polynucleotide chains. There are in respect of *mutation* in its broadest sense, small-scale and large-scale mutations.

Mutations can be classified in a variety of ways. Those that arise in gametes are *germ-line mutations*, all others being *somatic mutations*. Here, reproductive cells are not affected, so somatic mutations cannot be passed on to the progeny cells, and may not, in fact, be amenable to genetic studies. Mutations can also be classified in accordance with the manner in which they affect gene expressions. For example, the mutation that inactivates the complete gene function is a *loss-of-function mutation* (Frankenberg et al. 2002; Tatsumi et al. 1992). The same mutations can be labelled with different names, some of which are: '*null mutations*', '*knockout mutations*' and '*amorphic mutations*'. A type of mutation that reduces, but does not eliminate, the level of expression of a particular gene, or the activity of the gene product, is called a '*hypomorphic mutation*' (Stewart et al. 1999). These mutations result from

an amino acid replacement that impairs protein function (Ege et al. 2005; Zhang et al. 2005), or from those nucleotide substitutions that prevent proteins from being produced at the normal level. *Hypomorphic mutations* can cause cells to react differently. For example, *hypomorphic mutations* that have recently been identified in DNA ligase IV (Kuhne et al. 2004) exhibit a substantial repair defect up to 24 hours, but which continue to undergo several days' worth of repair, and consequently seem similar to that of wild-type cells that manage to reach the level of non-repaired DSBs.

The opposite of a '*hypomorphic mutation*' is a '*hypermorphic mutation*' (Van Raamsdonk et al. 2004). Here, by the mutation, the amount of gene product that a mutant produces is greater than normal level of gene expression, because, typically, the mutation changes the regulation of the gene so that the gene product is overproduced; for example, an amino acid-replacement may increase the activity of an enzyme or another protein. There are also mutations which qualitatively alter the action of a gene, and these are called *gain-of-function mutations* (Tatsumi et al. 1992). In such cases, mutations of this sort are dominant whereas, most *loss-of-function* and *hypomorphic mutations* on the whole, prove to be recessive (Zhang et al. 2005). And, in addition to this, because they are more likely to undergo mutation than others, certain DNA sequences on the genome are labelled as '*mutational hotspots*' (Drobetsky & Sage 1993; Thilly et al. 1989). So, *mutational hot spots* may, in fact, include monotonous runs of a single nucleotide, or involve tandem repetitions of some particular short sequence, such as an unstable tri-nucleotide-repeat, that may be expanded, or contracted by replication slippage, or by other mechanisms (Podlutsky et al. 1998). Typical *hot spots* can be found at various sites, throughout the genome itself, and also within the genes. Regarding genetic studies of mutation, the existence of *hot spots* would mean that a relatively small number of sites could decidedly account for a disproportionately large fraction of all mutations (Podlutsky et al. 1998; Thilly et al. 1989).

2.3.1.1 Small-Scale Mutations

In this section, classifications of small-scale mutations such as point mutations will be described. When we concern ourselves with the molecular nature of mutations, we are confronted with their simplest type, and that is a nucleotide base substitution, in which a nucleotide pair within a DNA duplex is replaced by a different nucleotide pair. For example, within an A→G substitution, an A is replaced with a G in one of the DNA strands. This substitution temporarily creates a mismatched G-T base-pair, therefore when the next immediate replication takes place, this particular kind of mismatching is resolved as a proper

G-C base-pair within one specific daughter-molecule, and additionally as a proper A-T base-pair within the other daughter-molecule. In this case, the G-C base-pair is the mutant and the A-T base-pair is a non-mutant. Some nucleotide substitutions replace one pyrimidine base with the other, or one purine base with the other. These are called *transition mutations* (O'Neill & Finette 1998; Vrieling et al. 1989). There can be 4 possible transition mutations: T→C or C→T (pyrimidine → pyrimidine); A→G or G→A (purine → purine). The other possible nucleotide substitutions replace a purine with a pyrimidine, or the other way round. These genetic changes are called *transversion mutations* (Silva et al. 2005). Eight possible transversion mutations are: A→T, A→C, G→T or G→C (purine → pyrimidine); T→A, T→G, C→A or C→G (pyrimidine → purine). Should these changes of bases occur in a random manner, then one would expect a 1:2 ratio of transitions to transversions. However, studies have shown, that spontaneous nucleotide substitutions are often biased in favour of transitions, and a particular ratio of base pair substitutions in the human genome is nearly 2:1.

The mutations that change the nucleotide sequence without changing the amino acid sequence are called *silent mutations* or *synonymous mutations* (Saffi et al. 2001), whereas the mutations with the other way round are *missense mutations* or *non-synonymous mutations* (Lee & Paull 2004; Oguchi et al. 2003). A change in the amino acid sequence of a protein may actually alter the biological characteristics of the protein here. Another classical example of the phenotypic effect of a single amino acid change is the change responsible for the human hereditary disease *sickle-cell anemia*. The *sickle-cell* mutation is an A-T → T-A transversion in the second codon position for the sixth amino acid in the β-globin chain of haemoglobin; particular mutation caused the normal glutamic acid to be replaced with valine (Kudsk et al. 1981; Markenson et al. 1978). Further, mutations that create a new stop codon resulting in the premature termination of translation and the production of a truncated polypeptide are called *nonsense mutations* (Hou 1994; O'Neill et al. 1998). Due to termination, the remaining polypeptide fragment finally becomes non-functional.

Mutations, in which small insertions and deletions occur instead of single base-pair substitutions are mostly limited to 1-6 base pairs in mammalian genomes. These types of mutations, however, cause the amino acids to be altered on their way downstream from the site of the mutation, and are termed *frameshift mutations*, considering their function in the reading frame of the codons in the mRNA (Giver et al. 1995; Nelson et al. 1994).

2.3.1.2 Large-Scale Mutations

Chromosomal-level aberrations belong to large-scale mutations. Should the irradiation be delivered early in the cell cycle before DNA replication has begun, then the chromosomes will not yet have duplicated, and the lesions will affect to whole chromosomes. This may be visible through chromosome-type aberrations (formed in G1 or G0) immediately after mitosis (Mognato et al. 2003; O'Neill et al. 1991; Virsik-Kopp et al. 2004). In contrast, chromatid-type aberrations (formed in G2) may arise following irradiation at a later stage during the cell cycle when each chromosome, will have divided into two chromatids, so that the damage may only be found in one of a pair of chromatids (Harvey et al. 1997; Helbig et al. 1994). Aberration formation is usually assessed using the long known breakage-and-reunion model and its current versions (Sachs et al. 2004). An aberration is formed when free ends from two or more different radiation-induced DSBs interact. However, recent evidence argues strongly for different mechanisms for chromosome- and chromatid-type aberrations, i.e. there is little or no correspondence in the relative frequencies between chromosome and chromatid aberrations (Bryant 2004).

In general, there are four basic structural aberration categories: terminal deletion or discontinuity; interchange; inter-arm intrachange; intra-arm intrachange. Terminal deletion or discontinuity of a chromosome can be thought to be from a single break while all other three categories require the interaction of a minimum two breaks. Of all these categories, interchanges such as translocations are the commonest form for chromosome-type aberrations, whereas various forms of intra-arm intrachanges between breaks in the sister chromatids (interstitial deletions or paracentric inversions) are believed to be the commonest among chromatid-type aberrations. Two rejoining modes, which yield either a dicentric (a chromosome with two centromeres and also resulted from interchanges) or a reciprocal translocation are thought to be equal, despite the fact that the latter are only visible when specialised staining techniques such as fluorescent *in situ* hybridisation (FISH) are employed (Nias 1998). The dicentrics, because they are much easier to score, have for some time been the basis of a technique of biological dosimetry (Ballarini & Ottolenghi 2003; Frankenberg et al. 2002; Nias 1998). In addition to reciprocal translocations, there are also its asymmetric form of chromosomal interchanges; non-reciprocal translocations. It has been reported, that a translocation can be used in radiological protection to supplement physical dosimetry in the event of a suspected accidental exposure to radiation (Boei & Natarajan 1998; Edwards 1997). In addition to these two chromosomal mutations (translocations and dicentrics), inversions, insertions, centric rings, duplications and deletions are the other chromosomal

aberrations that have been found among the radiation-induced chromosome-level aberrations (Bauchinger & Schmid 1997; Mognato et al. 2003).

An inversion whose inverse region is not equipped with a centromere is called a ‘*paracentric*’, while its antonym is known as a ‘*pericentric inversion*’ (Bauchinger & Schmid 1997; Brenner 1996; Ciampi et al. 2005). Centric rings and pericentric inversions are observed as inter-arm intrachanges while paracentric inversions and interstitial deletions are resulted by intra-arm interchanges (Hlatky et al. 1992). As deletions are generally thought to be harmful to the organism, one should bear the customary rule in mind: ‘*the larger the deletion, the greater the harm*’, notwithstanding, larger chromosomal deletions are usually lethal, even when the heterozygous element bears a normal chromosome. Small deletions are often viable when they are heterozygous with a structurally normal homolog, because the normal homolog supplies gene products that are necessary for cell survival. In any case, even small deletions if they are found homozygous, can be lethal (Edwards et al. 1997; Okano et al. 1999).

When two genetically equal regions are detected within chromosomes, they are known as ‘*duplications*’ (Mizuki et al. 2000). A duplication in which duplicated segment is in the same orientation immediately adjacent to the normal region is called a tandem duplication. An example is the *Bar* duplication in *Drosophila*, which is a tandem duplication of bands 16A1 through 16A7 in the X chromosome. Compared to duplications, deletions are however much more harmful, although, in such cases, the size of comparable duplications should definitely be considered. Large-scale chromosomal rearrangements generally represent the primary genetic lesion in a variety of situations important to human health. Chromosomal-scale events are frequently involved in carcinogenesis (Fearon & Vogelstein 1990) and represent a significant component of the mutational spectrum in loci associated with heritable diseases (Mohrenweiser 1994). Particularly, deletion and translocation mutations have been shown to play a significant role in the genesis of many cancers. It has been shown that tumours are often related with chromosomal rearrangements; translocations, inversions, and large deletions (Gisselsson et al. 2000; Grosovsky et al. 1996; Jostes 1996), when they were investigated cytogenetically. Further, these rearrangements are also seen as mutations in genetic diseases (Edelmann et al. 2001; Hu et al. 1991). Usually these are small percentage of possible mutations; however, for some genes, such as in Duchenne and Becker muscular dystrophy, large deletions can comprise a major percentage of mutations (Den Dunnen et al. 1989). In between, large-scale deletions below the limits of cytogenetic resolution have been

identified by molecular analysis at loci such as dystrophin (Den Dunnen et al. 1989), α -globin (Nicholls et al. 1987) and steroid sulfatase (Yen et al. 1990).

2.4 Mutagenesis Analysis

In order to have a clear picture of the frequency and nature of the mutations caused by exposure to a particular genotoxic agent, genes are being sought that are suitable as markers for induction of mutation (Albertini 2001). Ideally, such a marker gene should allow the identification of a mutant cell among a large number of cells with no mutation in the marker gene. Mutant cells might be identified visually for example by colour or by selective growth of the cells carrying the mutation. Furthermore, the marker gene should be sensitive to the many different types of mutations that might be generated by the genotoxic agent under investigation (Frankenberg-Schwager et al. 2002). Thus the types of mutation in the marker gene that cause a phenotype should include intragenic mutations such as base-pair changes, small deletions, insertions frame shift mutations and chromosomal mutations such as large deletions, translocations, gene conversions, mitotic recombination, chromosome losses etc (Giver et al. 1995; Grosovsky et al. 1996).

Following are two main mutation induction gene markers together with other markers that are being used in present day mutation analyses. Out of all these markers, HPRT gene locus has been used frequently in radiation-induced mutation evaluations and clinical studies.

2.4.1 Hypoxanthine-Guanine Phosphoribosyl Transferase (HGPRT or HPRT)

Hypoxanthine-guanine phosphoribosyl transferase (HGPRT or HPRT) is a purine salvage enzyme that catalyses the conversion of hypoxanthine and guanine into inosine mono phosphate (IMP) and guanosine mono phosphate (GMP), respectively (Cameron et al. 1993). In humans, HPRT deficiency is related to two clinical disorders, i.e. Lesch-Nyhan (LN) syndrome caused by a complete deficiency of HPRT (Lesch & Nyhan 1964; Nyhan 2005), and a milder disorder, known as the Kelly-Seegmiller syndrome, characterized by severe gout attacks and a superfluity of uric acid, or nephrolithiasis (Seegmiller et al. 1967). The former disorder is related to hyperuricemia, mental retardation, choreoathetosis, and compulsive self-mutilation (Jolly 1986; Yang et al. 1988). According to literature, *missense mutations* have been found in HPRT mutant clones which were derived from irradiated cell cultures (Brown et al. 1986; da Cruz & Glickman 1997).

The human hypoxanthine-guanine phosphoribosyl transferase gene is found within the X-chromosome (Xq26-27) (Jinnah et al. 2000) and is expressed in a constitutive manner. The gene is located within a 45-kilobase (kbp) region on the X-chromosome in humans and rodents (Kim et al. 1986; Melton et al. 1984; Morris & Thacker 1993). This gene is composed of nine exons and eight introns and is transcribed into 1.6 kb of mRNA, which encodes a protein of 218 amino acids (Jolly et al. 1983; Patel et al. 1986). This coding sequence is distributed among 9 exons ranging from 18 (exon 5) to 184 (exon 3) base pairs. Introns range from 170 (intron 7) to 13075 (intron 1) base pairs (Giver et al. 1993; Jolly 1986). Furthermore, the HPRT gene belongs to a class of housekeeping genes which includes DHFR, adenosine deaminase, and phosphoglycerate kinase, all of which have a similar organization of promoter elements (Cohen et al. 2002). The entire gene with all intronic sequences has already been cloned and sequenced (Edwards et al. 1990).

HPRT is a non-essential enzyme for cells in tissue culture. The base analogue, 6-thioguanine, is also a substrate for the enzyme, and can be converted into its corresponding mono-phosphate, which is actually toxic to cells. A mutation that inactivates the gene causing the loss of gene product makes the cell resistant to 6-thioguanine. Cells lacking the HPRT gene function are, therefore, able to grow in medium containing 6-thioguanine, whereas normal cells die. This selection procedure can in practice be applied to both male and female cells, because, in fact, both carry only a single active copy of the HPRT gene. Following exposure to a genotoxic agent, the cells need time to convert the DNA damage into a mutation, and subsequently allow the mutant to express its phenotype. For cells in culture, the time required for the full expression of HPRT mutations is seven to eight days (Morris et al. 1993; Morris & Thacker 1993; Van Zeeland & Simons 1975). This particular period of time in mutation-induction experiments is called '*expression time*' and it is probably dependent on the turnover of the HPRT-mRNA and the HPRT protein. The latter appears to be generally stable, and several cell-divisions are needed to dilute it. How long the '*expression time*' takes, however, varies to some extent according to the dose and the type of mutagen used. By isolating cells from peripheral blood, it is also possible to analyse HPRT mutations in human T cells.

The HPRT-gene has shown itself capable of bearing many mutation types including point mutations, deletions, insertions, and translocations and a mechanism such as illegitimate V(D)J recombination-mediated deletion (Rainville et al. 1995; Recio et al. 1990). Rearrangements, such as inversions, translocations, duplications, and large deletions have occurred, although only a small percentage of HPRT somatic mutations or those of germinal

Lesch-Nyhan mutations, can be made responsible for events among normal individuals (Nicklas et al. 1989). However, these mutations can increase to up to 60% of all mutations in *in vitro* irradiated cells or in radiation-exposed individuals (Albertini et al. 1997; Albertini et al. 1990a). Furthermore, the aforementioned gene happens to be one of the few genes that are suitable as a marker for mutation induction in animal systems and humans (Aghamohammadi et al. 1992; Albertini et al. 2000). Alternatively, the HPRT gene is widely used as a model gene in both *in vivo* studies of somatic mutation, and *in vitro* studies of mutation (Albertini et al. 1990b; Dobrovolsky et al. 2005).

2.4.2 Adenosine Phosphoribosyl Transferase (APRT)

The human Adenosine phosphoribosyltransferase (APRT) gene is found on chromosome 16, and is 2.6 kbp in length (Amundson et al. 1992; Miles et al. 1990; Paeratakul & Taylor 1986). Particular enzyme is able to convert adenine into adenosine monophosphate (AMP). As has been the case with HPRT, an additional biosynthesis pathway is available for AMP, so that the APRT gene product is not essential to the cell. Cells that have a mutation in their APRT gene can be selected from wild-type cell populations by using their resistance to 8-azoadenine and 2,6 diaminopurine. Because APRT mutations are recessive; the frequency of 8-azadenine-resistant mutants is very low in populations of wild-type cells, and therefore, only cell-lines already carrying a mutation in one of the two APRT alleles are suitable for assay of mutation induction (Sankaranarayanan 1991).

The spontaneous mutation frequency in mouse T lymphocytes at the APRT gene locus is reported to be 10 times higher than that at the HPRT gene locus. The length of the restriction-fragment in polymorphism analysis of genomic DNA of APRT negative clones has revealed that almost eighty percent had actually lost the germinally intact allele, but that in many of these allele-loss mutants the mutated APRT allele seemed to have been duplicated (Fujimori et al. 1992).

Apart from the above two loci that have been described, Na⁺/K⁺-ATPase gene locus, Dib-1 gene locus, Thymidine kinase gene (TK) and Dihydrofolate Reductase gene (DHFR) have also been used for mutation induction studies (Schmidt 1999; Winton et al. 1990).

2.5 Scope of this thesis

Although a number of investigations was reported on the molecular characterisation of radiation-induced mutations, little is still known about mutagenesis and the related molecular mechanisms of the formation of genomic rearrangements and deletions after cells' exposure to ionizing radiation. The hypoxanthine guanine phosphoribosyltransferase (HPRT) locus has been used in many of these studies because mutants in this X-linked, hemizygous, non-essential gene can easily be isolated in the presence of the purine analogue 6-thioguanine (6-TG).

A variety of methodologies have been used. They include: measurements of targeted enzyme activities, Southern hybridisations following restriction digestions, PCR studies using sequence tagged sites (STSs) for the Xq26 chromosomal region containing the HPRT locus, multiplex PCR based on only 3 HPRT exons, multiplex PCR based on all 9 HPRT exons, RT-PCR based on HPRT-mRNA, and combinations of two or more of the above mentioned methods. The targeted sequential regions of most of these analyses were either the HPRT gene or the coding sequences of the gene with 1 or less than 2 Mbp of adjacent sequences at either side of the gene. Importantly, the cell lines and cell cycle phases in which the cells were found during irradiations, play a crucial role in mutation spectra. Most of the studies were based on rodent cells and human tumour cells. Only a few studies were, however, carried out on human primary fibroblasts. Nevertheless, experimental procedures on primary fibroblasts were known to have encountered with difficulties due to the fact that cells reach their replicative senescence after a few dozen of cell divisions.

The present study was focused on the generation and molecular characterisation of X-radiation-induced HPRT deficient mutant clones in two different human cell-lines using hybridisation assay, as well as multiplex-PCR of HPRT exons, RT-PCR of HPRT-cDNA, 3-Dye-FISH and DNA sequencing analysis.

The experimental work described was directed towards:

- The characterisation of HPRT mutant clones following acute dose X-irradiation of a malignant human cell-line.
- The analysis of the effect of pharmaceutical inhibition of non-homologous end-joining on the frequency and the spectrum of X-ray-induced HPRT mutations.
- The characterisation of mutation patterns in telomerase-immortalised normal human primary fibroblasts following acute X-ray exposure.

- The characterisation of HPRT-mutant clones in telomerase-immortalised human primary fibroblasts following fractionated X-irradiation.

3 Materials and Methods

3.1 Primary Cell Culture

3.1.1 Human Bladder Carcinoma Cell Line - MGH-U1

This male human malignant cell line is also known as EJ, HM, RN, and RB (Lin et al. 1985) in previous reports. Particular cell line is gifted by Dr. S. Powell, Boston, MA, USA. Cells were derived from a human bladder carcinoma and have epithelial characteristics. These cells have been used for previous studies in our group (Lobrich et al. 2000; Rothkamm & Lobrich 1999) and also in Leonhardt et al. (2000) and the advantages of the cell line are rapid cell growth and easy handling in cell culture. Cytogenetically, the cells are hypertriploid to hypertetraploid (Kato et al. 1978; Young et al. 1985). Cells were grown to confluence as monolayers in Eagle's minimal essential medium (MEM) (Biochrom, Germany) containing 2 mM glutamine and supplemented with 10% foetal calf serum (FCS), 1% non essential amino acids (NEAA), streptomycin 0.1 mg/ml and penicillin 100 U/ml, at 37°C in 5% CO₂/95% air. Confluent cultures at a density of about 5×10^5 cells per cm² were used in all experiments. For mutation induction experiments, MEM culture medium with the above supplements was mixed with 2-amino-6-mercaptopurine /6-thioguanine (6-TG) to a concentration of 10 µg/ml before plating.

3.1.2 Immortalised Human Primary Fibroblasts Cell Line - 82-6 hTERT

Normally, human fibroblasts have definite cell divisions in cell culture but can be immortalized by transfection with a vector that carries the gene for the human telomerase reverse transcriptase (hTERT) catalytic subunit under the control of a constitutive promoter (Bodnar et al. 1998; Pirzio et al. 2004). Unlike normal somatic cells, most immortalized cell lines and tumour tissues process active telomerase, a ribonucleoprotein that adds enzymatically to the repeated TTAGGG sequences at chromosomal ends. Therefore, immortalised cells have an indefinite life span, but they are not tumorigenic, and they retain other characteristics of non-transformed fibroblasts, including normal karyotypes, cell cycle check point responses and growth requirements (Fernandez-Capetillo et al. 2002; Morales et al. 1999; Roques et al. 2001).

The immortalised human primary fibroblasts used in this study are a generous gift from Prof. Dr. R. Schiestl, UCLA School of Medicine and Public Health, Los Angeles, USA. For all the experiments, 82-6 hTERT cells were grown to confluence in culture flasks in

MEM supplemented with 20% foetal calf serum (FCS), 1% non-essential amino acids (NEAA), streptomycin 0.1 mg/ml and penicillin 100 U/ml, at 37°C in 5% CO₂ /95% air. Cytogenetic analyses revealed that cells are male and remain diploid (unpublished data, Löbrich et.al). To select the HPRT negative mutant clones, the same culture medium was used after adding 6-TG to a concentration of 10-20 µg/ml. At the confluent stage, the cell density of this cell line was about 7×10^4 cell per cm². The cells have shown relatively low 5-10% plating efficiencies.

In an attempt to generate a sub cell line with enhanced plating efficiency (PE), a separate selection experiment was carried out. In this selection experiment, cells showing 5% of cloning efficiency (original 82-6 hTERT cells) were seeded to obtain the surviving cells. After trypsination cells were replated. This procedure was repeated two more times. The selected cells then achieved plating efficiencies of at least 55%. The last two mutation induction experiments were based on this latter sub cell line.

3.2 Cell Irradiation

For all the radiation-induced experiments in this study, two different X-ray tubes were used. The X-ray tube used for the early experiments (with MGH-U1 cell line) was of type PW2184/00 (Philips), that was driven at 95 kV /25 mA and its dose rate was 5-Gy /min. The experiments carried out later were based on an another tube, MCN165/796704 (Philips), that was operated at 90kV /19mA with a dose rate of 2-Gy /min. Tubes were equipped with a wolfram anode and a beryllium window. The chosen filter plate was of 2 mm thick aluminium. The dose rates and the homogeneity of irradiation field were rechecked regularly using chemical dosimetry (Fricke-Dosimetry). Cells from the two above named cell lines as confluent monolayers covered with culture medium either in 25-cm² or 75-cm² flasks were exposed to irradiations at RT depending on the purpose of the experiment (survival experiments or mutation induction experiments) and subsequently incubated at the culture conditions as described in 3.1.

3.2.1 Cell Irradiation for Cell Survival Colony Forming Assay

3.2.1.1 MGH-U1 Cells and Cell Survival Colony Assay

Cells were prepared as monolayers that were grown to confluence in 75-cm² culture flasks. Cells in culture flasks filled with growth medium were then irradiated. For comparison, control cells that were not irradiated but handled with the same conditions were also analysed.

Doses of radiation administered were 1, 2, 4, and 6-Gy. Following exposure to radiation, cells were rinsed twice with 5 ml of phosphate-buffered saline (PBS) at RT and dispersed with 2 ml trypsin-EDTA (0.25% trypsin solution containing 0.5 mM EDTA) and incubated for 5 min at 37°C (see also Figure 3.1). The loosened cells were homogeneously resuspended with cell culture medium pre-warmed to 37°C. Then the cell density of each suspension was determined in a Neubauer cell counting chamber to prepare a dilution series. 1×10^2 - 1×10^3 cells /100-mm dish were then seeded in triplicate for each dose. To each petri dish, 10 ml of culture medium was added and the dishes were subsequently incubated for 12-14 days until cell colonies became visible. The seeding numbers of cells for each dose point were chosen by estimating how many cell colonies would later be counted in each dish after staining them with crystal violet (1 mg/ml (Sigma) dissolved in 25% ethanol). An average cell colony consisted of nearly 1×10^2 cells as seen /observed through a low-power microscope.

To obtain information about the survival of cells following irradiation in the absence of NHEJ, a separate survival experiment was performed. Here, confluent cells were treated with wortmannin, which is an enzymatic inhibitor also to DNA-dependent protein kinase (see also the review of the literature). Stock solutions of wortmannin were dissolved in DMSO at 10 mM. Cells were pre-treated with wortmannin (Sigma) at a concentration of 20 μ M (Okayasu et al. 1998; Price & Youmell 1996) or DMSO and incubated for 2 h. After that they were exposed to acute doses of X-rays at 1-6-Gy in the presence of wortmannin or DMSO. 16 h after irradiation, the cells were washed three times by complete changes of medium to remove wortmannin or DMSO and fresh medium was added. Following trypsination, cell densities were calculated. For the colony-forming assay, the number of cells per dish was chosen to ensure that 50-100 colonies would survive a particular treatment. The cells were then plated out at 1×10^2 to 5×10^3 cells /100-mm dish in triplicate. In parallel, unirradiated control monolayers were treated with 0.1% DMSO (Mosmann 1983) or with wortmannin. All groups of dishes were incubated for 12 days before staining with crystal violet. Cell colonies were examined under a low-power microscope and scored if each dish contained more than 50 cell colonies. Cell survival following irradiation was normalized to unirradiated controls exposed to the same concentration of DMSO or wortmannin.

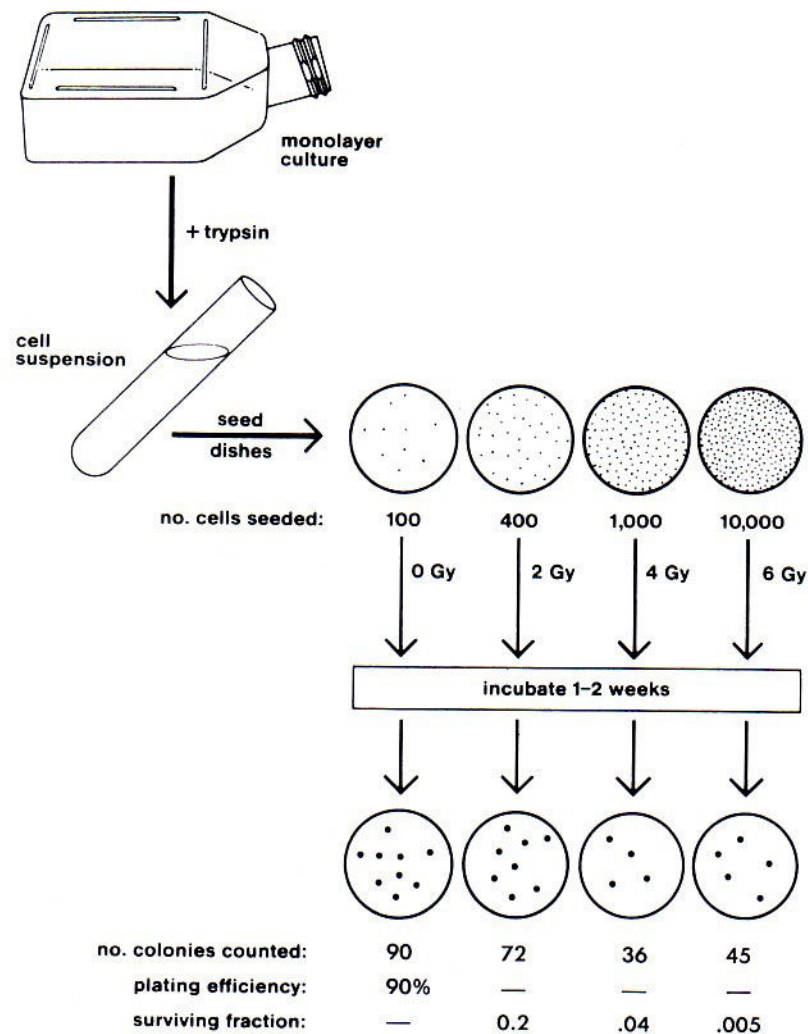


Figure 3.1. Representative diagram for cell survival colony forming assay: confluent cell monolayers were exposed to 0, 2, 4, and 6-Gy of X-rays and following trypsinisation, cells were detached. Then they were seeded as 100, 400, 1000 and 10000 cells with increasing of the administered dose of X-rays. After 1-2 weeks incubation, depending on the cell lines, the arising cell colonies were stained with crystal violet. Colonies were counted and plating efficiencies were calculated. Plating efficiencies of irradiated cells were corrected to that of unirradiated controls (From Hall, 2000).

3.2.1.2 Immortalised Human Fibroblasts and Cell Survival Colony Assay

Confluent cell monolayers of immortalised human fibroblasts were prepared as described for the malignant cells, MGH-U1. For this purpose, cells in early passages were grown starting from small numbers. Sufficient numbers of cells were then generated by subsequent splitting. In comparison to the bladder carcinoma MGH-U1 cells, cell growth of this immortalised cell line was relatively slow. Confluent cell monolayers were irradiated with single doses of 1, 2, 4, 6-Gy and subsequently plated out for cell survival at 1.5×10^2 - 5×10^4 cells /100-mm

plastic dish for each dose point in triplicate and the number of seeded cells was adapted to the dose points in a way that 50-100 colonies would survive a particular exposure to X-rays. After 16-18 days of incubation, dishes were stained with crystal violet. An average colony contained nearly 50 cells. Cell survival following exposure to X-rays was normalised to unexposed controls.

3.2.2 Acute Cell Irradiation for Mutation Induction

Confluent cell monolayers were exposed to an acute dose (single dose) irradiation of 2 and 6-Gy. Control cell cultures were treated under identical conditions without irradiation. Following irradiation, cells per dose were split into several flasks and incubated in previously described cell culture conditions. This step was mandatory to ensure the independent growth of the mutant clones (see section 3.3.3). Mutation expression times (Period needed for the decay of pre-existing HPRT products) were for 7-8 days (immortalised cells) and 10-11 days (malignant cells). These times are concordant with that of human fibroblasts (Morris et al. 1993) and previous data for MGH-U1 (Lobrich 1999). Following expression times, surviving cells that were grown independently were then seeded in 6-TG (10-20 µg/ml) containing culture medium (1 x 10⁶ cells per 100 mm-petri dish) to allow HPRT selection. Thioguanine resistant cell colonies became visible after 14-16 days (Lobrich 1999) and 21-28 days (Morris et al. 1993) for malignant cells and immortalised cells respectively. During this incubation period it was necessary to change the culture medium containing 6-TG at least once.

With the malignant cell line, three mutation induction experiments were carried out. The first experiment (Experiment I) only focused on one dose point (6-Gy), whereas the other two (Experiment II & III) were performed with an enzymatic inhibitor of DNA dependent protein kinase (see below). Similarly, three mutation induction experiments based on an acute dose were performed with the immortalised primary human fibroblasts (82-6 hTERT).

3.2.2.1 Acute Dose Cell Irradiation and Mutation Induction in Wortmannin -Treated Cells

To obtain information about the radiation-induced mutation in the absence of the NHEJ, confluent monolayers of MGH-U1 cells were pre-treated with 20 µM wortmannin and incubated for 2 h until they were then exposed to irradiations. Here, the doses used were 2-Gy with wortmannin and 6-Gy without wortmannin, with one control (0-Gy) that was treated with wortmannin (WM) and the other with DMSO. After exposure to X-rays, the cells were incubated for 16 h. Wortmannin treatment was carried out as before. After that, the cells were

washed three times with culture medium to remove the wortmannin. Then the cells were plated in flasks (25-cm²) to allow them to grow independently until they were introduced to selective culture medium. For selection with 6-TG, 5×10^5 - 1×10^6 cells per petri dish (100-mm) were seeded in thioguanine containing cell culture medium. Likewise, 40 petri dishes were prepared for mutation induction. The 6-TG concentration was as in 3.2.2. For the calculation of corresponding mutation induction frequencies, plating efficiency tests were carried out in parallel for all the dose points. To obtain sufficient numbers of HPRT mutant clones, this mutation induction experiment was repeated once.

3.2.3 Mutation Induction Following Dose Fractionation

Immortalised primary human fibroblasts grown to confluent monolayers were irradiated. By seeding small numbers of cells in culture flasks, cells were grown to confluence to minimize the spontaneously arising mutant colonies. The total doses chosen were 6-Gy and 18-Gy of X-rays with respective dose fractions of 0.2-Gy and 0.6-Gy twice a day for 15 days to a total number of 30 fractionated irradiations. Cells were allowed to recover for approximately 10 h before exposing to the next dose fraction. Control cells that were not exposed to irradiation were handled under identical conditions. After the last dose fraction, cell cultures were incubated for 7 days to allow phenotypic alterations to appear. To compare the mutation induction of fractionated irradiations with acute dose irradiation, a few monolayers were also grown to confluence and exposed to 2-Gy and 6-Gy (acute doses) and incubated until the cells were plated for thioguanine resistance. Control cells that were not exposed to irradiation were handled under identical conditions.

Two mutation induction experiments were performed using cells of two different plating efficiencies (~50% and ~10% see also 3.1.2) but that belonged to the same origin (82-6 h TERT). Confluent cells in 75-cm² flasks were irradiated as described above and incubated until the cells were seeded for mutation selection and corresponding plating efficiency tests. To recover sufficient numbers of surviving cells for each dose, the numbers of flasks or dishes required for each dose were established from survival data: 8 x 75-cm² for controls; 4 x 75-cm² for each acute doses (2 and 6-Gy); 8 x 75-cm² for 0.2-Gy x 30 and 8 x 75-cm² for 0.6-Gy x 30. After the final day of irradiation (15 day at last serial fractionated irradiation); flasks were kept in incubators leaving 7-8 days of expression time to allow phenotypic expression.

The expression times necessary for clearance of residual HPRT message and protein were 21 and 7 days for acute dose and fractionation respectively (see also 3.2.2). This

necessitated the passage of cells two or three times during the entire period of the experiments (from day 1 to day 15).

3.3 Mutation Selection

3.3.1 Mutation Selection Following Acute Dose Irradiation

The use of the purine analogue 6-TG, also known as an anti-cancer drug forms the basis for cell selection following irradiation. Cells without a mutation on the HPRT gene locus are poisoned by 6-TG, while mutant cells survive in the culture medium and form colonies. Those cells that are able to form colonies are assumed to be mutant cells resulting from either a spontaneous mutation or from an induced mutation caused by X-ray irradiation. Commercially available 6-TG in powder form (Sigma, Germany) was dissolved in distilled water in the presence of Na_2CO_3 (with a Na_2CO_3 to 6-TG ratio of 5:1) to a concentration of 1 mg/ml. These solutions were then filter-sterilized. Aliquots were frozen at -20°C for the following applications.

To select the cell populations resistant to 6-TG, cells both irradiated and unirradiated were first rinsed twice with a sufficient volume of PBS, trypsinised (Trypsin-EDTA) at 37°C for 5-10 min and diluted in culture medium that was pre-warmed to 37°C . After that the cell density was calculated and 5×10^5 - 1×10^6 cells were seeded in each 100-mm dish. Flasks normally contained sufficient cells for 5-10 platings.

For the mutation selection experiments, 6-12 ml of 6-TG stock solution (1 mg/ml) was added to 600 ml so that the final concentrations varied from 10-20 $\mu\text{g/ml}$ (60-120 μM) (Morris et al. 1993). 10 ml of culture medium containing 6-TG was pipetted in each petri dish. Plated dishes were subsequently incubated for either 14-16 days (MGH-U1 cells) or 21-28 days (immortalised human fibroblasts). In parallel, cells from each dose point were seeded in triplicate in dishes containing non-selective MEM medium for assessment of plating efficiency. These plating efficiency values were considered when scoring the corresponding mutation induction frequencies.

3.3.1.1 Isolation of Radiation-Induced 6-Thioguanine-resistant (6-TG^r) Mutant Sub Clones

Following the incubation period, one or two single colonies well separated from neighbouring colonies were picked from each petri dish containing 6-TG medium (i.e. from each culture) (Morris et al. 1993). By the time cells had grown enough to form colonies, they could be discerned by eye on the bottom of the dishes as cell clumps when observed carefully in

daylight. Well separated colonies were trypsinised with 30-50 μ l Trypsin-EDTA and carefully isolated under sterile conditions and were subsequently seeded /incubated in 6-well plates containing 3-4 ml of 6-TG containing medium /well to re-check the survival of the picked mutant clones.

Because of the relatively large variations in mutant frequency between replicates, it was necessary to determine the mutant frequency for each treated culture. Several mutant clones were selected from each untreated and from each treated culture in which the mutation frequency was considerably higher than the average for the untreated cultures in the same experiment. Each clone analysed was selected from a different expression culture, thus eliminating poliferation during the expression period as a source of duplicates. Nonetheless, any duplicate mutations from the same initial treated culture were later eliminated from the dataset.

3.3.1.2 Isolation of Spontaneous Mutant Clones

Cells, which had not been subjected to any mutagenic irradiation but were grown in parallel in 6-TG containing selective cell culture medium, also formed 6-TG^r cell colonies. Although this was a relatively rare event, one single colony per dish was picked using the same procedure as described in 3.3.1. The number of spontaneously arising HPRT mutant clones was smaller in immortalised cells than in MGH-U1 cells. To avoid off set losses, isolated mutant clones were first cultured in 6-thioguanine containing culture medium and then incubated in 6-TG-free culture medium. After picking cell colonies, dishes were stained with crystal violet and the number of colonies per total number of seeded cells was counted. Finally, respective mutation induction frequencies were scored relative to the plating efficiency values.

3.3.1.3 Expansion of HPRT-Deficient-Mutant Clones

After 5-7 days, cells recovered as healthy clones in 6-well plates were trypsinised and seeded in 25-cm² culture flasks containing 6-TG-free culture medium in order to allow cells to grow to sufficient numbers for cryopreservations and downstream analyses. The expansion of cells took at least 1-2 weeks, the majority of the induced mutant clones was observed to have slow growth. The morphological appearance of the cells under microscopic examination showed that there were no changes between wild type cells and each 6-TG^r mutant cell population. As it took relatively longer times for mutant clones until bulk numbers of cells were available, medium change was done several times during the incubation.

3.3.2 Mutation Selection Following Dose Fractionation

After the expression times, the cells in flasks were trypsinized, resuspended in culture medium, enumerated for both mutagenesis assays and plating efficiency tests. After determining the cell densities of each flask, $0.5\text{--}0.6 \times 10^6$ of cells were seeded in a 100-mm petri dish with 6-TG containing culture medium (MEM supplemented with 20% FCS and the other supplements as given also in 3.1.2). The cell content of a 75-cm² flask was sufficient for 10 platings. In parallel, two sets of triplicates /each dose were prepared in 100-mm dishes without 6-TG. Colonies were stained after 12-14 days to determine the plating efficiencies. The seeding numbers of cells for plating efficiency tests were as follows: $5 \times 10^2\text{--}8 \times 10^2$ for control; $1 \times 10^3\text{--}2 \times 10^3$ for 2-Gy; $1 \times 10^4\text{--}2 \times 10^4$ for 6-Gy; $8 \times 10^2\text{--}2.5 \times 10^2$ for 0.2-Gy; $1.5 \times 10^2\text{--}5 \times 10^3$ for 0.6-Gy. Total numbers of dishes prepared were as follows: 80 for control; 40 for each of the acute doses; 80 x for each of dose fractions.

Following an incubation period of 21-28 days, 6-TG^r colonies from the various radiation doses were isolated from the 100-mm mutagenesis plates prior to staining and individual colonies were cultured to confluence in 25-cm² flasks containing MEM with 20% FCS and 6-TG. The colony chosen from a culture here was picked randomly, irrespective of size. Then the total numbers of colonies surviving 6-TG and those growing in non-selective medium were counted to give an estimate of the 6-TG^r mutant frequency. The isolated mutant clones (sublines) were subsequently expanded in 25-cm² flasks /100-mm petri dishes in non-selective medium until sufficient numbers were available to freeze a stock in liquid nitrogen and for molecular analyses. To avoid offset losses, in a few cases, more than one colony was picked from the same petri dish and their mutation characteristics were compared in molecular analyses before grouping them as independent mutant clones.

3.3.3 Mutation Frequency and Independent Mutation Estimate

After isolating single HPRT mutant clones as described in 3.3.1 and 3.3.2, plastic dishes were stained with crystal violet and the colonies were counted (also considering the colonies that were picked before). Mutation frequencies were calculated from the number of colonies surviving selection and the total number of cells assayed, taking into account plating efficiency and cell survival after treatment, since mutation frequency is defined as the number of mutant clones detected divided by the number of cells seeded, corrected for plating efficiency (Dahle & Kvam 2003).

One mutant cell colony per culture was picked to ensure independence, but there were several cases where more than one mutant cell colony per culture was isolated to account for offset losses due to senescence. In such cases a mutant clone was considered as independently derived if it was found to have a molecular change in HPRT that was clearly different from those in mutants derived from the same culture.

All hTERT mutant clones were named after an arbitrary nomenclature starting from irradiated (0.6, 2 and 6-Gy) doses and unirradiated controls (K), number of the flask in which cell monolayers initially contained (i.e 1, 2, 3 etc.), the naming of the mutants from which petri dish they were isolated such as from a, b, c etc (cell contents in the flasks were seeded in several petri dishes for 6-TG selections) and if several mutant clones were isolated from the same dish, their designation was suffixed by roman numerals (i.e I, II, III, IV and V).

3.4 Molecular Characterisation of HPRT Mutant Clones

3.4.1 Genomic DNA embedded in Agarose Plugs and Cell Lyses

Cells of each mutant sub clone grown to confluent monolayers were washed twice with a sufficient volume of phosphate buffer saline (PBS) and detached with EDTA-trypsin for 10 min at 37°C. Detached cells were resuspended in MEM culture medium pre-warmed to 37°C in a water bath. Subsequently, cell densities were determined in a Neubauer cell counting chamber. Cell suspensions were spun down by centrifugation (Eppendorf) at 4°C and at 300 x g for 9 min. The supernatant was removed. Then one volume of PBS was added to each cell pellet and mixed well by repeated pipetting. Following addition of an equal volume of 1.4% low melting agarose (Type VII, Sigma) (final concentration of the plugs 0.7% dissolved), the mixture was cast into pre-cooled plug molds (Bio-rad) and kept at 4°C to allow the plugs to solidify. Depending on the used molds (40 µl, 80 µl), the cell concentrations of agarose plugs were 1.25×10^7 or 0.625×10^7 cells respectively. Plugs were then equilibrated in lysis solution at 4°C for 1 h to inhibit cellular nucleases and repair enzymes. Cell lysis was performed for 2-3 days at 50°C. The lysis solution contained 1 mg/ml Pronase E (Merck) and 1% (w/v) sodium-lauroyl-sarcosin (Merck) in 0.5 M Na₂EDTA (pH 8). After lysis, agarose plugs could then be stored at 4°C in 0.5 M Na₂ EDTA for longer periods without any sign of DNA degradation.

3.4.1.1 Restriction Digestion

To obtain more information on fragment distribution of the 6-TG^r mutant sub clones at the mega base pair (Mbp) level, genomic DNA embedded gel plugs were digested using the commercially available restriction enzyme *NotI* (MBI Fermentas), which has an eight-base recognition sequence that includes CpG dinucleotides that occur very infrequently in mammalian DNA (Kinashi et al. 1995). Plugs were first washed 7 times, for at least 30 min each in 3-4 ml TE buffer (10 mM Tris-HCl; 1 mM Na₂EDTA (pH 8)) at RT and then equilibrated in 200-250 µl (depending on the sizes of plugs) of restriction buffer provided by the manufacturer (MBI Fermentas) for 1 h. The subsequent digestion was performed at 37°C (at least 16 h, overnight) in an Eppendorf tube with the addition of 20-25 U of the *NotI* enzyme. The digestion was stopped by adding 35-40 µl of 0.5 M Na₂EDTA (pH 8) and incubating the reaction for 30 min at 4°C.

Preliminary experiments with different cell- and enzyme-concentrations showed that the conditions described were optimal for achieving complete DNA digestion since neither longer incubation times nor higher enzyme concentrations had any further effect on the DNA size distribution. The size of the DNA fragment cleaved by *NotI* for both human cell lines (MGH-U1 and 82-6 hTERT cells) was 2 Mbp. To maintain equal conditions for every mutant sample, a cocktail for several plugs was pre-prepared and aliquoted in each tube.

3.4.1.2 Pulse Field Gel Electrophoresis (PFGE)

Digested mutant genomic DNA was separated by pulse field gel electrophoresis which is the conventional method frequently used for the separation of large DNA molecules by periodic alteration of non-uniform electric fields. Later, Chu, Vollrath and Davis (Chu 1989) introduced an innovative modification of this method by applying the concept of contour-clamped homogeneous electric fields (CHEF). By employing a fixed reorientation angle of 120° and different pulse times, DNA molecules up to 10 Mbp in size can be separated by this modified method.

For examination of alteration in genomic DNA of isolated HPRT mutant clones, the above improved CHEF-PFGE was used in this study. *NotI* digested genomic DNA of independently grown HPRT mutant clones, wild type clones and standard DNA size markers such as *Saccharomyces cerevisiae* (Bio-rad), *Schizosaccharomyces pombe* (Bio-rad), and *Hansenula wingei* (Bio-rad) were loaded onto a 0.8% agarose (Pulsed-Field Certified-Agarose, Bio-rad) gel and subsequently the wells containing agarose plugs were well sealed

with low melting agarose (Type III, Sigma). Both agaroses were prepared in 0.5 x TBE buffer. The gel was submerged for at least 30 min in running 0.5 x TBE buffer (44.5 mM Tris, 44.5 mM Boric acid, 1 mM Na₂ EDTA (pH 8)). After equilibration, the electrophoresis was started with the CHEF-DR III-apparatus (Bio-rad, Hercules, CA) under a hexagonal array of 24 electrodes, which produces a field with reorientation angles of 120°C. Digested genomic DNA loaded on gels were run at 14°C in 0.5 x TBE with linearly increasing pulse times from 500 to 3000 s over 115 h at a field strength of 1.5 V/cm. The running buffer was recirculated through a pump-operated unit to keep the temperature constant and to avoid ion build-up at the electrodes.

Following electrophoretic separation, gels were stained overnight by submerging them in a staining bath (44.5 mM Tris, 44.5 mM Boric acid, 1 mM Na₂ EDTA (pH 8), ethidium bromide 10 µg/µl) and then destained for at least 1 h in the same buffer without ethidium bromide. The stained gels were then excited with a UV transilluminator resulting in a fluorescence emission with a maximum at 302 nm. The fluorescence signals were detected by a charge-coupled device camera system. The information from the gel picture was then digitalised and transferred to a personal computer.

3.4.1.3 DNA Transfer /Alkaline Vacuum Blotting

After documentation the gel was used for Southern Blotting. For DNA transfer onto a positively charged nylon membrane, vacu-blotters (Biometra) were used. The porous screen of the blotter was soaked in deionised water and replaced on the buffer collecting container of the apparatus. A 3 to 4-mm blotting sheet of at least 900-cm² was placed centrally on the top of the porous screen without air bubbles. 20.5 cm x 14 cm of Hybond-N nylon membrane (Hybond N⁺, Amersham Biosciences, Inc) was cut and moistened using deionised water and placed centrally on the blotting sheet. An appropriate rubber template was selected to cover the entire area of the vacu-blotter with the cross-sectional area of the gel carefully cut out to allow a 0.5-1.0 cm overlap at the gel periphery. This template was immersed in deionised water and placed on the top of the membrane, overlapping the periphery of the nylon membrane. The agarose gel was then placed on it ensuring that the gel-wells were on top of the template and the rest of the gel laid on the nylon membrane. The entire stack was then fixed with the plastic template of the apparatus.

The vacu-blotter was then connected to the vacuum pump and the pressure stabilised to 50 mbar. 100-200 ml of 0.25 N HCl were added to the middle of the gel. This partly depurinated the DNA of the loaded mutant clones. After 15-20 min all the excess HCl was

removed. After that the gel surface was washed with a sufficient volume of 0.5 N NaOH to neutralize the membrane, and the gel surface was again covered with 100-200 ml of 0.5 N NaOH for alkaline transfer and blotted for additional 90 min. During this time it was ensured that the membrane stayed covered with liquid. After blotting, the NaOH-solution was removed and the apparatus was then dismantled and the nylon membrane was placed in 400 ml of 2 x SSC for 10 min. The upper DNA-containing side was labelled on the nylon membrane. The nylon membrane was then wrapped moist in polythene and kept at 4°C until used for Southern hybridisations. For long-term storage, the membrane in the polythene was wrapped in a foil envelope.

3.4.1.4 Probes and Radioactive ^{32}P -Labelling

The DNA probe D21S4 (pPw233F) (Watkins et al. 1985) hybridizes to a 2 Mbp *NotI* restriction fragment on the proximal part of the long arm of human chromosome 21 located in a Giemsa dark staining region (Gardiner et al. 1990; Ichikawa et al. 1992; Lobrich et al. 2000). This DNA probe is 1.5 kbp long and was cloned into the *EcoRI* site of pBR328. The vector was propagated in *Escherichia Coli* strain LE392 (Rothkamm & Lobrich 1999). The other probe used for Southern analyses was DXS1327 (ATCC No.95474) that detects a 2 Mbp *NotI* fragment in MGH-U1 cells and also a 2 Mbp *NotI* restriction fragment in hTERT-immortalised fibroblasts (82-6 hTERT cells). This probe was cloned in a vector pUC19 and propagated in *Escherichia coli* JM101 strain. The size of the insert was 850 bp and this was cleaved out with *EcoRI* /*HindIII* (Rothkamm & Lobrich 1999). This restriction fragment is located in a Giemsa light-staining region at Xq26, which also contains the hypoxanthine guanine phosphoribosyl transferase (HPRT) locus 250 kbp centromeric of the hybridisation site (Lippert et al. 1995; Lobrich et al. 1996; Rothkamm & Lobrich 1999).

Radioactive labelling was carried out using a commercially available labelling kit (Rediprime II, Amersham Biosciences). The DNA to be labelled was diluted to a concentration of 2.5 to 25 ng in 45 µl of TE buffer (10 mM Tris-HCl pH 8.0, 1 mM EDTA). Then the DNA was denatured in a screw-top tube by heating to 95-100°C for 5 min in a boiling water bath. After snap-cooling the DNA by placing it on ice for 5 min, it was spun down briefly by a micro-centrifuge to bring tube-content to the bottom. Then the denatured DNA was added to the reaction tube containing coloured rediprime II. To label the DNA, 5 µl of Redivue TM [^{32}P] dCTP (> 222 TBq/mmol, Amersham Biosciences, Inc.) were added and mixed by pipetting up and down about 12 times. The DNA solution changed colour to purple when the blue pellet provided in the reaction tube has been completely dissolved and mixed

with the added Redivue. Following incubation at 37°C for 3 hours, unincorporated nucleotides were removed by spin column chromatography. Mobi spin S-200 from Mobi Tec, Göttingen were used. The tubes were first vortexed briefly before use to resuspend the resin. Then the cap was loosened and the bottom of the tube was snapped off. The spin-column was placed in an Eppendorf tube. The column was spun at 3700 rpm (1000 x g) for 1 min. Then the spin column was placed in a fresh Eppendorf and the labelled solution was added. These procedures were performed behind a protective shield (Amersham). The tube was spun for 2 min at 3700 rpm. The flow-through contained radiolabelled probe which was kept in a lead protector at 4°C until use. The specific activity of the labelled probe varied between 2 and 4 x 10⁹ dpm/μg.

3.4.1.5 Southern Hybridisation

To examine the alterations of mutant clones, genomic DNA transferred onto nylon membranes were serially Southern hybridised. Pre-hybridisation buffer mix (5 x SSPE (20 x SSPE containing 3 M NaCl, 0.2 M NaH₂PO₄; 20 mM Na₂EDTA (pH 7.4)), 5 x Denhardt's (50 x Denhardt's containing 10 g/l Ficoll 400, 10 g/l Polyvinylpyrrolidone, 10 g/l BSA, "Fraction V"), 3% (w/v) SDS) was poured into glass-cylinders pre-warmed to 65°C. The membranes were trimmed using a sterile blade and subsequently soaked in 200 ml of 2 x SSC for 5 min. Then they were inserted into the cylinders in a way that transferred DNA of the membrane faced inside. To block unspecific binding sites on the membrane, 200 μg/ml of salmon sperm DNA was boiled in a screw-top tube for 5 min in a water bath and placed on ice prior to use. After 30 min of pre-hybridisation denatured salmon sperm DNA was added to the pre-hybridisation solution. This pre-hybridisation was continued for 4-5 h. Before use, the radioactive probe was boiled in a mini-water bath for 5 min and cooled down for 5 min on ice. The labelled probe was then added to the pre-hybridisation mix. They were then left to hybridise for nearly 12-16 h at 65°C.

After hybridisation, the membranes were washed in three steps at 65°C with 3 different wash solutions containing SSPE and 0.1% SDS. The first wash consisting of 2 x SSPE /0.1% SDS was carried out 3 times, beginning with 5 min for the first wash followed by 30 min for the next two washes. Here, the very first wash was discarded in a radio-safe sink (i.e designated for radioactive waste) while the others were collected in another collection gallon. The second solution contained 1 x SSPE /0.1% SDS and only 1 wash was carried out with the solution for 25 min. The third solution contained 1 mM EDTA /40 mM NaH₂PO₄ x H₂O pH 7.2 /1% SDS and 2 washes for 30 min each were performed.

The radioactivity of the membrane was measured using a Geiger counter several times until nearly background was reached and then it was blotted on tissue to remove excess fluid and placed within a thin plastic bag with three edges heat-sealed. Through the remaining open end, excess fluid was removed. The open end was sealed enclosing the membrane in an airtight close fitting plastic envelope. For radioactive exposition, hybridised membranes in envelopes were kept in sealed cassettes facing to imaging screens. After 3-4 days, imaging screens were read by a phospho-imaging system (Cyclone, Canberra Packard) with the assistance of a software programme.

Since two serial hybridisations were necessary for the analysis of the HPRT mutant clones, after each hybridisation, membranes were stripped using 0.4 M NaOH at 45°C followed by a wash for 30 min with a neutralisation solution (5 ml 0.1 M x SSC, 5 ml 0.1% SDS, 20 ml 0.2 M Tris-HCl pH 7.5) at RT. The first hybridisation for all membranes was carried out with the HPRT specific probe DXS1327, and the subsequent one was with the reference probe D21S4.

The Southern blot pictures were evaluated using a software programme (Opti-quantem). With the software programme used, the length from the well to the radioactive signal could be measured. These migration lengths were varied from mutant sample to sample. To classify the HPRT mutations and to account for running artefacts in a lane, the migration distance of the corresponding reference probe was compared to the migration distance of the HPRT-probe. In addition, the two different migration lengths of each mutant clone were compared with that of a wild type sample. A difference of 2-3 mm and more classified a clone as altered.

3.4.2 Exon-Deletion Screening at HPRT Gene Locus

3.4.2.1 Genomic DNA Extraction

Genomic DNA from mutant sub clones was extracted using a commercially available molecular biological kit (QIAamp DNA Blood Mini Kit, Hilden Germany). Cell suspensions of 3×10^6 cells were first spun down (Eppendorf) at 300 x g for 5 min to obtain cell pellets and then carefully washed with 200 µl PBS at RT to remove residual cell culture medium. After removing the supernatants, 20 µl of QIAGEN protease and 200 µl buffer AL (contains guanidine hydrochloride) were added to the tube. Following vortexing for 15s the cell suspension was incubated at 56°C for 10 min for cell lysis. DNA was then precipitated with 200 µl of 96-100% ethanol. The total volume of 620 µl was pipetted into the provided

columns and subsequently spun down at 8000 rpm (Biofuge Pico Heraeus) for 1 min. The flow-through was discarded and set the column on a new cap (provided), 500 µl buffer AW1 (contains guanidine hydrochloride) were added and centrifuged the column again at 8000 rpm for 1 min. The filtrate was discarded, 500 µl buffer AW2 was added, tubes were centrifuged at 14000 rpm for 3 min. AW1 and AW2 buffers significantly improve the purity of the eluted DNA. Wash conditions ensure complete removal of any residual contaminants without affecting DNA binding. The genomic DNA bound to the column material was retrieved in 200 µl elution buffer AE (10 mM Tris-HCl, 0.5 mM EDTA; pH 9.0) by centrifugation at 8000 rpm for 1 min. Eluted genomic DNA extractions were kept at -20°C for downstream PCR analyses.

DNA concentrations of genomic DNA isolated for PCR analyses were first measured photometrically to estimate the amount of template to be used for each PCR reaction. Eluted genomic DNA was diluted to 1:100 with ddH₂O and, using a pre-cleaned crystal cuvette, measurements were taken as optical absorbance values at wavelengths of 260 and 280 nm with a spectral photometer (Amersham Pharmacia Biotech). DNA concentrations were determined as given below. To confirm the purity of the elutant, it was necessary to check whether the ratio between the absorbance values at $\lambda_{260} / \lambda_{280}$ was nearly 1.8 (QIAGEN, Instruction manual). DNA concentration = $\lambda_{260} * \text{Factor} * 100$, the factor for DNA concentration (µg/ml) is 50.

3.4.2.2 Multiplex Polymerase Chain Reaction (M-PCR)

Multiplex polymerase chain reaction (M-PCR) is a modification of the conventional standard PCR (Uniplex-PCR). In M-PCR, more than one target sequence can be amplified by including more than one pair of primers in a reaction. M-PCR has the potential to produce considerable savings of time and effort within the laboratory without compromising test utility. This has been successfully applied in many areas of nucleic acid diagnostics, including gene detection analysis (Chamberlain & Chamberlain 1994), mutation and polymorphism analysis (Shuber et al. 1993), quantitative analysis (Cirigliano et al. 2001), and RNA detection (Jin et al. 1996). Nevertheless, only a handful of publications discuss M-PCR (Chamberlain & Chamberlain 1994; Edwards & Gibbs 1994) so far, though a number of review and research articles have provided detailed descriptions of the key parameters that may influence the performance of standard single PCR (Cha & Thilly 1993; Robertson & Walsh-Weller 1998). However, the overall success of specific amplification in M-PCR reactions depend on the rate

Table 3.1. Primers (including the primers for exon 1) used for M-PCR to amplify targeted sequences at the human HPRT gene locus: From left to right: the exon number, oligonucleotide sequence, concentration of primer, sizes of PCR products and the positions of the primers according to a gene bank sequence of HPRT gene (M26434). In terms of the relevant exon-number, they have been classified considering the polarisation ends either 3' (reverse) or 5' (forward) directing forward and reverse primer oligonucleotides. Human exon have been abbreviated as *hex* here.

Primer Sequence		Concentration μM	PCR product Size (bp)	Position (M26434)
<u>Genomic DNA, M-PCR</u>				
hex 1.5	5'-TGGGACGTCTGGTCCAAGGATTCA-3'	0.2	636	1225-1248
hex 1.3	5'-TGACGTAAAGCCGAACCGGGAAA-5'	0.2		1861-1837
hex 2.5	5'-TGGGATTACACGTGTGAACCAACC-3'	0.4	572	14577-14601
hex 2.3	5'-GACTCTGGCTAGAGTTCCTTCTTC-3'	0.4		15149-15126
hex 3.5	5'-CCTTATGAAACATGAGGGCAAAGG-3'	0.32	1059	16252-16275
hex 3.3	5'-TGTGACACAGGCAGACTGTGGATC-3'	0.32		17310-17287
hex 4.5	5'-TAGCTAGCTAACTTCTCAAATCTTCTAG-3'	0.5	334	27766-27793
hex 4.3	5'-ATTAACCTAGACTGCTTCCAAGGG-3'	0.5		28099-28076
hex 5.5	5'-GCCAAGTGAGGGTTTATGGTGAGA-3'	0.4	766	31073-31097
hex 5.3	5'-GAGAGGTAGGAAGTATACCATTCC-3'	0.4		31839-31816
hex 6.5	5'-GACAGTATTGCAGTTATACATGGGG-3'	0.2	441	34851-34875
hex 6.3	5'-CCAAAATCCTCTGCCATG CTATTC-3'	0.2		35291-35268
hex 7.5	5'-GATCGCTAGAGCCCAAGAAGTCAAG-3'	0.36	1533	38668-38692
hex 8.3	5'-TATGAGGTGCTGGAAGGAGAAAAC-3'	0.36		40200-40176
hex 9.5	5'-GAGGCAGAAGTCCCATGGATG TGT-3'	0.32	1278	40444-40468
hex 9.3	5'-CCGCCCCAAGGGAACTGATAGTC-3'	0.32		41721-41699

at which primers anneal to their target and the rate at which annealed primers are extended along the selected sequence during the early and late cycles of the amplification.

To elucidate consequences of radiation in the mutants, genomic DNA from HPRT-deficient mutant clones was isolated (as described in 3.4.21) to screen for exon-level deletions (334 bp - 1533 bp) at the HPRT gene locus. Multiplex PCR was used to detect the presence and absence of specific exons (exons 2-9) of the HPRT locus. M-PCR reactions were optimised with two different Master Mixes: HotStarTaq Master Mix and QIAGEN Multiplex PCR Master Mix both from QIAGEN, Hilden, Germany. The PCR products were synthesized in two groups depending on product size. Short fragments amplifying exon 2, 4 and 6 and long fragments with regions in which exons 3, 5, 7 + 8 and 9 were amplified. Exons 7 and 8 were co-amplified as a single PCR product. A pair of primers was designed covering both exons 7+8 in one PCR product because the two exons were only 163 bp apart (Park et al. 1995). The primers were located in intronic regions enabling the synthesis of the targeted sequences without having spurious synthesis of non-specific signals. All primers except those for exon 1 were able to amplify the corresponding exons in the multiplex PCR reactions. Corresponding primer sequences (Oligonucleotides), sizes of amplified PCR products, the locations of target sequences on a Gene Bank sequence of the human HPRT gene (M26434)

and the concentrations of primers for PCR reactions are given in the Table 3.1. The primers starting with 3' end are the forward while that of with 5' ends are the reverse primers. All the oligonucleotide primers were synthesized by Roth, Karlsruhe, Germany and provided lyophilized oligos were dissolved at RT in water and stock solutions were stored at -20°C. For PCR amplifications, they were thawed on ice and diluted to 10 pmol / μ l using water supplied with the QIAGEN Kit.

For simultaneous amplification of the above mentioned two sets of targeted sequences, two Primer-Mixes were separately pre-prepared. To prepare primer Mixes, 10-25 pmol of each primer (see also Table 3.1) were pipetted into a Eppendorf tube on ice, water was added to give a final volume of 50 μ l. The final concentration of each primer in the Mixes varied from 0.2-0.5 μ M.

For multiplex reactions, genomic DNA template (100-150 ng) was mixed with 2.5 μ l of each Primer Mix in a total PCR volume of 25 μ l consisting of 12.5 μ l HotStarTaq Master Mix (5 U HotStarTaq DNA polymerase, 2 x PCR Buffer containing 3 mM MgCl₂ and 400 μ M of each dNTP) and the rest with water. To enhance the formation of short fragments, Q-solution (supplied with Kit) was added (2.5 μ l for a total reaction volume of 25 μ l) to the reactions with Mix I. To maintain the specificity of all these amplifications, a cocktail of all the PCR components but without the corresponding templates were mixed before and pipetted into the reaction tubes. As a last step, templates were added to each tube. A positive control with wild type genomic DNA and a template free negative control were run in each set of PCR. The thermocycle programme was as follows: thermal cycling was started with an initial denaturation at 95°C for 15 min to activate the HotStartTaq polymerase followed by 33 cycles with each cycle consisting of (a) denaturation at 94°C for 30s (b) annealing at 55-60 °C for 90s and (c) extension at 72°C for 90s. After the last cycle a 10-min extension was performed at 72°C.

10-15 μ l of the PCR product was used for analysis on a 1.5% agarose gel. A 100 bp plus DNA ladder (MBI Fermentas, dissolved in 10 mM Tris-HCl /pH 7.6, 10 mM EDTA 0.015% bromophenol blue, 0.015% xylene cyanol FF & 10% Glycerol) was used as a molecular weight marker. If genomic DNA of any particular mutant clone failed to give reliable results, multiplex PCR for the mutant clone was repeated several times with changing primer concentrations, amount of template and other parameters according to a standard PCR trouble shooting protocol. If the results obtained remained unchanged, the mutant clones were then subjected to single PCR amplifications as described in detail in 3.4.2.4.

3.4.2.3 Uniplex /Standard Polymerase Chain Reaction (Single-PCR)

Single PCRs were carried out to amplify specifically exon 1 and the other exons when desired. It was difficult to include exon 1 primers with the remaining set of primers without having spurious amplification of non-specific products. However, a plausible explanation for the failure of exon 1 amplification in the multiplex PCR could be that the primers of exon 1 may form primer-dimers (Brownie et al. 1997), leaving an insufficient concentration of primer molecules to anneal to the template. This problem has already been reported in several other protocols (Park et al. 1995; Yamada et al. 1996).

Amplification of exon 1 (636 bp) of all the mutant clones in this study was performed successfully with HotStarTaq DNA polymerase (QIAGEN). For the amplification, genomic DNA template (250 ng) was mixed with 20-30 pmol of each primer, 0.2 mM dNTPs (MBI, Fermentas), 1-2.5 U of HotStarTaq polymerase, 1x PCR buffer (Tris-HCl, KCl, $(\text{NH}_4)_2\text{SO}_4$, 1.5 mM MgCl_2 , pH 8.7 at 20°C), 1x Q-solution and water (QIAGEN) to give a final volume of 50 μl . After the initial activation of HotStarTaq polymerase at 95°C for 15 min, a total of 33 PCR cycles were performed in which each cycle consisted of (a) denaturation at 94°C for 60s (b) annealing at 60°C for 60s and (c) extension at 72°C for 60s. The last cycle was followed by a 10 min extension at 72°C. Oligonucleotides relevant to exon 1 are listed in Table 3.1. PCR products of exon 1 were electrophoretically separated and the size of the obtained PCR products were compared with DNA makers. If a mutant failed to give a PCR product, repeated amplifications were performed.

The other single amplifications (exons 2-9) were performed either with HotStarTaq polymerase for exon 1 or with QIAGEN Multiplex Master Mix. 25-50 μl reaction volume contained 125-250 ng genomic DNA, 0.2 mM dNTPS (MBI, Fermentas), 1-2.5U HotStarTaq polymerase, 1x PCR buffer (Tris-HCl, KCl, $(\text{NH}_4)_2\text{SO}_4$, 1.5 mM MgCl_2 , pH 8.7 at 20°C), 1x Q-solution (if necessary), 10-20 pmol of each primer. Thermal cycling began with an initial activation as described before followed by 30-33 thermo-cycles consisting of (a) denaturation at 94°C for 60s, (b) annealing at 55-60°C for 30-60s, (c) extension at 72°C for 60s and terminating with a 10-min extension step at 72°C. For analysis, aliquots of the synthesized PCR products were electrophoresed in an ethidium bromide containing 1.5% agarose gel and sizes of bands were compared with DNA markers.

Three single PCRs were performed to analyse specific regions of three selected mutant clones (Table 3.2). Two of these mutants (6/7aI and 2/10d) showed inter-chromosomal translocations in FISH analyses while the remaining mutant clone (6/10e) failed to give the

Table 3.2. Primers used for single-PCRs to amplify desired sequences at the human HPRT gene locus of three selected HPRT mutant clones (6/7aI, 2/10d and 6/10e): From left to right oligonucleotide sequence of forward (F) and reverse (R) primers, primer concentration, sizes of PCR products, corresponding annealing temperatures and the positions of the primers on a Gene Bank sequence (M262434) of the HPRT gene. Directions of all the primers are given as 5'→3' and names of respective mutant clones are given in bold.

Primer Sequence	Concentration μM	PCR product Size (bp)	Annealing T °C	Location (M26434)
<u>Genomic DNA, Single-PCR</u>				
<u>Mutant clone</u>				
6/7aI				
F 5'-CCT TAT GAA ACA TGA GGG CAA AGG-3'	0.5	620	60	16252-16275
R 5'-GCA AGT ATG GTT TGC AGA GAT TC-3'	0.5			16871-16849
F 5'-GAT AGA TCC ATT CCT ATG ACT GTA G-3'	0.5	575	60	17736-17760
R 5'-TGT GAC ACA GGC AGA CTG TGG ATC-5'	0.5			17310-17287
<u>Mutant clone</u>				
2/10d				
F 5'-GAT CGC TAG AGC CCA AGA AGT CAA G-3'	0.5	586	62	38668-38692
R 5'-CTA CAG GCA CCC GCC AGC ACT-3'	0.5			39253-39232
F 5'-CTT ACG CCT GTC ATT TCA GCA CT-3'	0.5	617	60	39105-39128
R 5'-TCC GTG CTG AGT GTA CCA TGG T-3'	0.5			39722-39701
F 5'-GTC TGT AGT GTC AAC TCATTG CTG C-3'	0.5	592	60	39609-39633
R 5'-TAT GAG GTG CTG GAA GGA GAA AAC-5'	0.5			40200-40177
<u>Mutant clone</u>				
6/10e				
F 5'-ATT ATG ATT CTT TTT AGT TGT TGG ATT T-3'	0.5	184	60	40017-40044
R 5'-TAT GAG GTG CTG GAA GGA GAA AAC-5'	0.5			40200-40177
F 5'-GTC TGT AGT GTC AAC TCATTG CTG C-3'	0.5	592	60	39609-39633
R 5'-TAT GAG GTG CTG GAA GGA GAA AAC-5'	0.5			40200-40177

sequence complementary to exon 8 after sequencing of cDNA. Corresponding PCRs were carried out as described in 3.4.2.3.

3.4.2.4 Agarose Gel Electrophoresis

Agarose gel electrophoresis was performed in a horizontal configuration with the gel submerged in the electrophoresis buffer (submarine gel). Standard gels were prepared on plastic gel forms, which were preset with a 10-15 tooth comb. The agarose (100 ml 0.5 x TBE buffer + agarose 1.5 g or 1.7 g) was melted in a microwave oven or on a hot plate and the evaporated volume of water was added back to the solution to maintain the ionic strength. 8-10 μl of ethidium bromide (10 μg/ml) were added after the mixture had cooled, and mixed gently into the agarose, to prevent air bubbles. The gel was poured slowly and any bubbles in the solution were removed. The gel was allowed to solidify for 30-40 min. The gels could be stored wrapped in plastic-wrap at 4°C.

To prevent contamination of samples from run-over from a neighbouring well, samples were loaded on the gel with a free well between each sample. DNA ladder markers (6-8 μ l) were pipetted either into the terminal or the middle wells. After loading samples, the gels were run at 80-100V and 35mA (usually 45 to 90 min) until the bromophenol-blue loading buffer dye front reached the base of the gel or the second row of wells. The gel was then visualised under UV light and photographed. When the electrophoresis results showed unclear band distribution, the samples were analysed on a 1.7% agarose.

3.4.3 RNA Isolation and Analysis of HPRT-mRNA -Transcripts

3.4.3.1 Total RNA Isolation

Total RNA isolation was carried out by using a commercially available molecular biological kit (RNeasy Mini Kit, QIAGEN). With the RNeasy procedure, all RNA molecules longer than 200 nucleotides can be isolated. A specialized high-salt buffer system allows up to 100 μ g of RNA to bind to the RNeasy silica-gel membrane. Cell suspensions are first lysed and homogenised in the presence of a highly denaturing guanidine isothiocyanate-containing buffer, which immediately inactivates RNases to ensure the isolation of intact RNA. Ethanol is then added to provide appropriate binding conditions, and the sample is then applied to an RNeasy mini column where the total RNA binds to the membrane and contaminants are efficiently washed away. High quality RNA is then eluted in 30-50 μ l of RNase free water provided.

The cells of 6-TG^r mutant clones that were grown to confluence were prepared following trypsination and diluting in culture medium. More than 3-4 million cells were used for total RNA isolation according to the instruction manual. Suspended cells were first centrifuged for 5 min at 300 x g and pellets were subsequently rinsed with 200 μ l ml PBS (at RT) to remove cell culture medium. After addition of 350 μ l of RLT lysis buffer containing guanidine isothiocyanate, the cell lysate was homogenized by passing through a sterile needle (with a diameter of 0.9 mm) at least 5-10 times. In this manner, high molecular weight DNA can be sheared and β -mercaptoethanol, a component of the RLT buffer facilitates proper disruption. After disruption and homogenisation, 350 μ l of 70% ethanol were added to the cell lysates to create optimal conditions for selective binding of RNA to the RNeasy silica-gel membrane. The RNeasy column was placed on a 2 ml collection tube and 700 μ l composition were added. The tube was then centrifuged at 8000 x g for 15s. The flow through was discarded and the RNeasy column placed back in the tube. Then 700 μ l RW1 buffer

composition (wash buffer) were added to the column and centrifuged for 15 s at 8000 x g. After transferring the RNeasy column to a new collection tube, 500 µl of RPE buffer (wash buffer) were pipetted on the RNeasy column and centrifuged for 15 seconds at 8000 x g to wash the column. The filtrate was discarded and another 500 µl of RPE buffer were added and centrifuged for 2 min at 8000 g to dry the RNeasy silica-gel membrane. In case of incomplete drying, this step was repeated once for 1 min at the same g value. After that, to elute the RNA bound to the silica membranes, RNeasy column was transferred to a 1.5 ml collection tube. After pipetting 50 µl of the provided RNase free water onto the membrane, the column was centrifuged for 1 min at 8000 x g. The eluted RNA from each mutant was kept at -20°C for downstream PCR applications.

The concentrations of individual mutant total RNA from each mutant clone were determined by measuring the optical density absorbance at 260 nm (λ_{260}) and 280 nm (λ_{280}) in a spectral photometer. In order to measure the values, RNA samples were diluted to 1:100 by using RNase free water for analysis in a quartz cuvette that was pre-cleaned several times with a solution of methanol + concentrated HCl (v/v; 1:1). Photometric values were taken and concentrations were calculated as given below ($\text{RNA concentration} = \lambda_{260} * \text{Factor} * 100$; factor for RNA concentration (µg/ml) is 40). The ratio of readings at 260 nm and 280 nm ($\lambda_{260}/\lambda_{280}$) provided an estimate of the purity of RNA with respect to contaminants that absorb in the UV range, such as protein.

3.4.3.2 Reverse Transcriptase Polymerase Chain Reaction (RT-PCR)

First-strand cDNA analysis was carried out using 50 ng to 2 µg of total RNA from the mutant clones with the commercially available Omniscript™ Reverse Transcriptase Kit (QIAGEN, Hilden, Germany). The reverse transcriptase transcribed the mRNA of mutant clones with an oligo-dT primer (Roth, Karlsruhe, Germany) that consisted of 12 nucleotides. The reverse transcriptase used here was a multi-functional enzyme with three distinct enzymatic activities: an RNA-dependent DNA polymerase, a hybrid-dependent exoribonuclease (RNase H), and a DNA-dependent DNA polymerase. The RNA-dependent DNA-polymerase activity transcribes complementary DNA (cDNA) from an RNA template, whereas RNase H of the Omniscript™ reverse transcriptase specifically degrades only the RNA in RNA:DNA hybrids.

3 MATERIALS & METHODS

```

1 tcttgctgcg cctccgcct cctcctctgct ccg ccaccggcttctcctcctgagcagtc

61 agcccgcgcg ccggccggct ccgttatggc gaccgcgacg cctggcgctg tgattagtga
121 tgatgaacca gggtatgacc ttgatttatt ttgcatacct aatcattatg ctgaggattt
181 ggaaaggggtg tttattcctc atggactaat tatggacagg actgaacgctc ttgctcgaga
241 tgtgatgaag gagatgggag gccatcacat tgtagccctc tgtgtgctca aggggggcta
301 taaattcctt gctgacctgc tggattacat caaagcactg aatagaaata gtgatagatc
361 cattcctatg actgtagatt ttatcagact gaagagctat tgtaatgacc agtcaacagg
421 ggacataaaa gtaattgggtg gagatgatct ctcaacttta actggaaaga atgtcttgat
481 tgtggaagat ataattgaca ctggcaaaac aatgcagact ttgctttcct tggtcaggca
541 gtataatcca aagatgggtc aggtcgcaag cttgctggtg aaaaggaccc cacgaagtgt
601 tggatataag ccagactttg ttggatttga aattccagac aagtttggtg taggatatgc
661 ccttgactat aatgaatact tcagggattt gaatcatggt tgtgtcatta gtgaaactgg
721 aaagcaaaa taaaaagcct aagatgagag ttcaagttga gtttggaaac atctggagtc

781 ctattgacat cgccagtaaa attatcaatg ttctagtctt gtggccatct gcttagtaga
841 gctttttgca tgtatcttct aagaatttta tctgttttgt actttagaaa tgtcagttgc
901 tgcattccta aactgtttat ttgcactatg agcctataga ctatcagttc cctttgggcg
961 gattgtgtgt taacttgtaa atgaaaaaat tctcttaaac cacagcacta ttgagtgaag
1021 cattgaactc atatctgtaa gaaataaaga gaagatatat tagtttttta attggtatgt
1081 taatttttat atatgcagga aagaatagaa gtgattgaat attgttaatt ataccaccgt
1141 gtgtagaaa agtaagaagc agtcaatttt cacatcaaag acagcatcta agaagttttg
1201 ttctgtcctg gaattatttt agtagtggtt cagtaatggt gactgtatgt tccaacttgt
1261 tcaaattatt accagtgaat ctttgtcagc agttcccttt taaatgcaaa tcaataaatt
1321 cccaaaaatt t

```

Figure 3.2. Gene bank sequence of the human HPRT cDNA (NM_000194) showing the locations of the primers for RT-PCR: Right pointed arrows indicate the locations of forward primers, while left pointed arrows show the starting locations of reverse primers. Blue arrows indicate the primer-start locations of first PCR product of 761 bp; red arrows show the primer-start locations for nested PCR product of 737 bp; the underlined are the primer sequences including overlapping regions.

According to the instructions provided by the manufacturer, a RT reaction volume of 20 µl containing of 2 µl 10-x buffer composition RT, 2 µl oligo d (T)₁₂ primer (10 µM) 2 µl dNTPs (5 mM each d NTP), 1 µl Omniscript™ Reverse Transcriptase (4 Units) and isolated mutant RNA was prepared in a 0.5 µl-tubes on ice. The reverse transcription reaction was incubated for 1h at 37°C in the thermo cycler (Biometra) and stopped at 93°C for 5 min. As a control, wild type cDNA was synthesized in each reverse transcription-run of new cDNA synthesis. If no cDNA was present, the syntheses were repeated once using increased amounts of templates and the reaction constituents were placed on ice during mixture preparations and pipetting. For long-term storage, the tubes containing synthesized cDNA were preserved at -20° C.

PCR was used to amplify HPRT expression products from cDNA in a total reaction volume of 25 µl, which contained 12.5 µl QIAGEN Multiplex Master Mix, 2.5 µl of cDNA, 1-1.25 µl of each primer (0.4-0.5 µM), 1x Q-solution (if necessary). Cycling began with an initial activation step of 15 min at 95°C and followed by 33-35 cycles each consisting of (a) denaturation for 30s at 94°C (b) annealing temperature for 90s at 55-56°C (c) extension for 90s at 72°C and after the last cycle was finished with 10-min extension at 72°C. The primary PCR product (761 bp) was reconfirmed by a nested PCR that was run with an inner primer set

using 1-2 µl of primary PCR product. Primers used for these amplifications were as follows: primary PCR product with forward primer 5'-CCT CCT CTG CTCCGCCACCG-3' and reverse primer 5'-GACTCC AGA TGT TTC CAAAC-3' while the second was nested PCR amplified with a forward primer of 5'-CCA CCG GCT TCC TCC TCC TGA-3' and a reverse primer of 5'-GTT TCC AAA CTC AAC TTG AAT TCT CAT C-3'. The positions of the primers in HPRT cDNA is depicted in Figure 3.2. These pairs of primers were used in previous reports (Horikawa et al. 2002). PCR products were analysed by 1.5% agarose gel electrophoresis and ethidium bromide staining.

3.4.4 DNA Sequencing of cDNA Products of Mutant Clones

A limited number of samples which gave RT-PCR products was sent out to get DNA sequenced. Purification of PCR products and the DNA sequencing of both DNA strands of each mutant were carried out by the Medigenomix GmbH, Martinsried, Germany and QIAGEN, Hilden, Germany. These mutant clones belong to one of the mutation induction experiments performed using immortalised human fibroblasts. There were 10 samples including wild type as a control and both 2-Gy and 6-Gy induced mutant clones. Sequenced samples were K/28a, K/40f (spontaneous mutant clones) 2/15b, 2/14eI, 2/14eII, 2/11d, 2/16cII (2-Gy mutant clones), 6/10e, 6/20cII (6-Gy mutant clones) and wild type. Detailed mutation signatures of these mutant clones are given in Table 8.1. Mutations on sequenced data were assessed comparing the sequences of each mutant clone with gene bank sequence NM_000194 using a software programme BioEdit version 5.0.6.

3.5 Categories of Mutations

Mutant clones were divided into several categories according to the method used for their analysis. In M-PCR analysis, "Total deletion (TD)" mutant clones include mutants for which no representative exon fragment was synthesized. "Partial deletion (PD)" mutants consist of either intragenic or end deletions at the HPRT gene locus. Intragenic deletion mutants contain two break points within the HPRT gene, whereas end-deletion mutants have only one break point within the HPRT gene. Mutants with "Normal pattern (WT)" represent those which contain all exon PCR products of desired sizes. These mutants could have transitions, transversions, frameshifts or small deletions, which would not be detected by PCR. In *NotI* restricted Southern hybridisation analyses, radioactive signals registered on blots were compared to those of respective wild type signals and were then grouped into altered (small or

large) when deviations were more than 3 mm compared to WT or unaltered (normal) or no signals where no banding pattern could be observed in the lanes of the corresponding blots. Similarly, in RT-PCR, mutants were divided into two groups: mutants that retained a PCR product were scored as positive and the others as negative.

3.6 Fluorescent *in situ* Hybridisation (FISH)

The method of *in situ* hybridisation also called chromosome painting was used to identify the chromosomal location of a specific DNA or RNA probe. The theory is the same as for Southern hybridisation, except that the DNA to which the probe will hybridise is the actual chromosome. The probe was labelled with a fluorescent dye. It was then added to a chromosomal preparation from the species of interest. After a sufficient time for annealing, the chromosomes were viewed using a fluorescent microscope. The probe will hybridise to the chromosome carrying the sequence of interest. If the species has been characterized cytogenetically, the marker can be assigned to the appropriate chromosome. Because this technique uses a fluorescent probe it is called fluorescent *in situ* hybridisation or FISH. Several additional technical steps increase the utility of the FISH technique. If FISH was coupled with chromosome banding, the probe can be localized to a specific band of the chromosome. Chromosomes can also be characterized simultaneously with two probes, each labelled with a different label. This permits the ordering to any two probes on a specific chromosome. In this manner, physical linkages can be determined using FISH.

In the current study, an X-chromosome specific probe was used to detect inter chromosomal aberrations such as reciprocal or non-reciprocal translocations between X chromosome and the autosomes of radiation-induced and spontaneously arising HPRT mutant clones. Chromosome painting probes for chromosome 1 (green), 2 (yellow) and X (red) (MetaSystems, Altussheim, Germany) were used by Dr. Salam A. Warda to hybridise metaphase spreads of mutant clones. Hybridised metaphase-spreads were examined with a Zeiss Axioskop 2 mot fluorescence microscope using the ISIS software (MetaSystems, Altussheim, Germany).

4 Results

4.1 Human Bladder Carcinoma Cells-MGH-U1

4.1.1 Cell Survival Colony-Forming Assay

Radiation-induced cell survival was examined in a human bladder carcinoma cell line and measured by a cell colony-forming assay. Crystal violet stained cell colonies were scored from survival experiments in which cells were seeded and incubated in plastic dishes for 12-16 days. Only dishes that contained at least 50 colonies were counted for the assessment (a colony consisted of at least 50-100 cells). Confluent cells were irradiated with X-rays as described in Materials and Methods. In comparison, untreated control cells were held in the same conditions. The doses administered for these experiments were 1, 2, 4 and 6-Gy. Three survival experiments were carried out and the mean values were taken for the final survival curves.

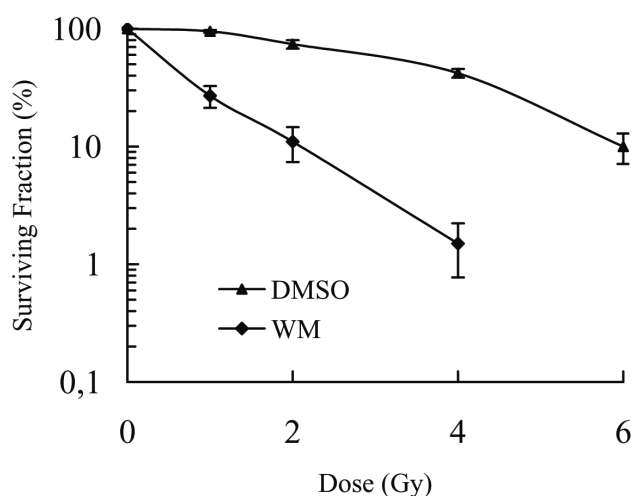


Figure 4.1. Cell survival of MGH-U1 tumour cells as a function of dose of X-rays in the presence or absence of 20 μ M wortmannin (WM). Since wortmannin is dissolved in DMSO, control cells were treated with 0.1% of DMSO. Confluent cultures were treated with wortmannin 2 h prior to X-irradiation and both treated and untreated groups of cells were incubated for 16 h before plating them for colony formation. Each dose point represents the mean of three determinations ($n = 3$).

To investigate the effect of radiation on cell survival in the absence of a significant repair mechanism, the tumour cells grown to confluence were treated with wortmannin 2 h prior to irradiation. Wortmannin is an enzymatic inhibitor (PI-Kinase family) also for non-homologous end-joining which is the predominant repair pathway of mammalian cells. Cell monolayers were irradiated with acute doses. Irradiated cells were then incubated for 16 h. After removing the wortmannin-containing culture medium, both untreated control and wortmannin treated cell cultures were plated for the colony-forming assay.

In Figure 4.1, survival curves of MGH-U1 cells in the presence and the absence of wortmannin are shown. Cell survival without wortmannin treatment reveals a characteristic shouldered response while the survival results of wortmannin-treated cultures are consistent with previous reports (Chernikova et al. 2001; Delacote et al. 2002) indicating that wortmannin is a potent radiosensitizer. A concentration of 20 μ M was chosen because at this level wortmannin displays minimal cytotoxicity (Rosenzweig et al. 1997 and own observation). Since wortmannin is dissolved in DMSO, controls were also treated with the same solvent.

To avoid cytotoxicity a minimal concentration of DMSO ($< 0.1\%$) was added to the cell cultures 2 h prior to irradiations. Surviving fractions of cells exposed to wortmannin combined with X-irradiation are compared with those of cells that were only exposed to X-irradiation in the presence of DMSO. For cells treated with wortmannin + 2-Gy X-rays and for cells treated with DMSO + 6-Gy X-rays, a cell survival level of 10 % could be observed.

4.1.2 Isolation of Independent HPRT Mutant Clones

To analyse the nature of mutations at the HPRT gene locus, confluent monolayers of MGH-U1 cells were exposed to single doses of 2 and 6-Gy X-rays. Parallel control cells were unexposed but held under the same conditions during the entire experimental procedures.

Isolations were made from two mutation experiments though a total number of three was carried out with the tumour cell line. The first experiment (Exp I) comprised unirradiated controls and cells exposed to 6-Gy X-rays. Mutation induction and selection of HPRT-deficient mutants were performed as described in detail under Materials and Methods. Mutant clones arising after 14-16 days were isolated as a colony per dish and the resistance to 6-thioguanine further confirmed by expanding them first in selective medium containing 6-thioguanine and then in 6-thioguanine free culture medium. After the isolation of mutant clones, all culture dishes were stained with crystal violet to determine mutation frequencies. From cultures of independently grown mutant clones, aliquots were used for cryopreservation, DNA isolations and further molecular analyses. All mutant clones varied widely in their growth capacity, and clonal expansion after isolation was extremely poor. 18 spontaneously arising mutant clones and 9 x 6-Gy induced mutant clones could be recovered for molecular analyses such as PFGE coupled *NotI* restriction fragment analysis, multiplex PCR and FISH. The values in plating efficiency tests (88% for 0-Gy and 10% for 6-Gy) that were carried out parallel to mutation induction experiments were considered in assessing the corresponding mutation frequencies for each treatment group.

Table 4.1. Mutation Frequencies of 6-TG^r HPRT MGH-U1 mutant clones depending on the parameters chosen; values are number of mutants per million survivors.

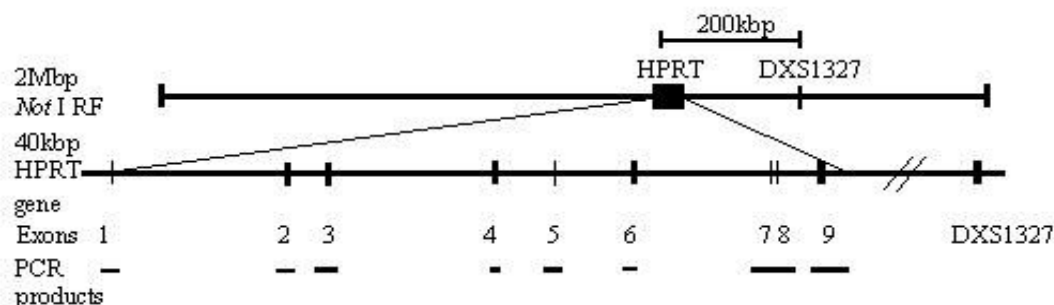
Experiment I X-rays		Experiment II X-rays + DMSO		Experiment II X-rays + wortmannin	
0-Gy:	5.9 ^a	0-Gy:	0.9 ^a	0-Gy:	1.1 ^a
6-Gy:	63 ^a	6-Gy:	16.5 ^a	2-Gy :	2.6 ^a

^a HPRT mutant clones were isolated from these samples.

The parameters chosen for other two experiments were different from the first. Cells grown to confluence in four 75-cm² culture flasks were taken for each experiment. Two of these were exposed to X-rays while the remaining two were used as controls (wortmannin + 0-Gy and DMSO + 0-Gy). 2 h prior to X-irradiation, two cultures were treated with wortmannin and the other two were treated with DMSO (< 0.1% DMSO). Two cultures were then exposed to X-irradiation so that a wortmannin-treated culture was irradiated with 2-Gy and a DMSO-treated culture with a dose of 6-Gy. 6-TG^r HPRT mutant colonies of the experiment (Exp II) were isolated from each group.

After 14-16 days incubation, 6-thioguanine resistant mutant cell colonies were isolated and expanded. From independently grown mutant clone cultures, cells were taken for genomic DNA isolations, frozen stocks and FISH analyses. Similar to the previous experiment, the mutant clones varied widely in their growth capacity leaving 13 x spontaneously arisen, 9 x 2-Gy combined with wortmannin treatment and 9 x 6-Gy (without wortmannin) mutant clones. The third experiment (Exp III) was performed using the same protocol in order to increase the number of 6-TG^r mutants but the mutation frequencies were relatively varied from the first two experiments and therefore mutants were not subjected to further analysis.

Table 4.1 summarizes the mutation data collected on all HPRT mutant cell clones isolated from both experiments. Mutation induction frequencies for HPRT gene inactivation, as measured by 6-thioguanine resistance, were corrected for corresponding plating efficiencies of non-irradiated and irradiated cells and are given as the numbers of mutants per million of cell survivors. These data indicate that irradiation of MGH-U1 cells with 6-Gy of X-rays has reduced the relative cloning efficiency (survival) to 10% (see Figure. 4.1) and resulted in at least a 10-fold increase in HPRT gene mutation above background levels for both mutation experiments. The mutation frequency for cells that were exposed to 2-Gy in the presence of wortmannin was 2.5-fold higher than the corresponding background level (unirradiated cells treated with wortmannin).

4.1.3 *NotI* Digested Restriction Fragment Analysis**Figure 4.2.** Schematic diagram of human HPRT gene locus viewing single copy probe binding site and the sizes of exons and the PCR amplification products.

HPRT mutations were investigated at the Mbp level by Southern hybridisation. All mutant clones isolated were used for the analysis. Genomic DNA embedded in agarose-plugs was cleaved with the rare-cutting restriction enzyme *NotI* and separated by pulse field gel electrophoresis (PFGE). The approximate number of cells embedded in an agarose plug was roughly 6×10^5 .

Following UV imaging, the gel was transferred onto a nylon membrane and later hybridised with two different radioactive probes. The first α - ^{32}P dCTP labelled radioactive probe was DXS1327, which hybridises to a 2 Mbp *NotI* fragment in MGH-U1 cells. A schematised diagram of the HPRT gene showing the binding site of the hybridisation probe and the HPRT exons are given in Figure 4.2. The HPRT gene locus lies on the restriction fragment and the hybridisation binding site is 200 kb telomeric to the gene on the *NotI* restriction fragment. The second was the D21S4 probe, which served as the reference to the first and detects a 2 Mbp restriction fragment located on the proximal part of the long arm of human chromosome 21.

A representative diagram including the UV picture, DXS1327 hybridisation and D21S4 as a reference is illustrated in Figure 4.3. Genomic DNA from *Saccharomyces cerevisiae* (Sc), *Schizosaccharomyces pombe* (Sp) and *Hansenula wingei* (Hw) were used as DNA molecular size markers. On Southern blots, migration lengths were sorted into 4 categories. These four categories were large (> 2 Mbp), small (< 2 Mbp) and normal (2 Mbp), and the combination of two bands (i.e small and normal or large and small). The migration length which was at least 3 mm larger or smaller than 2 Mbp was grouped as aberrant bands. Mutant clones that gave no radioactive signals with HPRT specific probe were grouped as “no signals”. All samples with no signals were detected with the reference probe D21S4. Summarised data of all the analytical methods are tabulated in the Table 4.2.

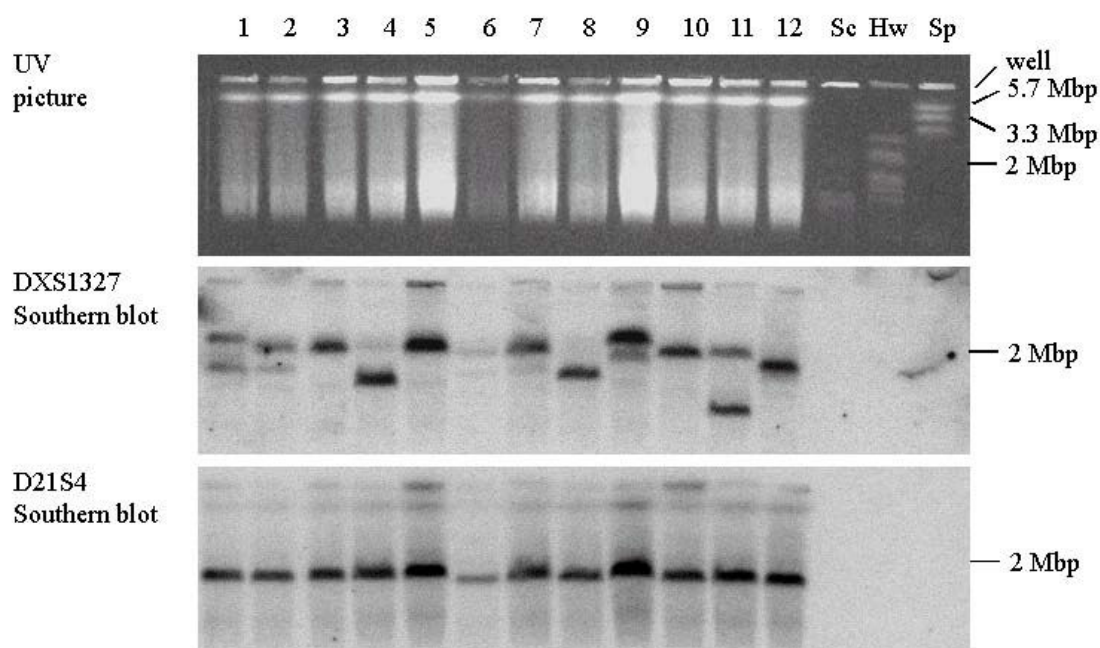


Figure 4.3. Representative picture of restriction fragment migration patterns of 12 HPRT mutant clones in MGH-U1 cells. Genomic DNA samples were digested with a rare-cutting restriction enzyme, *NotI* and the restriction fragments were separated in a 0.8% agarose gel by pulse field gel electrophoresis (PFGE). Following exposure to UV light (302 nm), the fragments were transferred to a nylon membrane. The membrane was hybridised to a radioactive marker specific to the HPRT gene region. After stripping the membrane, it was re-hybridised with D21S4, which served as a reference. Genomic DNA of *Saccharomyces cerevisiae* (Sc), *Schizosaccharomyces pombe* (Sp) and *Hansenula wingei* (Hw) was used as DNA molecular size markers and are displayed on the last three lanes of EtBr-stained gel. Upper panel: UV-photograph of EtBr-stained gel; Middle panel: Southern blot picture with DXS1327 probe (binding site is 200 kbp telomeric of the HPRT gene) detects to a 2 Mbp fragment, which also contains the HPRT gene. Lower Panel: Southern blot picture with D21S4 probe which hybridises to a 2 Mbp fragment located on longer arm of chromosome 21 and this serves as a reference; Lanes 1-5: spontaneously arising mutants; Lane 6: 6-Gy mutant; Lanes 7-11: spontaneously arising mutants; Lane 12: genomic DNA of wild type MGH-U1 cells as a positive control. Restriction band alterations of independently grown HPRT mutant clones can be observed in the middle panel while constant migration lengths (2 Mbp) are seen in the lower panel where the D21S4 probe served as a reference. Complete digestions of samples can be noted in EtBr-stained UV picture.

The results of the restriction fragment analysis:

From a total number of 31 spontaneously arising mutant clones: 2 x normal bands; 18 x large bands; 1 x small band; 3 x large /large bands; 2 x large /small bands (these mutants with double bands were later removed from the data set) and 5 x gave no signal.

Among 18 x 6-Gy mutant clones, the results were as follows: 2 x normal bands; 7 x large restriction bands; 2 x small bands; 4 x no signal and 3 mutant clones with double bands (2 x large /normal and 1 x large /small) which were later removed from the data set. Additionally, 9 x 2-Gy + wortmannin mutant clones: 5 x large bands; 2 x small bands; 1 x large /normal; 1 x large/large band. The latter two mutant clones with double bands were not included to the final data set.

4.1.4 Multiplex PCR-based HPRT Exon-Deletion Analysis

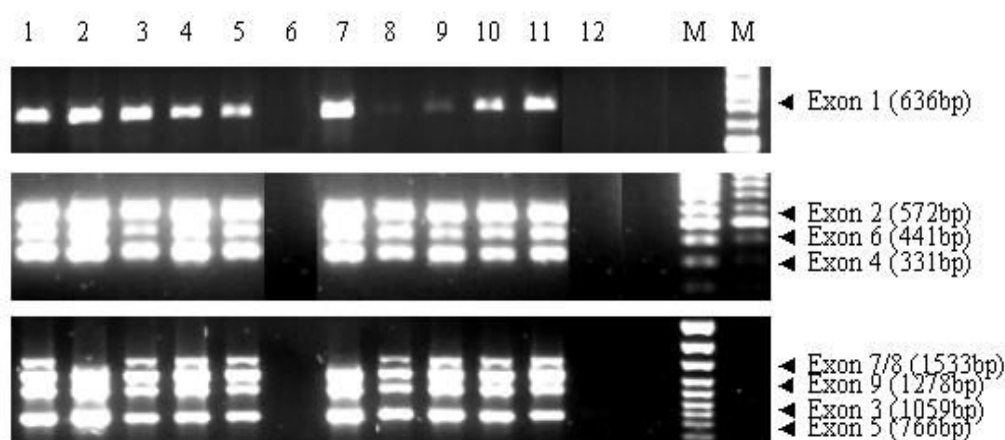


Figure 4.4. Multiplex-PCR based exon-deletion screening at the HPRT gene locus of the mutant clones in human bladder carcinoma (MGH-U1) cells. Exon-containing fragments were amplified as follows: Exon 1 as a monoplex-product individually, exons 2, 4 and 6 as a triplex-product and exons 3, 5, 7/8 and 9 as a tetraplex-product. *Upper panel:* Exon 1 as a single product. *Middle panel:* Exons 2, 4 and 6 as a triplex-product. *Lower panel:* Amplification of exons 3, 5, 7/8 and 9 as a tetraplex-product. 10-15 μ l of each reaction product was electrophoretically separated in a 1.5% agarose gel and stained with EtBr. Apparent fragments were determined by a DNA molecular size marker (M). Mutant clones in lanes 6 and 12 demonstrate the absence of all exons (total deletion) while mutants in lanes 2 and 7 lacked only exon 7/8 (partial deletion) and lane 8 gave no product in upper panel. Remaining samples gave all fragments (wild-type). Sizes of fragments containing exons were given in parentheses.

The genomic DNA from each of the 58 mutant clones was analysed at the HPRT gene locus by multiplex PCR to screen for exon-deletions. It was time saving to amplify a couple of exons as a multiplex-product rather than synthesizing all exons as single fragments in separate PCR reaction volumes. For each mutant genomic DNA, all 9 exons were amplified in three different reaction volumes: Exons 2, 4, and 6 as triplex-products; exons 3, 5, 9 and 7/8 as tetraplex-products and exon 1 as a single product. Since exons 7 and 8 are only 163 bp apart these two were amplified as a single fragment.

To guarantee the accuracy of PCR results, the mutants that gave unclear products were repeated. PCR results, in every reaction was compared with a positive control using wild type genomic DNA and a negative control with template-free reaction volume. The apparent sizes of fragments amplified ranged from 331(exon 4)-to 1533 bp (exon 7/8). Figure 4.4 shows the representative panels of various mutations analysed by multiplex and single PCR. The resolution of electrophoretic conditions used in this analysis was sensitive enough to clearly distinguish the migration lengths of PCR products. The sizes of exons and the PCR amplification products can be seen in Figure 4.4. Table 4.2 shows a summary of PCR. 3 classifications were made here, considering the exon-presence and absence in corresponding

4 RESULTS

Table 4.2. Comparison of spontaneous and X-ray-induced HPRT mutant clones in human MGH-U1 cells

X-rays	Number of Analysed Clones	PCR Analysis		Restriction Fragment Analysis
		Pattern	Failed Exons	
6-Gy	15	9 WT	none	5 x large ^a 2 x small 2 x normal ^b
		4 PD	2-3 2-3 and 7-8 1 3 and 7-8	1 x large 1 x large 1 x no signal 1 x no signal
		2 TD	all	2 x no signal
2-Gy + WM	7	5 WT	none	4 x large 1 x small
		2 PD	7-8 7-8	1 x large 1 x small
0-Gy	26	16 WT	none	13 x large 1 x no signal 2 x normal
		9 PD	3 2-3 1 7-9	3 x large 2 x large 3 x no signal 1 x small
		1 TD	all	1 x no signal

Abbreviations:

WT- wild type pattern including all HPRT exons; PD-partial deletions missing one or multiple number of HPRT exons; TD-total deletions missing all HPRT exons; normal = 2 Mbp restriction fragment; Large > 2 Mbp; small < 2 Mbp; WM-wortmannin which was used to generate NHEJ deficient cells.

^a one of these mutant clones gave a translocation between X-chromosome and the autosomes.

^b one of these mutant clones gave a translocation between X-chromosome and the autosomes.

PCR products (Wild type WT, Total deletion TD or partial deletion PD). All of the mutants, which belong to either “normal” or “no signal” category, showed almost identical results both in restriction fragment analysis and PCR based studies.

The results for spontaneously derived mutant clones: 20 mutants retained WT pattern, 10 PD pattern and 1 TD pattern. In the 10 partial deletions there were intragenic and end deletions in the gene: 3 clones missed exon 1; 3 clones exon 3; 2 clones lacked exon 2/3; 1 clone had a deletion of exons 7-9 and 1 mutant clone lacked exons 7/8. HPRT mutant clones arising following X-irradiation in the absence of wortmannin produced a spectrum of mutations significantly different from that of spontaneously arising HPRT mutations. Distinguishable difference lies in the proportions “wild type” and “total deletions”. However, it is difficult to make a final conclusion, because the total number of induced mutants

analysed in this study are relatively low, especially for the wortmannin treated cell group. In Table 4.2, mutation signatures of 26 spontaneous mutant clones and 22 radiation-induced mutant clones are given. 10 Mutant clones with double restriction bands were removed from the initially collected number of mutant clones in preparing the final data set. Those were: 3 x 6-Gy mutant clones; 2 x 2-Gy + WM mutant clones and 5 x spontaneous mutant clones.

4.1.5 Cytogenetic Screening Using Fluorescence *in situ* Hybridisation (FISH)

Fluorescent *in situ* hybridisation (FISH) was performed to examine the genomic rearrangements and cytogenetic nature of the mutant clones. For this purpose, exponentially growing cells were treated with 80 ng/ml colcemid for 4 h, trypsinized and incubated in 75 mM KCl at 37 °C for 10 min, fixed 3 times in methanol: glacial acid 3:1 and dropped onto wet glass slides. Followed by denaturation, hybridisation with chromosome painting probes for selected chromosomes 1, 2 and X was carried out.

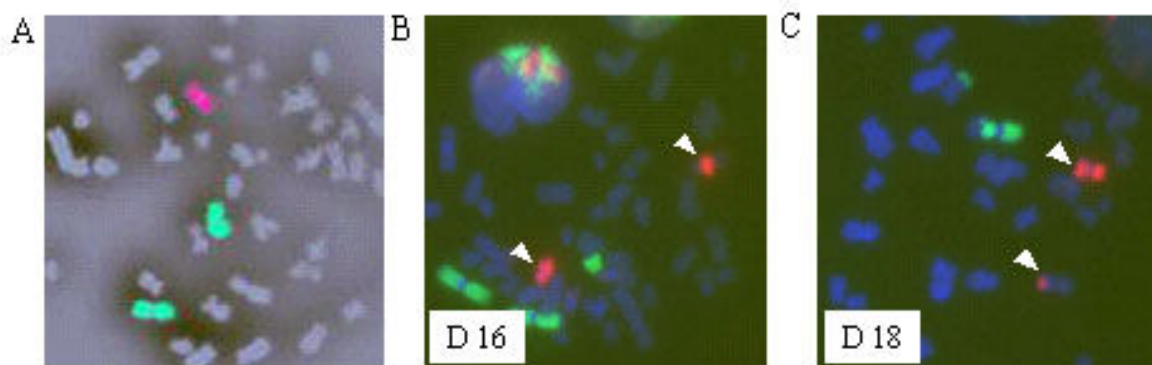


Figure 4.5. Examination of cytogenetically visible aberrations of HPRT mutant clones in human bladder carcinoma (MGH-U1) cells. Exponentially grown cells were used for metaphase-slides preparations. The number of metaphases analysed was variable. X-chromosome is painted in red and chromosome 1 in hell green, while the remaining chromosomes are painted in DAPI. In the panels from A to C: untreated mutant clone with no chromosomal exchanges, a mutant clone (D16) with normal restriction fragment size but gave a non-reciprocal translocation while the other mutant clone (D18) with aberrant restriction fragment also gave a non-reciprocal translocation. Changes to X-chromosome (red) are designated by white arrow heads.

Only two out of a total of 31 mutants examined (all mutants from Exp II), contained non-reciprocal translocations. The clones were 6-Gy induced HPRT mutants. Both chromosomal translocations were detected between X-chromosome and the autosomes. One mutant had surprisingly retained a normal sized restriction band while the other showed an aberrant (large) restriction band in Southern analysis. These results suggest that intra chromosomal exchanges rather than inter chromosomal ones cause the inactivation of the HPRT gene in mutant clones. Figure 4.5 shows translocations found in HPRT mutant clones in MGH-U1 cells.

4.2 Acute-Dose-Irradiation and Immortalised-Human Primary Fibroblasts (82-6 h TERT Cells)

To further elucidate the radiation-induced mutation spectrum at the HPRT gene locus, several mutation induction experiments were performed using an immortalised primary fibroblasts-cell line (82-6 hTERT). Although these cells have an indefinite life span, they are not tumorigenic, and they retain other characteristics of non-transformed fibroblasts, including normal karyotypes, cell cycle checkpoint responses, and growth requirements. As already described in detail under Materials and Methods, cloning efficiency (plating efficiency) of this particular cell line is relatively low and ranged between 5-10%. However, the sub cell line that was later produced using early-passages of original 82-6 hTERT cells possessed a cloning efficiency of at least 50%. The first two mutation induction experiments used cells showing at least 5% of cloning efficiency while cells that had at least 50% of cloning efficiency were used for the last experiment. Before performing both survival and mutation-induction experiments, cell passages were examined for their karyotypes and they were all found to have a normal cytogenetic profile.

4.2.1 Cell Survival and HPRT Mutation Frequency

Table 4.3. Mutation Frequencies of 6-TG^r HPRT 82-6 hTERT mutant clones depending on acute X-ray doses employed; values are number of mutants per million survivors.

Experiment I	Experiment II	Experiment III
<u>Acute dose</u>	<u>Acute dose</u>	<u>Acute dose</u>
0-Gy : 0.12 ^a	0-Gy : 1.25 ^a	0-Gy : 19.5 ^b
2-Gy : 3.78 ^a	2-Gy : 4.26 ^a	2-Gy : 31.9 ^b
6-Gy : 16.4 ^a	6-Gy : 21.4 ^a	6-Gy : 70.15 ^b

^a Average plating efficiency of confluent cells used for mutation induction was 5%, HPRT mutant clones isolated from these samples

^b Average plating efficiency of confluent cells used for mutation induction was 50%, HPRT mutant clones isolated from these samples

Radiation-induced cell survival was determined by a colony-forming assay. Sufficient numbers of cells were generated from a mass culture of 82-6 hTERT cells. In comparison to the bladder carcinoma MGH-U1 cells, cell growth of this immortalised cell line was relatively slow. Surviving fractions were determined after cells were exposed to acute doses of X-rays *in vitro* and seeded in plastic dishes. Survival and mutation induction experiments were carried out in the same manner to the experiments that were performed previously with MGH-U1 cells. For both survival and mutation induction experiments, arising colonies were counted following crystal violet staining. In assessing mutation induction frequencies, all the values

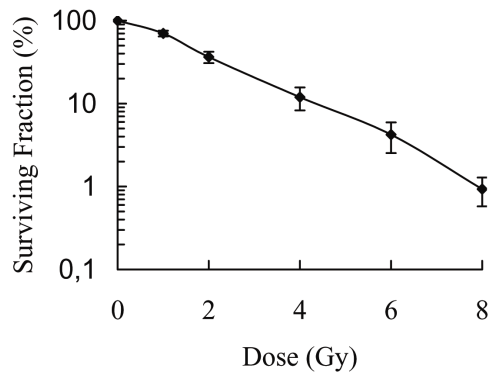


Figure 4.6. Cell survival of hTERT-immortalised primary fibroblasts (82-6 hTERT) as a function of increasing dose of X-rays. Confluent cultures were exposed to X-irradiation and incubated for 16 h prior to plating for the colony-forming assay. Colonies were made visible after 14-16 day incubation and relative survival fractions were assessed for each dose point. Control cell cultures were held in the same conditions during the entire period. Each point represents the mean of two determinations ($n=2$).

were normalized to respective plating efficiencies, because the mutation induction frequency is defined as the number of HPRT mutant clones in a million of cell survivors.

The doses employed for cell surviving assays were 1, 2, 4, 6 and 8 Gy while the mutant induction experiments were performed only with 2 and 6-Gy dose points. Initial dose-response studies showed that the irradiation of 82-6 hTERT cells at 2-Gy and 6-Gy of X-rays reduced its relative cloning efficiency (survival) by up to 36% and 4% (Figure 4.6) respectively. HPRT mutation induction frequencies suggest at least a 4- or 20-fold increase above the background levels for 2 and 6-Gy respectively (Table 4.3). However these values are valid only for Experiment I and II, since the last experiment performed with the cells whose cloning efficiency was 5-10 times more efficient gave higher frequencies for spontaneously arising 6-TG^r HPRT mutant clones. The cell survival curve for 82-6 hTERT cells is demonstrated in Figure 4.6. It can be seen that this has a characteristic shouldered response while cells seem to be sensitive to increasing of doses of X-rays. All mutation induction frequencies depending on the experiments and the dose points are tabulated in Table 4.3. Increase in the mutation frequencies of the Experiment III following X-irradiation can clearly be seen in the corresponding frequencies.

4.2.2 Isolation of Independent HPRT Mutant Clones

82-6 hTERT cells grown to confluence as monolayers were irradiated with acute doses of X-rays, and independently arising HPRT mutants were detected by resistance to 6-thioguanine. Mutant colonies were isolated from plastic dishes and expanded individually. As also observed in previously produced HPRT mutants, isolated clones of these experiments varied

widely in their growth capacity. Clonal expansion after selection was extremely poor. Each experiment was started from a small number of cells to minimize the inclusion of pre-existing spontaneous HPRT mutants. Untreated cultures were held under the same conditions but without exposure to irradiation.

Given below are the number of mutant clones for each experiment that were initially isolated and expanded independently for analytical methods such as genomic DNA and RNA based analyses as described in detail under Materials and Methods.

Experiment I:

28 HPRT mutant clones were initially examined by several analytical methods. These mutant clones consisted of 2 spontaneous mutants, 7 x 2-Gy mutants and 19 x 6-Gy mutants. Some mutant clones with identical genetic patterns were removed from the final data set.

Experiment II:

15 HPRT mutant clones were the total number of collected mutant clones. There were 6 spontaneous mutants and 9 x 2-Gy mutants. None of the 6-Gy-induced mutants were expanded here, because the colonies only became visible after being stained for counting assessments. A few of the mutants clones were excluded from the final data set because they showed identical patterns.

Experiment III:

28 HPRT mutant clones were collected from this experiment. 13 x spontaneously arising mutants; 15 x 6-Gy-induced mutants. 2-Gy induced mutant clones were not isolated for the analyses. Following background correction, a few mutant clones were excluded from the final assessments, since the corresponding spontaneous mutation frequency was relatively high in this experiment .

Isolating one cell colony per dish ensured independence, but sometimes more than one mutant colony from the same dish was picked to offset losses attributable to senescence. In such cases a mutant was considered as independently derived if it was found to have a molecular change in the HPRT gene that was clearly different from those in mutants derived from the same culture. Apart from this, mutant colonies were isolated randomly, without regard to colony size. Every mutant clone isolated was put through a screening process in which the resistance to 6-thioguanine was further tested to confirm the HPRT mutation of the mutants. Mutant clones were expanded in cell culture until sufficient numbers of cells were made available for isolations of genomic DNA and RNA. The growth of mutant clones was almost comparable with that of wild-type cells, though the mutant clones that had larger deletions (total deletions) showed retardation of cell growth after a few doublings of cells.

Genomic and complementary DNA of these mutant clones were analysed by several methods including Pulse Field Gel Electrophoresis (PFGE), Southern hybridisation, Multiplex PCR, RT-PCR, Fluorescent *in situ* hybridisation (FISH) and DNA sequencing.

4.2.3 *NotI* Cleaved Restriction Analysis of HPRT Mutation

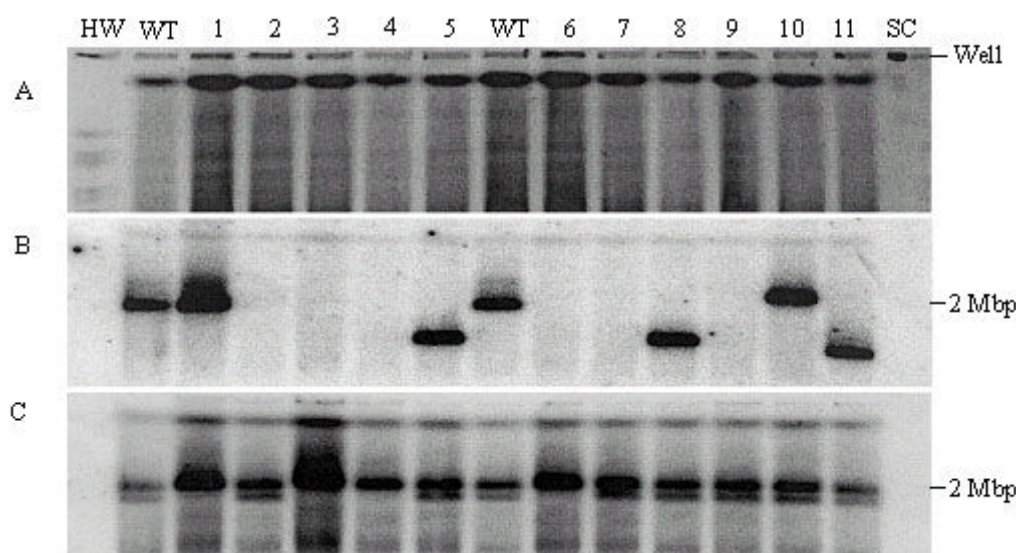


Figure 4.7. Representative diagram showing the restriction banding patterns of *NotI* digested genomic DNA of 11 x HPRT deficient mutant clones in 82-6 hTERT cells that were exposed to 6-Gy of X-rays. Fragment patterns were visualized by Southern hybridisations using two different [32 P] dCTP radioactive single probes serially: DXS1327 radioactive probe which detects a *NotI* fragment of 2 Mbp containing the HPRT gene and with the binding site 200 kbp telomeric from the gene; D21S4 hybridises to a *NotI* fragment of 2 Mbp and serves as a reference for each mutant genomic DNA. *Panel A:* Ethidium bromide-stained UV picture; both end lanes are loaded with chromosomal DNA of *Saccharomyces cerevisiae* (Sc) and *Hansenula wingei* (Hw) as size markers, while the complete *NotI* enzymatic digestion can be seen in all the lanes. *Panel B:* Southern blot picture of genomic DNA of mutant clones with WT genomic DNA; starting with wt, samples 1 and 10 display normal banding patterns, 5, 8 and 11 exhibit aberrant banding patterns (small) and the remaining samples 2-4, 6, 7 and 9 give no signals indicating the occurrence of large deletions in mutant genomic DNA. *Panel C:* Southern hybridisation picture of the same membrane with probe D21S4 which served as the reference; regardless of the Southern banding pattern with probe DXS1327, all the samples show a band size of 2 Mbp confirming that the mutation only occurred in the HPRT gene locus. Failure to form 2 bands instead 1 band with D21S4 probe did not affect the final classification of mutants.

As expected, the restriction band distribution patterns of the mutant clones were comparable with those of the previously analysed MGH-U1 HPRT mutant clones. Figure 4.7 shows a representative diagram of the Southern-blot-banding patterns of 11 HPRT mutant clones in hTERT-immortalised primary fibroblasts.

The results of *NotI* digested restriction fragment analysis:

Experiment I:

The two spontaneous mutant clones analysed, showed normal band sizes. Among the 2-Gy-induced mutants (7), 5 retained normal band sizes. One of the remaining mutants gave no signal on Southern blots, while the other mutant had an aberrant (large) band size. Among 6-Gy mutants (19), 2 showed normal band size. 3 gave no signal, and one mutant had a small/large double restriction band while the remaining 13 exhibited aberrant restriction fragments.

Experiment II:

Of six spontaneously arising mutant clones 4 showed normal band sizes. The other 2 had single aberrant bands representing large and small sizes. Among the 2-Gy-induced mutants (9), 2 showed normal band size, 3 gave no signals and the remaining 4 mutants displayed aberrant band sizes (3 x small, 1 x large).

Experiment III:

There have been thirteen spontaneous mutants that were exclusively analysed by restriction fragment analysis. Of those, only two mutant clones retained aberrant restriction bands (2 x large) while the remaining 11 had normal restriction bands. Of 15 x 6-Gy induced mutant clones, the majority appeared to have normal band size in *NotI* digested fragment analysis, compared to the spontaneous mutation rate it can be assumed that these clones arose spontaneously, because the spontaneous mutation induction frequency in this experiment was significantly higher than in the other two experiments. However, 3 mutant clones were found to have altered *NotI* fragments (2 x small and 1x large), while 2 mutant clones gave no radioactive signal suggesting a deletion in the probe binding sites of their genomes. All the remaining mutant clones (10) retained an unaltered restriction band size on the corresponding blots indicating a mutation may have been a result of point mutation in the exons of the gene. Since the spontaneous mutation frequency is found to be higher in the experiment, the final number of radiation-induced mutant clones was later calculated by subtracting the respective

Background mutation correction (as given in Schmidt & Kiefer, 1998)

Mutation frequencies of spontaneously arising mutant clones and 6-Gy-induced mutant clones of Experiment III were 19.5×10^{-6} and 70.5×10^{-6} respectively (Table 4.3). Since markedly elevated spontaneous mutation frequency was observed and these mutant clones contribute significantly in the fraction of radiation-induced mutation, background mutation correction is mandatory. This correction was made as has been explained in a previous report in which radiation-induced mutation in a CHO cell line was investigated (Schmidt & Kiefer 1998). To correct the complete pattern, each mutant type present in the background mutation fraction was weighted considering its relative distribution in the number of initially collected (assuming all these were radiation-induced) mutant clones and then proportionally subtracted from the total number.

Table 4.4a. X-ray-induced mutant clones

Pattern of Restriction Fragment	Total	%	Induced	%
Normal	10	66.7	0	0
Large	1	6.7	0	0
Small	2	13.3	2	50
No signal	2	13.3	2	50
	15	100	4	100

Table 4.4b. Spontaneous mutant clones

Pattern of Restriction Fragment	Total	%
Normal	11	84.6
Large	2	15.4
Small	0	0
No signal	0	0
	13	100

number of spontaneously arising mutant clones from the total number of mutant clones that were initially collected for the analysis. Thus, the absolute number (radiation-induced mutant clones) was only 4 mutant clones. Among these 4 mutant clones 2 mutant clones gave no signals and the other two were aberrant (small) in their band formation (Table 4.4a. and b).

An explanation for the mutant clones showing unaltered migration lengths (equal to 2 Mbp) may be that the mutation that occurred is of the small-scale type such as base pair changes in the HPRT exon sequences. The aberrant fragment sizes indicate that genomic rearrangements are responsible for the inactivation of the HPRT gene in the affected mutant clones. The lack of a hybridisation signal on Southern blots suggests the deletions of the probe-binding site. Double-restriction bands such as small /large may be a result of two sub clones or duplication of the HPRT gene in that mutant clone (see also 4.2.3.1).

4.2.3.1 Detailed Analysis of Mutants with Double-Restriction Bands

Among the examined HPRT mutant clones a small number showed two differing sizes of *NotI* restriction fragments with the HPRT specific radioactive probe (see Figure 4.8). These represented small /normal, normal /large, large /large and large /small. To find out what caused two different sizes of restriction fragments, a separate experiment based on sub-cell clones (sub clones made of original HPRT mutant clones) was designed.

Fresh cell cultures (from frozen stocks) were prepared by thawing two selected mutant clones. The cells were grown to confluence before being used for the experiment. 200 cells of each HPRT mutant clone were seeded 2 x in triplicate and selected for their resistance to 6-thioguanine. After 12 day of incubation, 6 independent sub clones were isolated from each mutant clone. Figure 4.8 depicts the distribution of band migration of the mutant sub clones in Southern hybridisation analysis. The reference panel demonstrates only a single band of 2 Mbp for all the samples. Among the size alterations of sub clones: 2 Mbp (normal), > 2 Mbp

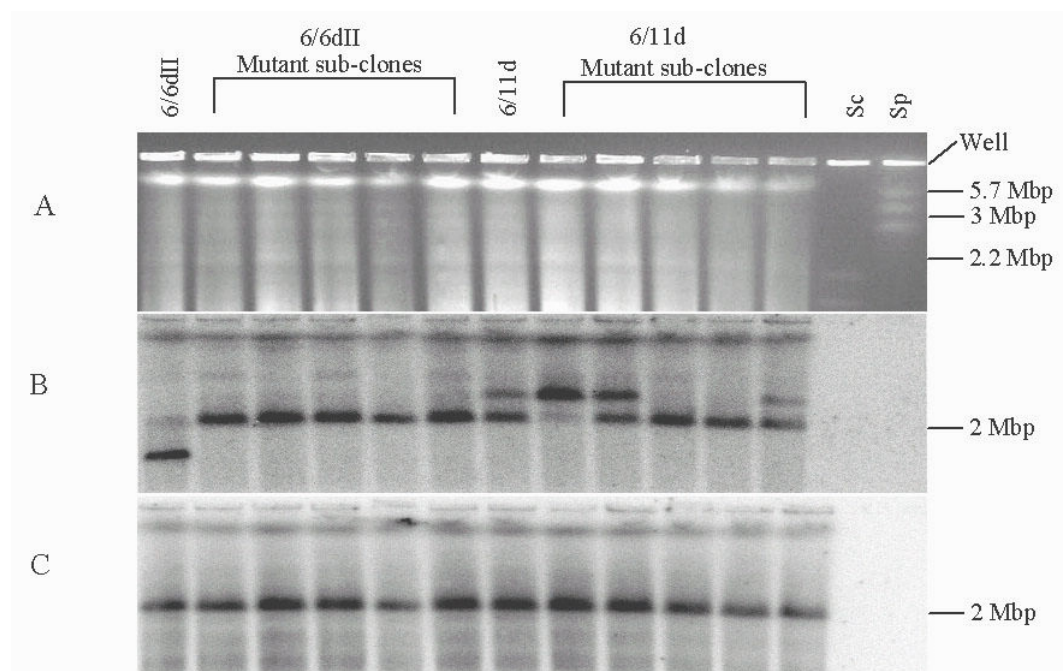


Figure 4.8. Detailed fragment analysis of mutant clones 6/6dII and 6/11d: Two selected HPRT mutant clones whose genomic DNA already showed two unequal sizes of *NotI* restriction migration lengths on Southern blots with DXS1327 radioactive probe have further been examined for their double band formation. *Panel A:* Ethidium bromide-stained UV picture. The last two lanes of this gel picture were loaded with chromosomal DNA of *S.cerevisiae* (Sc) and *S.pombe* (Sp) as size markers, while the complete *NotI* digestion can be seen in all the lanes in which genomic DNA of sub clones were loaded. *Panel B:* Southern blot picture of genomic DNA of loaded sub- clones and the original mutant clones. Lane 1: genomic DNA of original mutant clone 6/6dII; Lanes 2-6: genomic DNA of sub- clones of 6/6dII; Lane 7: genomic DNA of original mutant clone 6/11d; Lanes 8-12: genomic DNA of sub- clones of 6/11d. The fragment migration lengths remained as measured for original clones, while a few of sub- clones still show two different sizes of bands as seen in original clones. *Panel C:* Southern hybridisation picture of the same membrane with D21S4 probe which served as the reference as described above. All the samples show hybridisation band size of 2 Mbp confirming the mutation is only based on HPRT gene locus.

(large), < 2 Mbp (small) and combination of all types as two bands can be seen on the blot. All 6/6dII sub clones showed a normal fragment size, although this represented the minor band in the original DNA preparation. Three of 6/11d sub clones retained the double fragment pattern, while 2 clones exhibited normal band sizes. A potential explanation for the reappearance of two different sizes of bands representing original samples could be that these mutant clones were mixed with two different sub clones.

4.2.4 Multiplex PCR-based HPRT Exon- Deletion Analysis

Intragenic and end deletions at the HPRT gene locus were screened by multiplex PCR. Only mutant clones of the first two experiments were analysed by multiplex PCR.

Multiplex PCR results of the mutant clones:

Experiment I:

The two spontaneous mutant clones retained all 9 exons (wild-type). Of 7 x 2-Gy induced mutants, 5 gave wild type pattern, one had none of the exons (total deletion) and the other (2/10d) lacked exons 7+8 (partial deletion) indicating an interstitial deletion in the HPRT gene. The mutant clone that had a total deletion in the coding sequence gave no hybridisation signal with a HPRT gene specific single copy probe in *NotI* coupled hybridisation analysis, which indicates that this mutant clone has a minimum deletion of 200-250 kbp in the HPRT gene region.

Among the 6-Gy-induced mutant clones (19), 14 had all exons in their HPRT gene. Of these, two had normal restriction band size and some mutant clones were isolated from the same plastic dishes. For example, mutants 6/5dI, 6/5dII and 6/5dIII were picked from the same dish and gave similar results both in restriction fragment analysis and in multiplex analysis. However, there were mutants picked from the same culture dish which showed distinct mutational patterns. 6/6dI and 6/6dIII for example showed the same size of aberrant *NotI* restriction band on respective Southern blots, while 6/6dII gave double-band (see also Figure 4.8) but all 3 retained all HPRT exons in the coding sequence. Also, 6/20cI and 6/20cII have wild-type patterns in PCR analysis but in restriction fragment analysis they showed small and normal sizes of *NotI* restriction bands respectively.

6/6b and 6/9d had total deletions in PCR analysis and both gave no-signals on their Southern blots indicating a minimum deletion of 200-250 kbp in their genomes. Of the 3 mutant clones with partial deletions, one (6/3b) had an end deletion of exons 7-9 while the other 2 had intragenic deletions that resulted in the loss of exon 3 (a minimum deletion of 1059 bp). These two latter mutants (6/7aI and 6/7aII) had been picked from the same dish and showed the same size of restriction band (small). The mutant that lacked exons 7-9 (interstitial) had a no-signal pattern on the corresponding Southern blot. This may have either resulted from a minimum deletion of 203 kbp in the gene or may represent a rearrangement most likely starting from the end of the gene and spanning beyond it. Cleavage of genomic DNA of this mutant may have produced a larger *NotI* fragment, that may not be separable as a result of resolution limits in PFGE. Mutant clone 6/11d which was analysed in detail by Southern hybridisation due to the double band patterns also retained all exons.

Experiment II:

Of 6 spontaneous mutant clones, 3 retained all exons and had normal restriction bands in Southern analysis. 2 mutant clones that displayed normal and small band sizes according to

4 RESULTS

Table 4.5. Comparison of spontaneous and X-ray-induced HPRT mutant clones in human hTERT-immortalised fibroblasts (82-6 hTERT cells).

X-rays	Number of Analysed Clones	Pattern	PCR Analysis	Restriction Fragment Analysis	RT-PCR Analysis
			Failed Exons		
6-Gy	14	10 WT	none	4 x large ^a 3 x small ^b 3 x normal	no products no products 3 x products
		2 PD	7-9 3	1 x no signal 1 x small ^c	no product no product
		2 TD	all	2 x no signal	no products
		4**		2 x no signal 2 x small	
2-Gy	11	4 WT	none	4 x normal	4 x products
		3 PD	7-8 1-5 1-2	1 x large ^c 1 x small 1 x small ^c	no product no product no product
		4 TD	all	1 x normal 3 x no signal	no product no products
0-Gy	5	4 WT	none	4 x normal	4 x products
		1 PD	1-3	1 x large	no product
		13**		2 x large 11 x normal	

Abbreviations: WT- wild type pattern including all HPRT exons; PD-partial deletions missing one or multiple number of HPRT exons; TD - total deletions missing all HPRT exons; normal = 2 Mbp restriction fragment; Large > 2 Mbp; small < 2 Mbp.

^a one of these WT mutant clones (6/12d) gave a reciprocal translocation between X-chromosome and chromosome 2

^b one of these WT mutant clones (6/6dI) gave a non-reciprocal translocation between X-chromosome and the autosomes.

^c these three PD mutant clones (6/7aI, 2/10d and 2/11d*) each gave a non-reciprocal translocation between X-chromosome and the autosomes.

Two mutant clones whose namings appeared to be the same, therefore, one of them (from Experiment II) was named as 2/11d*.

** these mutant clones were examined only by restriction fragment analysis
only mutant clones with unaltered fragment gave a product in RT-PCR analysis

restriction fragment analysis lacked all exons (total deletion). Both of these mutants should have a minimum deletion of 50 kbp, representing the size of the HPRT gene. The remaining spontaneous mutant had an interstitial deletion missing exons 1-3 and gave a large *NotI* fragment in Southern blot analysis.

In the group of 2-Gy induced HPRT mutant clones, there were 7 total deletions missing all exons and 2 partial deletions. Of these 7 total deletions, 3 mutant clones gave no signals in Southern blots. One of them (2/2c) was an independent mutant clone while the

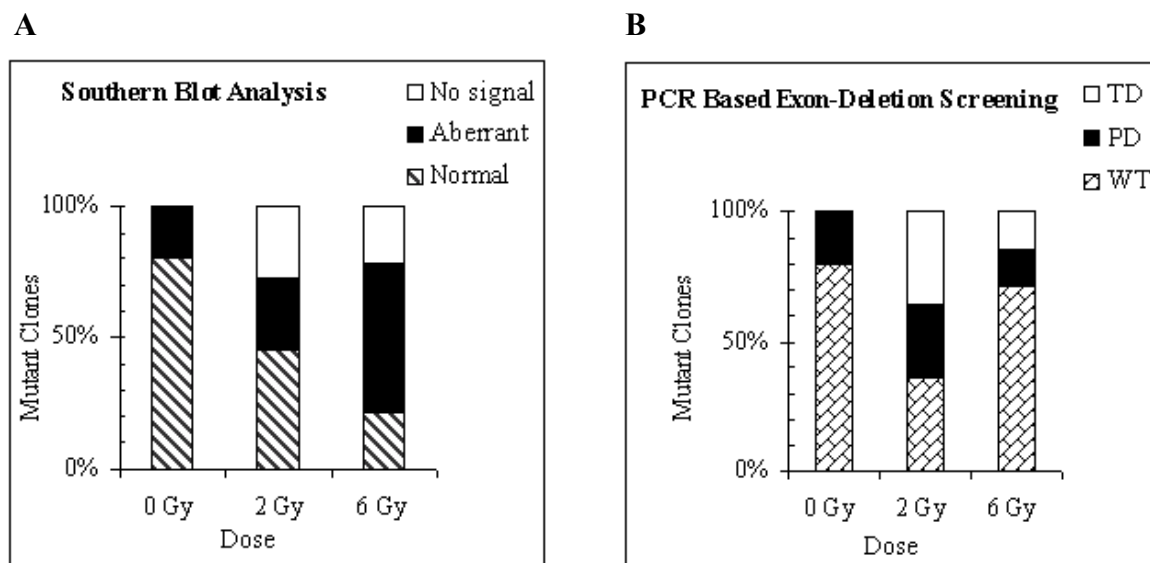


Figure 4.9. Mutation patterns of 5 x spontaneous, 11 x 2-Gy X-ray-induced and 14 x 6-Gy X-ray-induced mutant clones. Panel A: Southern blot results of *NotI* restriction fragment alterations according to hybridisation assay. Panel B: PCR results of genomic DNA of mutant clones in which a wild-type pattern of exons (WT), partial deletions (PD) and total deletions (TD) of HPRT 1-9 exons are screened.

other two (2/7cI and 2/7c II) were picked from the same dish and could be dependent. The remaining 4 mutant clones with total deletions in the gene showed varying characteristics. Two of them (2/5cI and 2/5cII) were picked from the same dish and hybridised to the same sized unaltered restriction fragment. The other two retained aberrant fragments (small).

Of two partial deletions, one mutant clone had a deletion of exons 1-2 (a minimum size of ~1200 bp) and the other missed exons 1-5 (a minimum size of ~3360 bp). Both of the mutant clones contained altered restriction fragments (large and small). To have a total deletion in the gene, mutant clones should have lost at least a sequence sized 50 kbp, while the mutant clones with total deletions both in Southern hybridisation and PCR screening should have a minimum deletion of 200-250 kbp in the gene.

Table 4.5 summarises all the mutant clones according to the patterns that they showed in each analytical method. Mutant clones that gave double hybridisation bands and the mutation signatures were found to be the same (mutant clones that were picked from the same petri dish and retained similar mutant characteristics) were removed from the number of mutant clones that were initially subjected to analysis. Restriction fragment size alterations and PCR patterns obtained for all 30 mutant clones derived from hTERT-immortalised fibroblasts are given in Figure 4.9. Panel A clearly demonstrates that the mutant patterns obtained by Southern analysis based on hybridisation assay are dose dependent. However, small sampling of the mutant clones has caused the decrease in the no signal fraction with increasing the doses (compare also Figure 4.17 Panel A). By contrast, PCR results give no

such a dose-dependence tendency for 2 and 6-Gy mutant clones (Panel B) (compare also with Figure 4.17 Panel B), although the PCR results for 0-Gy mutant clones are comparable with that of Southern blot results. Further, A considerable fraction of aberrant HPRT mutant clones are related to WT patterns rather than to PD patterns. This can clearly be seen in the fraction of 6-Gy mutant clones (Panel B). Furthermore, TD pattern of 2-Gy mutant clones is increased because one single 2-Gy mutant clone with normal restriction fragment retained a TD pattern (see Table 4.5).

4.2.4.1 Break Point Mapping of Two Selected HPRT Mutant Clones

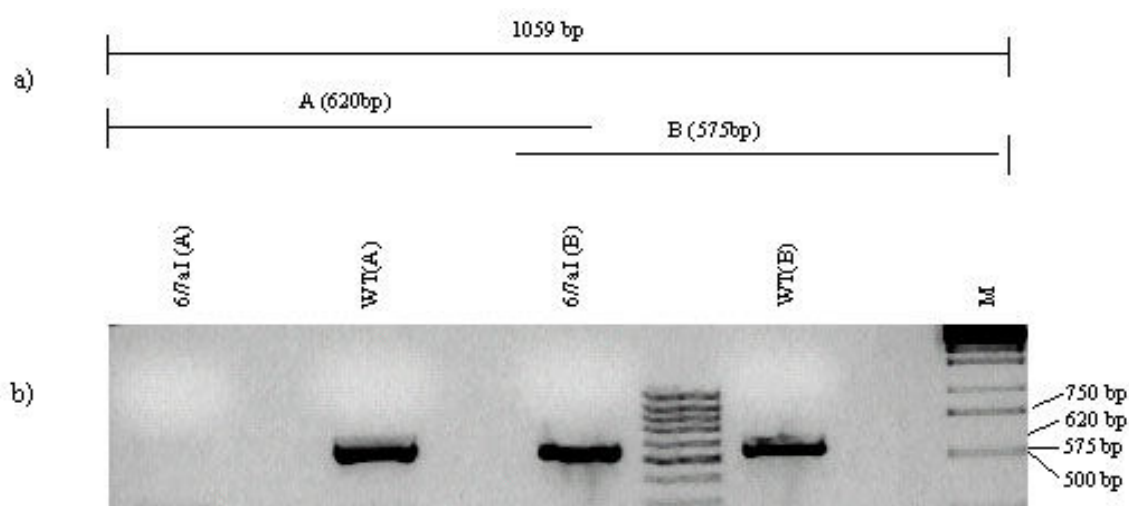


Figure 4.10. Detailed analysis of genomic DNA of HPRT mutant clone 6/7aI which rendered a translocation between the X-chromosome and the autosomes: a) Schematic diagram of two newly designed fragment sizes of a 1059bp-fragment (Part A and B with respective sizes of 620 bp and 575 bp), that amplified previously to detect exon 3 in HPRT gene; b) Ethidium bromide-stained 1.5% agarose gel picture of electrophoretically separated PCR products of wild-type and 6/7aI mutant clone. From left to right: Part A of mutant clone indicating a deletion in targeted region and the presence of its Part B in the mutant genomic DNA, M is a DNA size marker.

Two mutant clones (6/7aI and 2/10d) that had translocations according to cytogenetic studies (Figure 4.13) with probes specific for the X-chromosome were subjected to further analysis. These mutants had intragenic deletions according to multiplex PCR analysis. Mutant clone 2/10d had a deletion in exon 7/8, while the other mutant clone (6/7aI) lacked exon 3. The genomic rearrangements that caused these two mutant clones to form aberrant *NotI* restriction bands, should have occurred within the HPRT gene. To find out the regions neighbouring the break points on the gene, a nested-PCR was performed with new sets of primers. For the mutant clone 6/7aI (Figure 4.10a), two PCR reactions were performed to amplify two fragments within the 1059 bp original PCR product.

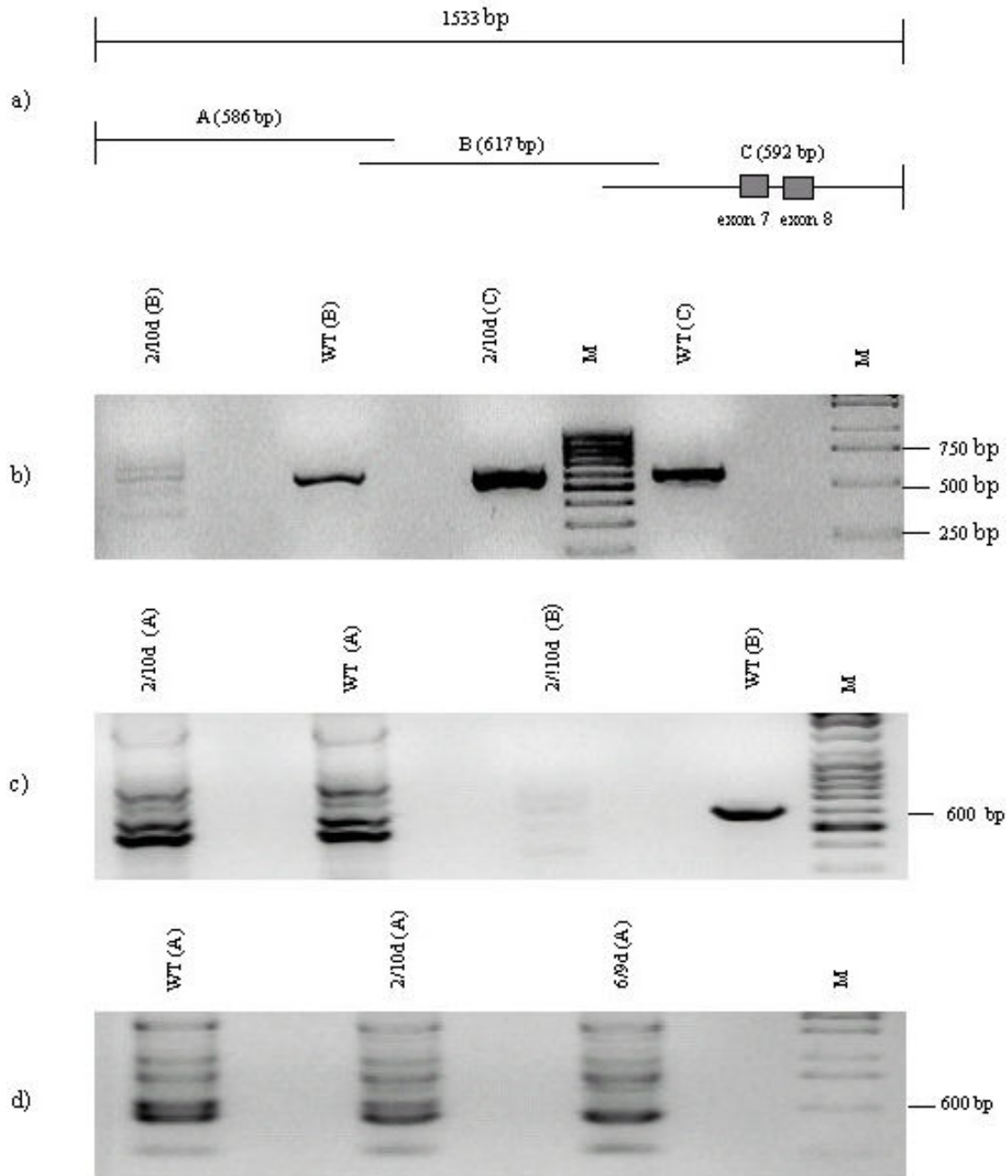


Figure 4.11. Detailed analysis of genomic DNA of mutant clone 2/10d which had a non-reciprocal translocation between the X-chromosome and the autosomes: a): Schematic diagram showing parts A, B and C along the fragment that was amplified during exon-deletion screening whereby Part C contains both exons 7 and 8; b): Ethidium bromide-stained gel picture of electrophoretically separated PCR products of Part B and C of both wild type-control and the mutant clone indicating presence of Part C and absence of Part B; c): Gel picture of repeated amplification of Part B together with Part A confirming the absence of Part B while showing the presence of Part A; d): Reconfirmation of the presence of Part A in mutant genomic DNA with a known mutant clone (6/9d) which has a total deletion covering the entire HPRT gene. Besides non-specific PCR products, it clearly shows the presence of the targeted 586-bp fragment (Part A) in the mutant and WT, whereas Part B seems to be lost in the mutant.

A picture of an ethidium bromide-stained gel of electrophoretically separated fragments of mutant clone 6/7aI is shown in Figure 4.10b. It can be seen that mutant clone 6/7a I failed to give a PCR product for amplicon A (contains exon 3 sequence), whereas the WT control was positive. The fact that fragment A could not be amplified suggests that the breakpoint has occurred in this region. This suggests that the break point should be located between 16252 to 16872 bp (620 bp) on HPRT gene (Gene bank sequence).

Since the clone 2/10d gave no product for exons 7+8 in multiplex PCR screening and had a large *NotI* fragment according to restriction fragment analysis, it seemed likely that a genomic rearrangement caused the mutation. To locate the approximate regions of the breakpoint, new primers were designed to amplify specific fragments within the original 1533 bp-long PCR-fragment. Figure 4.11a shows a schematic drawing of the fragment sizes and their locations. The picture of the ethidium bromide-stained gel in Figure 4.11b shows the amplification of parts B and C compared to the wild-type positive control. Here, it can be seen, that part B was not amplified whereas part C gave the expected PCR product. Figure 4.11c shows the gel picture of the PCR products of part A and B compared with positive controls. Amplification of part B again failed whereas PCR of fragment A using both mutant and control genomic DNA gave non-specific products. The fragment representing part A was re-amplified to ensure the accuracy of the PCR results. Two different controls were included. These controls were wild-type and a HPRT mutant clone with a deletion covering the entire HPRT gene (6/9d). As can be seen in the gel picture in Figure 4.11d, PCR products were not present in 6/9d indicating this fragment is available in the genome of the 2/10d mutant clone.

In conclusion, the mutant clone 2/10d retained the two exons but missed an intronic sequence spanning from 39106 to 39723 bp on the HPRT gene (Gene Bank sequence; M26434). According to these results, the break point for the genomic rearrangement within the HPRT gene of the mutant clone 2/10d should be within this sequence.

4.2.5 mRNA Isolation and RT-PCR

The majority of the mutant clones whose genomic DNA displayed wild-type pattern according to multiplex PCR screening showed restriction fragment alterations. This is an indication for the formation of genomic rearrangements either in regulatory regions or in intronic sequences of the HPRT gene of mutant clones. To confirm the HPRT mutations mRNA-HPRT transcripts of clones were examined. The total RNA, including HPRT-mRNA of mutant cells, was isolated and subsequently, HPRT-mRNA was converted into HPRT-cDNA using dT primers. Two sets of primers (outer and inner) were used to amplify PCR

products of 761 bp and 737 bp so that both products contained all 9 exons of the HPRT coding sequence. The first PCR product was subjected to a nested PCR in order to guarantee the accuracy of PCR results. A representative UV-agarose picture of electrophoretically separated RT-PCR products is demonstrated in Figure 4.16.

Only mutant clones that gave an unaltered restriction band pattern in *NotI* restriction fragment analysis synthesised PCR products, while the mutants that showed aberrant restriction bands or no hybridisation-signals gave no RT-PCR products. This is an indicator of whether the intact HPRT gene is located on one chromosome or scattered on unrelated chromosomal parts. In order to give RT-PCR products, exons of the mutant clones should be on the same chromosome or at least the entire coding sequence should be intact, since the primer positions were designed to cover all the coding sequence together with the flanking sequences of the HPRT gene. Since the predominant number of mutant clones gave no HPRT-mRNA transcripts, though more than 75% of the clones showed wild-type exon pattern, further confirms that the break points caused by X-rays occurred in intronic HPRT gene regions rather than in other sites of the gene.

However, there were very few HPRT deficient clones whose restriction band sizes were aberrant but nonetheless synthesized the RT-PCR products. These particular mutant clones may be mixed with mutant clones whose genomic DNA retained normal restriction band size or consisted of some exons and therefore could produce unexpected results in the analysis. This was revealed by a detailed analysis carried out with the respective mutants and are described in 4.2.3.1.

Experiment I:

Both spontaneous mutants gave RT-PCR products indicating the presence of all 9 exons within the normal sized restriction band as revealed by Southern analysis. Of the 2-Gy induced mutant clones, 5 retained HPRT-mRNA transcripts, while two mutant clones failed to amplify the fragment specific to coding region of HPRT gene. One of these two contained an aberrant restriction fragment and the other gave no-signal pattern on Southern blot. All mutant clones that showed HPRT mRNA transcripts gave a normal banding pattern on their Southern blots. This indicates that the genomic DNA of this type of mutants have WT- exon-order in the coding region; while the other type of mutants with aberrant restriction fragments have exons scattered in different parts of chromosomes.

Among the 6-Gy mutant clones, only 4 mutant clones formed HPRT-transcripts, while the remaining 15 failed to produce RT-PCR products indicating no transcripts can be formed. All 4 mutant clones that gave amplicons also displayed normal restriction bands on their

Southern blots. All mutants that failed to produce PCR products gave either no-signal pattern or aberrant *NotI* fragments in Southern analyses. This is significant evidence that the exons of mutant clones are located in unrelated parts of chromosomes or not similar to the manner in the genomic DNA of wild-type cells.

Mutant clones 6/6dII and 6/11d also gave products proving the presence of their sequential order of exons, in contrast, 6/6dII had an aberrant restriction band (small) whereas 6/11d gave a combination of two aberrant bands (large and small). Therefore, both were further analysed as described under 4.2.3.1 and revealed that both had been mixed. In conclusion, mutant clones that retained normal restriction band on Southern blots were the only ones that synthesized transcripts and all mutant clones that failed to show Southern hybridisation signals have been unable to give RT-PCR products.

Experiment II:

Of 6 spontaneous mutant clones, all except one synthesized RT-PCR products and the remaining mutant was the one with a terminal deletion that resulted in the loss of exons 1-3. Surprisingly, two mutants that gave total deletion patterns in multiplex PCR analysis, gave RT-PCR products. The coding sequence of the HPRT gene must have been there so that these two mutant clones could produce mRNA transcripts. However, this could not be explained by any means. All the other 3 mutants retained the normal pattern of restriction fragment in Southern analyses. Of 2-Gy induced mutant clones, only two mutant clones gave PCR products indicating these two may have the coding sequence of the HPRT gene. But according to PCR exon-deletion screening, both missed 9 exons in the coding sequence of the gene. Both mutant clones retained an aberrant size of restriction fragment (small). No explanation for the amplification of transcripts in the absence of all 9 exons could be found here. However, as before, the mutant clones that showed aberrant restriction fragments synthesized no HPRT-m RNA transcripts.

4.2.6 DNA Sequencing

To verify the mutations and to identify the nature of small scale mutations (point mutations in the HPRT gene locus), 10 samples were subjected to automated DNA sequencing.

Only nine RT-PCR products (Experiment I), i.e. those which gave unaltered restriction fragment bands in corresponding Southern blots and no exon-deletions in the HPRT gene, as suggested by multiplex PCR studies based on genomic DNA, were subjected to sequencing. One sample of wild type cells, from which mutant clones were originally selected, was added

to the group as a control. Further, none of these clones exhibited cytogenetic visible chromosomal aberrations in the examinations carried out in search of such abnormalities. The reason for the small number of mutant clones was that only a small number of mutant clones that retained normal restriction fragments could render RT-PCR products.

The samples were as follows:

Wild type cells as a control; spontaneously arising mutant clones K/28a and K/40f; 2-Gy X-ray-induced 2/11d, 2/15b, 2/14eI, 2/14eII, 2/16cII; 6-Gy X-ray-induced 6/10e and 6/20cII (see also Appendix Table 8.1).

Bio Edit version 5.0.6 (2001) of DNA sequencing software programme was used to compare sequences. Alignments were made with the Gene Bank sequence of the human HPRT cDNA (Data Bank: BC000578 Homo sapiens) as a consensus sequence. The control sample rendered no single base pair substitutions, deletions or insertions in its genome. The two spontaneously arising mutant clones, K/28a and K/40f, showed no sequence changes, though corresponding chromatograms were monitored repeatedly for the single base substitutions, deletions or insertions. At critical positions on such sequences, both strands were repeatedly examined. One credible explanation could be any kind of genetic changes in the sequence of the HPRT mutant clones beyond the focused regions or alterations in exon-intron junctions or regulatory sequential regions such as promotor, enhancing and silencing elements.

Of the 2-Gy-induced mutant clones subjected to DNA sequencing, only two mutants gave single base pair substitutions. Mutant clones 2/11d retained a single base substitution from A to C in exon 9. This transversion mutation caused a tyrosine to serine change. Formation of an aberrant HPRT gene product may most probably be the reason for the mutation of the mutant clone. The mutant clone 2/15b gave a single base substitution in exon 6. This leads to a C to T transition changing glycine to a stop codon, leading to nonsense mRNA and decay of the mutant transcript. Similar data have previously been reported (Hunter et al. 1996).

Of two 6-Gy-induced mutant clones, one mutant clone 6/10e showed a 77 bp long deletion in the complementary DNA of the mutant clone, whereas the other mutant clone gave no noticeable changes in corresponding sequencing data. The deletion found in 6/10e coincided entirely with the size of exon 8 of the HPRT gene. This deletion could also be noticed in the RT-PCR data, because the size of the PCR product was obviously smaller than 737 bp. As these data are solely based on cDNA, the mutation was analysed on the basis of

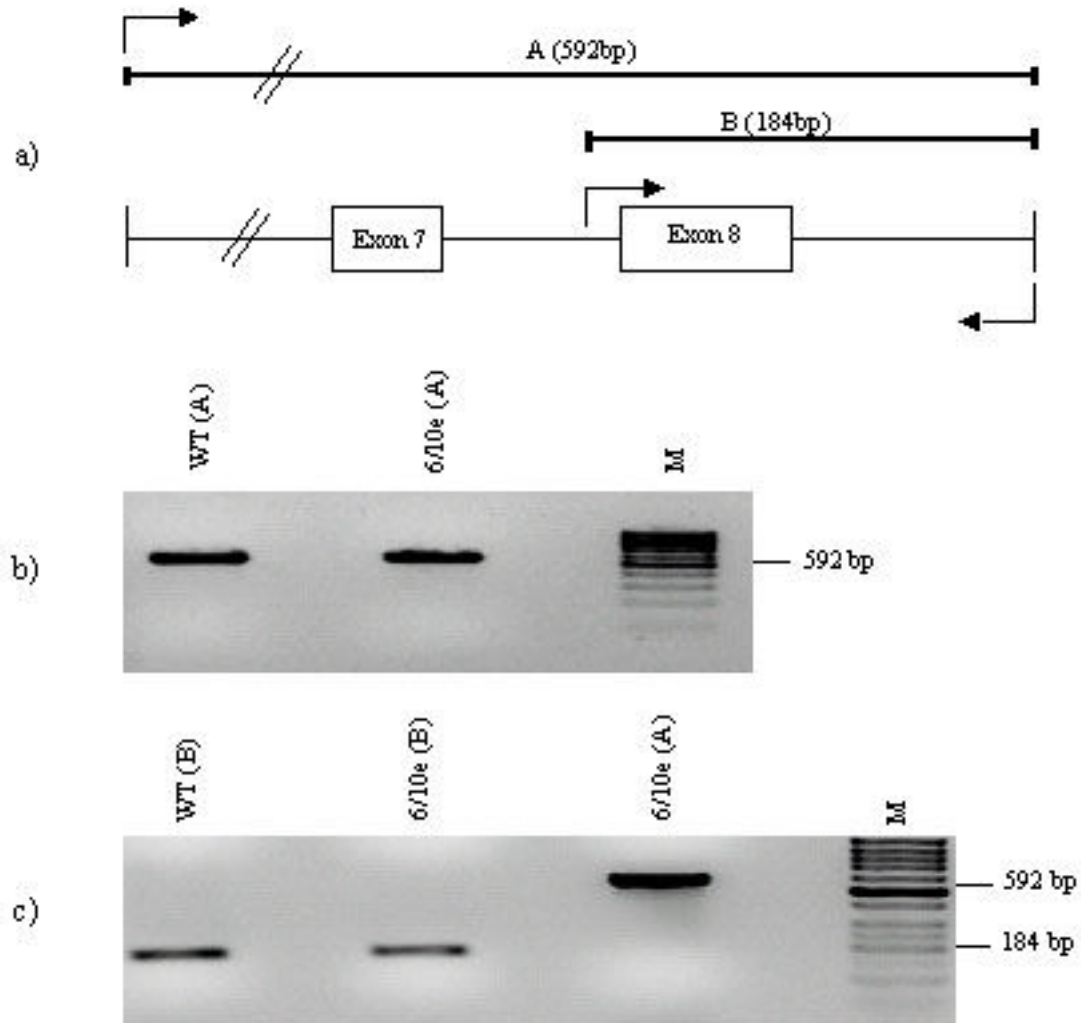


Figure 4.12. PCR amplification of genomic DNA from mutant clone (6/10e) that was missing the entire exon 8 in complementary DNA and identification of the deletion. DNA sequencing analysis of the mutant clone showed a total loss of exon 8 which is 77 bp long. To find out if this deletion is detectable on genomic DNA of the mutant clone, genomic DNA of the mutant clone was re-examined by PCR. The reaction products were separated on a 1.5% agarose gel and stained with ethidium bromide. Sizes of fragments were determined using a DNA size marker (M) loaded on the very right of the gel pictures: (a) Schematic drawing of the region of genomic DNA involved in the deletion, here two sets of primers were used for the amplifications. As seen in the diagram, the smaller fragment A (184 bp) represents exon 8 while the other fragment 592 bp in size is for both exons 7 and 8. (b) A gel showing the presence of both exons compared to a wild-type control. (c) A gel displaying the presence of exon 8 also compared to wild-type control. Results suggest that the deletion is only present on complementary DNA.

genomic DNA. Multiplex PCR previously rendered no exon-deletions in the genomic DNA of the mutant clone. As exons 7 and 8 have often been co- amplified as a single 1533 bp- fragment, amplifications were performed using two sets of inner primers for targeted products of 184 bp and 592 bp for exon 8 and exons 7+8 respectively. These results revealed that the

mutant clone has no deletions in genomic DNA. Figure 4.12 depicts the electrophoretically separated PCR results of 6/10e mutant clone.

Since there was no explanation for a deletion of this sort, a PCR product sized 592 bp (contained both exons 7 and 8 and end intronic regions) was synthesized using genomic DNA of 6/10e that got DNA sequenced on both strands. The sequence was compared with M26434 containing the 592 bp-fragment.

Sequential data of genomic DNA of the mutant clones revealed a single base substitution in the 3' end of intron 7. This mutation is a T to G transversion and lies 13 base pairs upstream to exon 8. Mutations in the exon or the intron outside of the consensus sequence can have strong effects (Andersson et al. 1992; O'Neill et al. 1998). Similar mutations of single base substitution such as this have been already reported (Leonhardt et al. 2000) and were discussed to cause splicing errors. Based on this information, it is likely that 6/10e mutant clone may most likely have a single nucleotide substitution in the 3' splice consensus sequences of intron 7.

4.2.7 Cytogenetic Screening Using Fluorescence *in situ* Hybridisation (FISH)

All the mutant clones from Experiment I and II were screened using chromosomal fluorescent *in situ* hybridisation (FISH) and 3 different fluorescent markers per chromosome: 1 (green), 2 (yellow) and X (red). This study focused mainly on the cytogenetic analysis of structural aberrations triggered in chromosomes after cells were exposed to single doses of X-irradiation. Translocations could be detected by heterogeneous scattering of fluorescent markers on the chromosomes that were focused for the painting. A large majority of mutant clones retained an intact X-chromosome indicating genetic rearrangements may actually be intra-chromosomal changes. Similarly, the ratio of the presence of these cytogenetically visible exchanges has been the same as other autosomal chromosomes (chromosomes 1 and 2).

Out of the 43 mutant clones examined in the study, including mutant clones with double Southern bands and identical characteristics (which were later removed from the final data set), only six mutant clones produced visible chromosome aberrations between the X-chromosome and the autosomes. Mutant clones 6/7aI and 6/7aII were later found to be identical (see Appendix Table 8.1). Therefore mutant clone 6/7aII was removed in the final

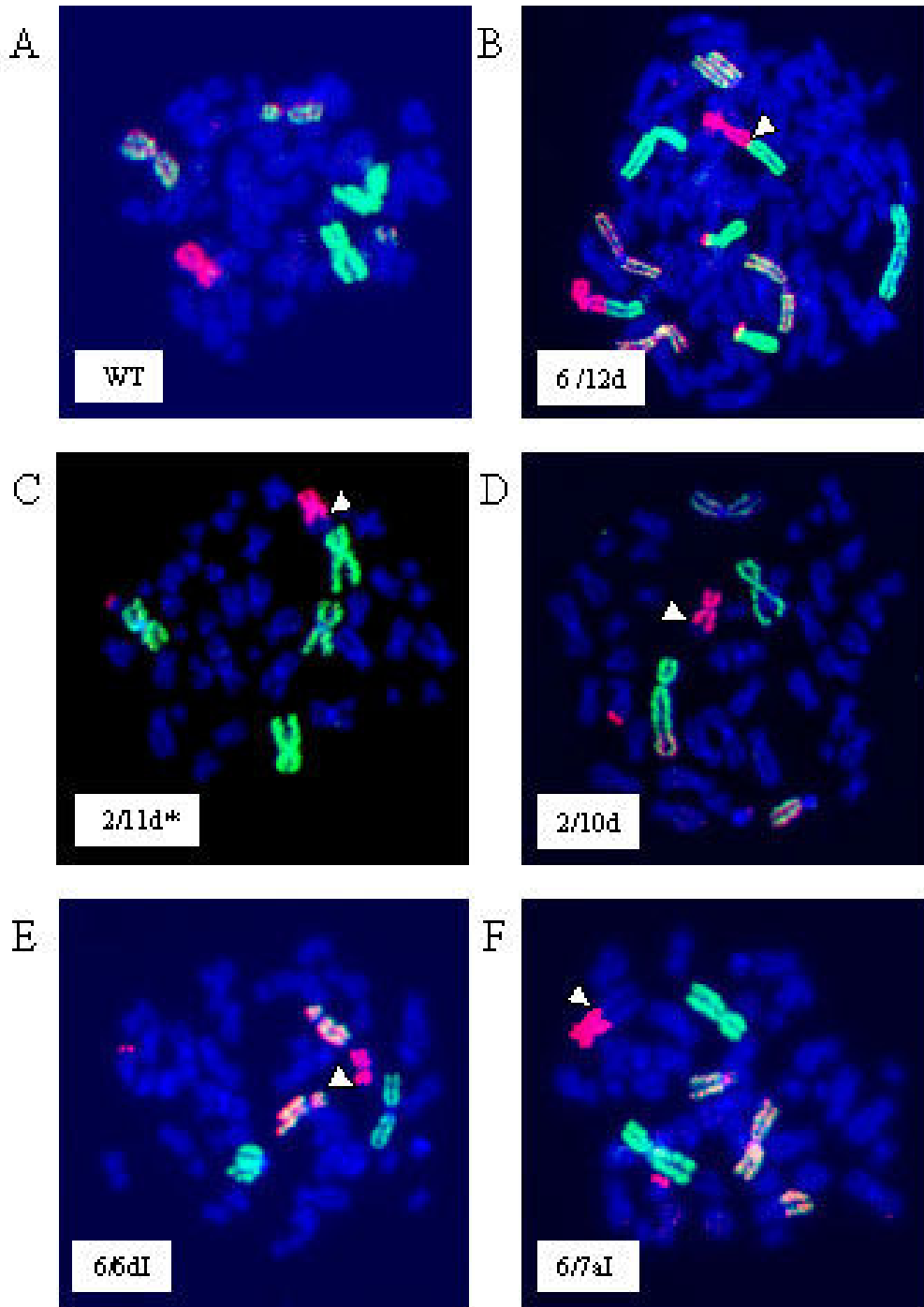


Figure 4.13. Fluorescence *in situ* hybridisation analysis of HPRT mutant clones in hTERT-immortalised fibroblasts: Metaphase spreading from mutant clones were painted with specific fluorescent probes for chromosomes 1 (green), 2 (yellow) and X (red). The remaining chromosomes are visualized by the blue counter-stain DAPI. *Panel A:* the presence of intact X-chromosome in a wild type hTERT-immortalised cell; *Panel B:* A reciprocal translocation between the X and 2 chromosomes of mutant clone 6/12d; *Panel C:* A non-reciprocal translocation between the X and targeted chromosomes in mutant clone 2/11d*; *Panel D:* A non-reciprocal translocation between the X and the other two chromosomes in mutant clone 2/10d; *Panel E:* A non-reciprocal translocation between chromosome X and the targeted chromosomes in mutant clone 6/6dI; *Panel F:* A non-reciprocal translocation between the X and the other two chromosomes. Changes to the X-chromosome are designated by white arrow heads.

data set. Figure 4.13 shows the results of the FISH analysis for one wild type (WT) and 5 x IR-induced HPRT mutant clones displaying translocations during the analysis. Mutant clone 6/12d gave a reciprocal translocation between the X and 2 chromosomes while all other mutant clones retained non-reciprocal changes between the X and the two chromosomes. Among 5 mutant clones, there were two mutant clones (6/12d and 6/6dI) accompanied by a WT pattern with the presence of all HPRT exons including aberrant restriction *NotI* fragments. The other three mutants with partial deletions (2/10d, 2/11d* and 6/7aI) in the coding segments of the gene also retained aberrant restriction fragments indicating gene inactivation as caused by genomic rearrangements (see Table 8.1 in Appendix).

The results obtained indicate that intra-chromosomal exchanges rather than inter-chromosomal exchanges may occur in genomic rearrangements after cells have been exposed to X-irradiation.

4.3 Fractionated Irradiation /Mutation Induction in hTERT-Immortalised Primary Fibroblasts

To explore the mutation induction mechanisms at low doses of X-irradiations, hTERT-immortalised primary fibroblasts (82-6 hTERT cells) were grown to confluence as implemented in the previous experiments and two independent mutation induction experiments were performed serially. The cells used for the first induction experiment showed at least 50% of plating efficiency (PE) at the time the cells were taken for the experiment, while the second one was based on cells of the same origin with a PE of was 10%. Conditions for cell growth and radiation were kept constant.

It is difficult to generate radiation-induced mutant clones after exposing them to a single low-dose of radiation, compared to single doses such as 2 and 6-Gy. To circumvent this problem, we have chosen fractionated irradiation of cells as the most appropriate alternative. Unlike 1-step single dose irradiations, cells were irradiated with smaller fractionated doses for a prolonged period of time in equal intervals. During the entire period of the partial irradiations, the control cell cultures were treated in an identical manner without exposing them to the X-ray source. Irradiations were administered in fractions to cell monolayers in 75-cm² flasks filled with culture medium. The total doses of X-rays of 6 and 18-Gy (with 0.2 and 0.6-Gy single fractions respectively) were delivered to a total number of 30 fractions: twice a day, consecutively, for a period of 15 days. To allow for DNA repair, cells were incubated for at least 10 h after every fractionated irradiation. Parallel to this, to compare the mutation with acute dose irradiations, several flasks of cells as confluent monolayers were also exposed to 2 and 6-Gy of single doses of X-rays and incubated at equal culture conditions. During the entire period of irradiations, changes of culture medium were made three times by replacing old medium with fresh MEM medium.

4.3.1 Surviving Fractions and Mutation Frequencies of Fractionated X-irradiated Cells

Survival rates for the immortalised fibroblasts were described previously and are given in Figure 4.6 (the diagram on the surviving data of hTERT-immortalised cells). In fact, the mutation-induction frequencies of Experiment I (Table 4.6) showed extensive variations even though the cells used for the experiments belonged to the same origin. After isolating the mutant clones, cell colonies were stained to determine the mutation frequencies. In calculating the mutation frequencies, the respective cultures of plating efficiency values for each dose

4 RESULTS

Table 4.6. Mutation Frequencies of 6-TG^r HPRT 82-6 hTERT-mutant clones depending on acute and fractionated X-ray doses employed; values are the number of mutants per million survivors.

<u>Experiment I</u>		<u>Experiment II</u>	
Acute dose ^c	Fractionated dose ^d	Acute dose ^c	Fractionated dose ^d
0-Gy : 18.16 ^a	0-Gy : 18.16 ^a	0-Gy : 5 ^b	0-Gy : 5 ^b
2-Gy : 60.2 ^a	0.2-Gy : 11.4 ^a	2-Gy : 23.9 ^b	0.2-Gy : 6.2 ^b
6-Gy : 73.7 ^a	0.6-Gy : 58.1 ^a	6-Gy : 101.8 ^b	0.6-Gy : 51.28 ^b

^a Average plating efficiency of confluent cells used for mutation induction was 50%. HPRT mutant clones isolated from these samples and the values are normalised by controls.

^b Average plating efficiency of confluent cells used for mutation induction was 10%. HPRT mutant clones isolated from these samples and the values are normalised by controls.

^c Cells were treated with 2 and 6-Gy of X-rays as single doses at the beginning of the experiments and were incubated under identical conditions till used for plating efficiency tests and thioguanine selections.

^d Cells were treated with fractions of 0.2 and 0.6-Gy for the total doses of 6 and 18-Gy of X-rays respectively. These fractions were delivered to confluent cell monolayers for 15 days consecutively as twice a day to a total of 30 serial irradiations. Between fractionated irradiations, at least 10 h was given cells to recover the lesions encompassed by radiation.

point were considered. All the frequencies are given in the Table 4.6 as the HPRT deficient mutant clones per million of surviving cells. Surviving fractions of the treated and untreated cells are illustrated in the Figure 4.14. As can be seen in the diagram, the cells exposed to fractionated irradiations of X-rays, have significantly increased cell survival compared to the cells exposed to X-rays of acute doses. At a total dose of 6-Gy, the cell survival following acute dose X-rays and fractionated X-irradiations showed 30% and 62% compared to control values with the respective mutation frequencies of 101.8×10^{-6} and 6.2×10^{-6} . Mutagenesis seems to have decreased to a 17-fold with a 2-fold increase of vitality in the cells after fractionated X-irradiation in the Experiment II. A 4-fold increase of the induced mutation frequency (Table 4.6) at equitoxic levels (survival rates at 2-Gy acute dose irradiation and 6-Gy fractionated irradiation were both ~60% as can be seen in Figure 4.14) further confirms the marked decrease in the incidence of HPRT mutations at fractionated irradiations. Comparable values for Experiment I were 73.2×10^{-6} and 11.4×10^{-6} for acute dose and fractionated irradiations for a total dose of 6-Gy of X-rays, resulting in a 1.2-fold increase in the survival following fractionated irradiation. Discrepancies among data are due to the variations in PE values of the cells used for the experiments. However, cells in both experiments (6-Gy fractionated X-irradiations (0.2-Gy x 30)) reduced the mutability of cells. Subsequently, cells were treated 30-times with fractions of 0.6-Gy, and it could be observed that at a total dose of 18-Gy the mutation frequency scored was $\sim 55 \times 10^{-6}$ for both experiments. When compared to the data for 6-Gy, despite a 3-fold increase in the dose, mutagenesis values of the cells were reduced ~2-fold in Experiment II and ~1.3-fold in

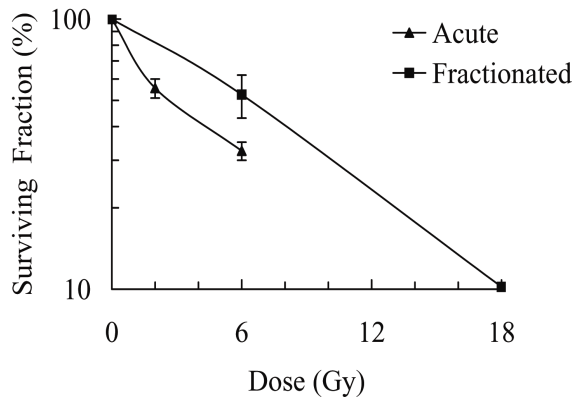


Figure 4.14. Survival data for fractionated X-irradiated experiments: Cells as confluent cultures were X-irradiated in two different ways. At the beginning of the experiments, several confluent cultures were irradiated with acute doses of 2 and 6-Gy of X-rays, whereas other cultures were exposed to the fractions of 0.2 and 0.6-Gy of X-rays for 15 days twice a day consecutively for total doses of 6 and 18-Gy respectively. Parallel to this, control cell cultures were handled with identical conditions except that they were not exposed to irradiations. After 22 day-(15 day-prolonged irradiation and the 7 day- expression time) incubation period, the cells of each group were plated in three sets of petridishes to determine the cloning efficiencies. Mean values of two independent experiments ($n = 2$) are shown in the diagram.

Experiment I. Cell survival at 18-Gy (fractionated irradiation) showed a ~ 3 -fold increase compared to that of the acute dose irradiation at 6-Gy. Furthermore, the mutation frequencies for 2-Gy acute dose irradiations in both experiments have shown markedly elevated values compared to fractionated 6-Gy irradiations. Overall data of these results suggest that mutation induction at the HPRT gene locus at fractionated irradiations of X-rays decreased significantly.

The mutation frequency of 6-Gy-fractionated cell cultures in Experiment II was nearly the same as the corresponding spontaneous mutation frequency (Table 4.6). Spontaneously arising mutant clones in Experiment I showed an unexpected mutation frequency, resulting in an 1.6-fold increase even above the value for 0.2-Gy fractionated irradiation. A plausible explanation for the markedly elevated mutation frequency in the spontaneously arising mutant clones in Experiment I may be due to the plating efficiency (at least 55%) of the cells used for the experiment.

4.3.2 Independence of Spontaneous /X-ray-induced Mutant Clones

During the two independently transacted mutation induction experiments, the HPRT mutant clones were isolated *en masse* in large X-irradiated cultures of the following treatment groups: (i) 0-Gy control cultures (ii) 2-Gy, with single dose irradiation; (iii) 6-Gy, with single dose irradiation; (iv) 6-Gy, split into equal fractions of 0.2-Gy (v) 18-Gy, split into equal fractions of 0.6-Gy. The HPRT negative cell colonies were selected in a 6-TG containing culture medium. The thioguanine-concentrations used here were the same as in previous experiments.

Following the last serial irradiation, the cell cultures were incubated for 7 days, allowing phenotypic alterations in the genome of the cells to appear. From the five treatment groups, a total number of 104 sub clones was collected. Control cell cultures were treated with identical culture conditions during the entire period of fractionated irradiations.

In most cases, one HPRT mutant clone per dish was chosen for the expansion of cells to conduct of downstream molecular analysis. However, in certain cases, more than one mutant cell colony was segregated. Because of the original experimental design, not all mutant clones displaying the same deletion patterns could unequivocally be considered to be independent mutants. However, the strategies used in selecting mutant clones throughout this entire study ensure in a proficient manner, the independence of a high proportion of selected mutant clones.

Experiment I

A total number of 47 HPRT mutant clones was isolated from independent cultures of unirradiated and irradiated with acute doses of 2 and 6-Gy and fractionated doses of 0.6-Gy. The mutant clones isolated in this experiment are as follows: 22 spontaneously arising mutant clones; 15 x 0.6-Gy induced mutant clones; 10 x 6-Gy induced mutant clones. 2-Gy mutant clones were not isolated because the respective mutation frequency was relatively higher and was virtually comparable to the evidences of 6-Gy induced mutant clones.

Experiment II

A total number of 57 HPRT mutant clones was isolated from independent cultures of unirradiated and irradiated with acute doses of 2 and 6-Gy, as well as fractionated dose 0.6-Gy. Numbers of the mutant clones are as follows: 8 x spontaneously arising mutant clones; 19 of 2-Gy induced mutant clones; 20 x 6-Gy induced mutant clones; 10 x 0.6-Gy (a total dose of 18-Gy). The total number of X-ray-induced mutant clones was 49. Subsequently, eight spontaneously arising mutant clones were isolated from untreated cell cultures in this experiment. 0.2-Gy mutant clones were not included for DNA analysis.

4.3.3 *NotI* Cleaved Restriction Fragment Analysis

In order to observe alterations occurring in areas at large DNA sequential levels (2 Mbp), the genomic DNA from all 104 mutant clones was examined by Southern blot analysis using the DXS1327 probe and D21S4 as its reference. *NotI* cleaved-wild-type genomic DNA served as a control in each Southern blot. Failed reactions were hybridised repeatedly with both probes

until reliable results could be obtained. Mutant clones that gave double bands with the HPRT specific probe were later removed from the final data set, since the occurrence of double-bands could not be explained for a X-chromosomal gene in a male cell line (see also 4.2.3.1).

Experiment I

All, except one, of the spontaneously arising twenty-two mutant clones gave a *NotI* restriction band size that matched the standard. The aberrant pattern of the single mutant clone had two bands (both large and normal) on the Southern blots and, was therefore, excluded from the data set.

In the fifteen mutant clones isolated from cultures that were exposed to 0.6-Gy fractionated irradiation were shown to be dependent (see Table 4.7). Subsequent results further suggested that the mutant clones were dependent and one of them was sufficient to represent the pattern during the final assessments. To account for spontaneous clones, seven mutant clones were removed from the total number of collected mutant clones. Four out of the eight independently arising mutant clones gave normal band sizes whereas the remaining four mutant clones had a smaller band size, indicating these mutant clones had emerged through genomic rearrangements. Though a dose of 0.6-Gy was administered 30 times to the cells in order to produce these mutant clones, the lesions resulting from these irradiations seemed to be relatively low. This can further be observed by comparing the mutation frequencies of both 6-Gy acute and fractionated 0.2-Gy x 30 irradiations (see also Table 4.6).

Of 10 mutant clones that had been selected from 6-Gy cultures, the mutant genomic DNA following *NotI* digestion showed either aberrant signals, or an absence of them on their Southern blots. Only a single mutant clone gave a normal band, whereas three retained small bands and the remaining six gave no signals. All these mutant clones were isolated from independent cultures. Genomic DNAs of these mutant clones either had a deletion in the probe binding site, or a larger deletion also encompassing the neighbouring gene regions. Since the spontaneous mutation frequency was markedly elevated, it was mandatory to go through a background correction to separate the fraction of radiation-induced mutants (see Table 4.4a. and b). Mutant clones derived from Experiment I were analysed only by hybridisation assay. When one considers mutants after exposure to ionizing radiation, it seems evident that all 0.6-Gy mutants analysed produce aberrant *NotI* fragments and this further indicates the gene inactivation is rather through genomic rearrangements. Among the 6-Gy induced mutants 66,7% of mutant clones showed large deletions of ≥ 250 kb whereas 33.3% displayed aberrant *NotI* fragment, this being entirely consistent with the formation of genomic

4 RESULTS

Table 4.7. Patterns of *NotI* digested fragments of isolated HPRT mutant clones from mutation induction Experiment I on corresponding Southern blots. Numbers of independently isolated mutant clones are given in brackets. Background mutation was corrected by subtracting previously existing spontaneous mutant fractions in the initial numbers of X-ray-induced mutant clones.

	Total ¹	%	Induced ²	%
<u>0.6-Gy mutant clones (8)</u>				
Pattern				
Normal (2 Mbp)	4	50	0	0
Aberrant (> or < 2 Mbp)	4 (< 2 Mbp)	50	4	100
No signal	0	0	0	0
<u>6-Gy mutant clones (10)</u>				
Pattern				
Normal (2 Mbp)	1	10	0	0
Aberrant (> or < 2 Mbp)	3 (< 2 Mbp)	30	3	33.3
No signal	6	60	6	66.7
<u>Background mutant clones (21)</u>				
Pattern				
Normal (2 Mbp)	21	100		
Aberrant (> or < 2 Mbp)	0	0		
No signal	0	0		

¹ Without background correction

² With background correction

Mutation frequency of spontaneously arising mutant clones for Experiment I was 18.16×10^{-6} .

rearrangements of the cells following 6-Gy of X-rays (see Table 4.7).

Experiment II :

In Experiment II, which was carried out using cells with a 10% of plating efficiency, there were eight spontaneously arising mutant clones. All the mutant clones retained unaltered normal band sizes on their Southern blots indicating that point mutations were most likely responsible for disrupting HPRT gene function. All spontaneous mutant clones gave PCR products both in RT-PCR and M-PCR.

Figure 4.15 shows the Southern blot-banding patterns of all 0.6-Gy mutant clones. Of the 10 mutant clones, that were selected from the cultures exposed to fractionated irradiations, there were 3 mutant clones, that gave altered sizes of bands (2 x large, 1 x small) suggesting genomic rearrangements. According to M-PCR screening, all three mutant clones had retained all the exons from the HPRT gene. However, RT-PCR products could not be observed in cDNA analysis. Among the remaining 7 mutant clones, there were five mutant clones that were picked from the same petri dish and all gave normal Southern band sizes. But according to RT-PCR analysis, only 2 of these 5 mutant clones synthesized the HPRT transcripts. This

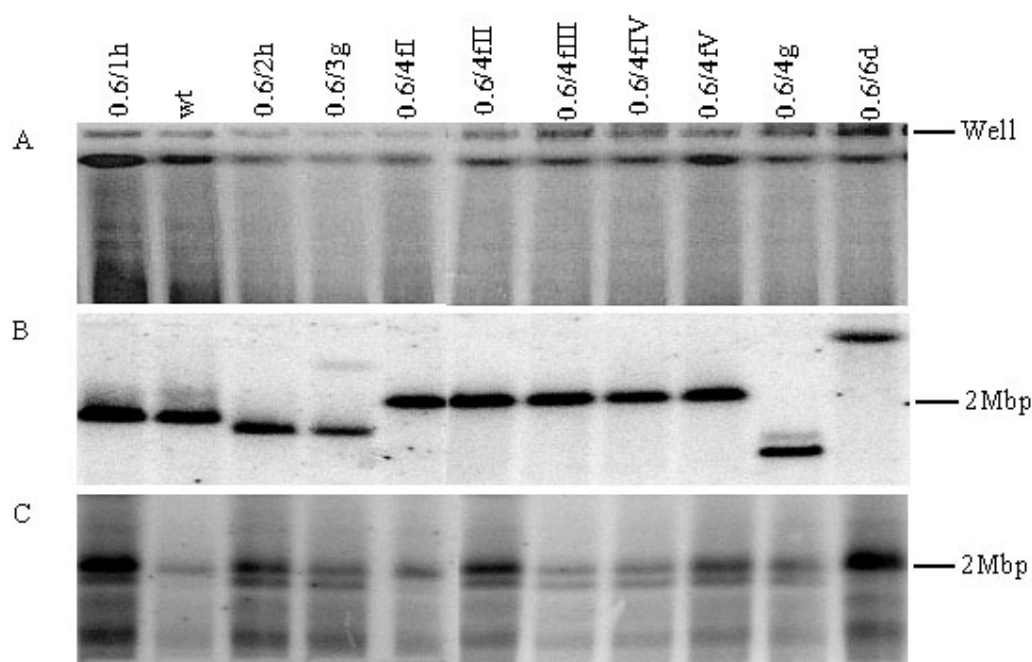


Figure 4.15. Restriction fragment analysis of 10 x 0.6-Gy human HPRT mutant clones: To collect these mutant clones, hTERT-immortalised primary fibroblasts (82-6 hTERT cells) as confluent cell monolayers were X-irradiated with a fraction of 0.6-Gy (to a total dose of 18-Gy) twice a day leaving at least 10 h after each serial irradiation for a period of 15 days and incubating further 7 days to allow phenotypic expression, HPRT negative mutant clones were selected against 6-thioguanine. Following *NotI* digestion, genomic DNA of mutant clones together with wild type (wt) as a positive control, were loaded on a 0.8% agarose gel and electrophoretically separated by PFGE. The membrane was serially hybridised with two different [32 P] dCTP radioactive single probes: DXS1327 probe hybridises to a 2 Mbp of *NotI* digested fragment contained the HPRT gene locus; D21S4 probe serves as the reference that hybridises to a *NotI* restriction fragment of 2 Mbp. Panel A: EtBr stained UV photograph taken prior to vacuum blotting, shows the complete digestions of all samples. Panel B: Southern-blot-banding picture of mutant clones hybridised with DXS1327 probe; normal and aberrant sizes of fragments can be observed here. Panel C: Southern-blot-banding picture of mutant clones hybridised with D21S4 radioactive probe, which serves as the reference for every individual probe.

suggests two independent mutants had arisen. These clones were grouped into two patterns and the rest of the clones with identical patterns were removed from the final data set. M-PCR results showed that all five mutant clones had a combined 1-3 exonic-terminal deletion (at least 2250 bp) at the centromeric site of the HPRT gene. The two mutant clones which were positive with RT-PCR could be explained that those mutant clones may contain sub clones with small mutations (see 4.2.3.1). The remaining 2 mutant clones also gave normal band size on Southern blots but RT-PCR analysis revealed that one mutant clone had retained the HPRT mRNA transcript, whereas the other had not.

Among 18 x 2-Gy mutant clones: 7 x normal; 10 x aberrant (small) bands; 1 x no signal. Six mutant clones displaying normal bands retained all the exons in the HPRT gene whereas 1 mutant clone failed to amplify the fragment containing exon 1 and all clones synthesized RT-PCR products. Only 2 out of ten mutant clones with aberrant bands, yielded

4 RESULTS

Table 4.8. Patterns of *NotI* digested fragments on Southern blots in isolated HPRT deficient mutant clones from mutation induction Experiment II. Numbers given in brackets are independently isolated mutant clones. Background mutation (considering results obtained in Southern hybridisations) was corrected by subtracting previously existing spontaneous mutant fractions in the initial numbers of X-ray-induced mutant clones.

	Total ¹	%	Induced ²	%
<u>0.6-Gy mutant clones (7)</u>				
Pattern				
Normal (2 Mbp)	4	40	0	0
Aberrant (> or < 2 Mbp)	3 (2 x > and 1x < 2 Mbp)	30	3	100
No signal	0	0	0	0
<u>2-Gy mutant clones (18)</u>				
Pattern				
Normal (2 Mbp)	7	38.8	2	15.4
Aberrant (> or < 2 Mbp)	10 (10 x < 2 Mbp)	55.5	10	76.9
No signal	1	5.7	1	7.7
<u>6-Gy mutant clones (19)</u>				
Pattern				
Normal (2 Mbp)	5	26.4	0	0
Aberrant (> or < 2 Mbp)	7 (2 x > and 5x < 2 Mbp)	36.8	7	50
No signal	7	36.8	7	50
<u>Background mutant clones (8)</u>				
Pattern				
Normal (2 Mbp)	8	100		
Aberrant (> or < 2 Mbp)	0	0		
No signal	0	0		

¹ Without background correction

² With background correction

Mutation frequency of spontaneously arising mutant clones for Experiment II was 5×10^{-6} .

cDNA transcripts with one of them having a deletion of 636 bp including exon 1. In the remaining 8 mutants with aberrant fragments, except for one mutant with a deletion of the sequence also containing exon 1, showed a wild type pattern in M-PCR analysis. The mutant clone that showed no signal also did not amplify products in M-PCR and RT-PCR. As given in the Table 4.8, the portion of aberrant fragments cells following X-rays was 77%, while 15% and 8% were for normal bands and no signal respectively.

Of 19 x 6-Gy mutant clones: 5 x normal; 7 x aberrant (2 x large, 5 x small) bands; 7 x no signal. All the mutant clones that gave no signals on Southern blots yielded no PCR products. One mutant with an aberrant restriction band of small size showed a total deletion. Three mutant clones with normal restriction bands synthesized mRNA-HPRT products and one of them had a deletion in exon 1. Following background correction, these two mutant clones were removed from the data set. Furthermore, 6 out of 7 mutant clones displaying aberrant *NotI* restriction-fragmentation had retained all exons according to M-PCR and none

of them produced RT-PCR products. Since the cells used for the Experiments contained also spontaneous HPRT mutant cells, it was necessary to remove the respective portions of mutant clones from each dose-point by considering corresponding background-mutation frequency. This correction was made also considering the results obtained in PCR analysis, 5 and 2 mutant clones were removed from 2-Gy and 6-Gy mutant fractions respectively. Table 4.8 summarises the restriction fragment-analysis-data collected on all the HPRT mutant clones in Experiment II with probable numbers of X-ray-induced mutant clones, while the respective net numbers of X-ray-induced mutant clones for 2-Gy and 6-Gy are 13 and 17 as given in the Table 4.11 as a comparison of combined results that were collected from both experiments.

4.3.4 RT-PCR-based HPRT mRNA Analysis

Total RNA of 57 mutant sub clones grown to confluence was isolated as described in the Materials and Methods section. Mutant cDNA was examined prior to HPRT-exon screening based on genomic DNA because the focus was to determine mutant spectra without using M-PCR. For all the mutants in Experiment II, HPRT cDNA was yielded, making use of a RNeasy kit together with Omniscript reverse transcriptase by QIAGEN.

Table 4.9. Summary of RT-PCR analyses of both spontaneous and X-ray-induced HPRT mutant clones in hTERT-immortalised human fibroblasts

Treatment	Number analysed	Number showing RT-PCR transcripts	
		Presence (+)	Absence (-)
Spontaneous	8	8 (100%)	0 (0%)
X-ray (Gy)			
0.6	7	4 (57%)	3 (43%)
2	18	8 (44%)	10 (56%)
6	19	3 (16%)	16 (84%)

Aliquots of PCR products together with DNA size markers were loaded on a 1.5% agarose gel containing ethidium bromide and were electrophoretically separated and UV-photographed. After that, according to RT-PCR results, mutant clones were grouped into categories. Virtually all the mutant clones, that gave an unaltered size of *NotI* restriction band were able to synthesize RT-PCR products of the expected size, while the mutant clones that gave altered restriction fragments did not produce HPRT mRNA transcripts.

However, there was a minority of mutant clones which retained HPRT mRNA-transcripts, though their Southern hybridisation signals were aberrant. These mutant clones were re-examined by repeated RT-PCRs using freshly synthesised cDNA.

Summarized RT-PCR results are given in the Table 4.9. By increasing the dose of administered X-rays, a trend of failure to amplify RT-PCR products is seen. Significantly, 0.6 mutant clones, having obtained a total of 18-Gy show substantially higher rates than the 6-Gy mutant clones. A failure in the amplification of RT-PCR products despite normal Southern banding may result from splicing errors in either exonic or intronic regions. cDNA from spontaneously arising mutant clones of Experiment I failed to synthesize targeted PCR products even though they were tested several times.

4.3.5 Multiplex PCR-based HPRT Exon-Deletion Analysis

Table 4.10. Summary of M-PCR analyses of both spontaneous and X-ray-induced HPRT mutant clones in hTERT-immortalised human fibroblasts

Treatment	Number analysed	<u>Number showing PCR changes</u>		Number showing no change (WT)
		Total deletion (TD)	Partial deletion (PD)	
Spontaneous	8	0 (0%)	0 (0%)	8 (100%)
X-ray (Gy)				
0.6	7	0 (0%)	2 (29%)	5 (71%)
2	18	1 (5%)	3 (17%)	14 (78%)
6	19	8 (42%)	1 (5%)	10 (53%)

A total of 104 mutant clones isolated in these two mutagenesis experiments had lesions in the HPRT gene locus that were undetectable in restriction analysis and RT-PCR. Thus, it was necessary to carry out individual exon-deletion screening at the HPRT gene locus using multiplex PCR. M-PCR was performed on 57 of the 104 mutant clones. Aliquots of PCR products loaded on a 1.5% agarose gel were electrophoretically separated together with DNA ladder markers (100 bp plus or 1kb marker, Fermentas).

Virtually, all the mutant clones which belong to either the “normal” or “no signal” category showed identical results regardless of the analytical methods chosen. However, 0.6/4fI and 0.6/4fII mutant clones (also removed mutant clones, 0.6/4fIII, 0.6/4fIV and 0.6/4fV) (see Figure 4.16) unexpectedly gave interstitial centromeric 1-3 exonic deletions although these particular two retained normal size of restriction fragments on Southern blots. Also the mutant clone, 2/2c did not amplify a PCR product related to exon 1 despite the mutant clone had normal band pattern on Southern analysis.

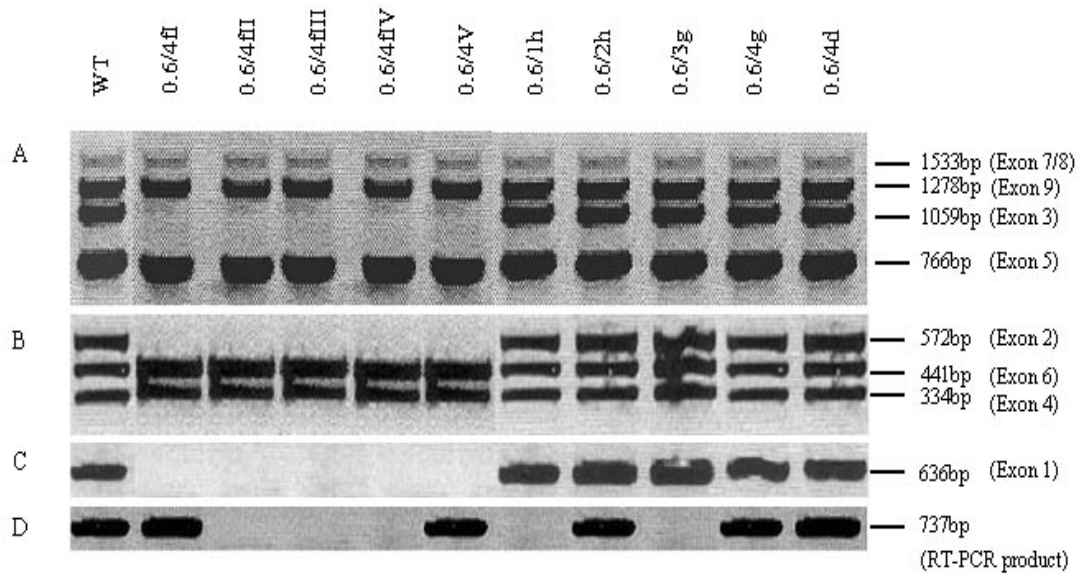


Figure 4.16. Agarose gel electrophoretic UV-picture of multiplex PCR and reverse transcriptase PCR analyses of human-HPRT-deficient-mutant clones in hTERT-immortalised-primary fibroblasts after exposure to dose fractions of 0.6-Gy of X-rays. The mutant clones illustrated here are 10 x 0.6-Gy those were isolated from confluent cell cultures following 0.6-Gy x 30 (for a total dose of 18-Gy) X-irradiation for 15 days consecutively. Genomic DNA of the mutant sub clones were isolated and PCR amplified in two different multiplex reactions: HPRT exons 3, 5, 7/8 and 9 as long fragments and exons 2, 4 and 6 as short fragments; exon 1 was amplified as a single fragment in a separate PCR reaction. From left to right: PCR products starting with wild type (WT) as a positive control and the 10x mutant clones are loaded as can be seen by the names given at the top of diagram, and the sizes of fragmented PCR products containing HPRT exons together with end-intronic sequences are pointed on the right-hand side. *Panel A:* separation of large fragments of the mutant clones; with starting wild type (wt) on the far left, 2-6 lanes represent 0.6-Gy mutants segregated from the same plate showing common exon 3 partial deletion with exons 5, 7, 8 9 present; plus lanes 7-11 show the presence of all large fragments in mutant genomic DNA. *Panel B:* separation of small fragments in mutant clones: lanes 2-6: Separation of short fragments rendering a partial deletion in exon2 with presence of exons 4 and 6; lanes 7-11: presence of all three short fragments. *Panel C:* separately amplified exon 1 fragments: lanes 2-6: partial deletion in exon 1; lanes 7-11: presence of exon 1 in genomic DNA of mutant clones. *Panel D:* separation of RT-PCR products; lanes 2, 6, 8, 10 and 11: plus including presence of HPRT cDNA transcript; lanes 3-5 and 7, 9 ergo: absence of the synthesis of transcript.

The results of the remaining mutant clones were partial deletions. All these newly detected partial deletions were continuous-deletions at the HPRT gene and discontinuous-deletions were not observed as in the previously-examined mutant clones (see MGH-U1 mutant clones in Table 4.2).

In addition, it was necessary to re-check the presence and absence of exon 3 and exons 7+8 in certain mutant clones. With the implementation of single PCRs, genomic DNA of the following mutant clones were re-examined: 2/3fI, 2/3aII and 6/3d for exon 3; 6/3c, 6/3f, 2/3fI, 2/3dI, 2/3eII, 2/2dI, 2/3aII, 2/3c and 2/1g for exons 7 and 8 (see Appendix Table 8.2). All 5 mutant clones isolated from a 0.6-Gy single cell culture gave 1-3 exonic end deletions at

4 RESULTS

Table 4.11. Comparison of spontaneous and X-ray-induced HPRT mutant clones in hTERT-immortalised fibroblasts (82-6 hTERT cells) following fractionated irradiations

X-rays	Number of Analysed Clones	Pattern	PCR Analysis Failed Exons	Restriction Fragment Analysis	RT-PCR Analysis
Acute Dose					
6-Gy	17	8 WT	none	2 x large 4 x small 2 x normal	no products no products no products
		1 PD	1	1 x normal	1 x product
		8 TD	all	7 x no signal 1 x small	no products no product

	9*		6 x no signal 3 x small		

2-Gy	13	9 WT	none	8 x small 1 x normal	1 x product no product
		3 PD	1	1 x normal 2 x small	1 x product 1 x product
		1 TD	all	1 x no signal	no product

Fractionated Dose					
0.6-Gy	6	4 WT	none	2 x large 1 x small 1 x normal	1 x product 1 x product 1 x product
		2 PD	1-3	2 x normal	1 x product

	4*		4 x small		

0-Gy	8	8 WT	none	8 x normal	8 x products
	21*			21 x normal	

Abbreviations:

WT- wild type pattern including all HPRT exons; PD - partial deletions missing one or multiple number of HPRT exons; TD - total deletions missing all HPRT exons; normal = 2 Mbp restriction fragment; Large > 2 Mbp; small < 2 Mbp.

* these mutant clones were exclusively analysed with hybridisation assay

the HPRT gene. These results were instrumental in both detecting the individuality of those 5 x 0.6-Gy mutant clones and making further comparisons with data obtained through RT-PCR results and restriction fragment analyses. All partial deletions were caused by exon 1 containing regions. Summarized PCR results for spontaneously-derived and X-ray-induced mutant clones analysed at the HPRT gene locus are given in the Table 4.10. These results are compared with those of the other analytical methods and are given in Table 4.11, while Figure 4.17 illustrates the mutation patterns of 44 mutant clones separately. The mutant clones in Table 4.11 were categorized into groups as wild type, total or partial (5' and 3' end

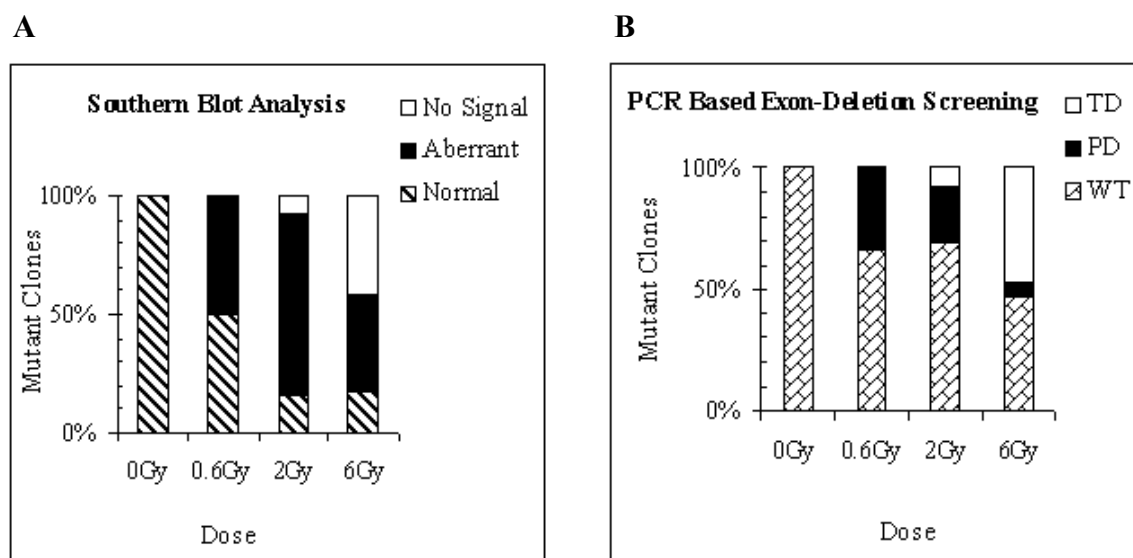


Figure 4.17. Mutation patterns of 8 x spontaneous, 6 x 0.6-Gy fractionated dose, 13 x 2-Gy acute dose and 17 x 6-Gy acute dose of X-ray-induced HPRT mutant clones were examined by hybridisation assay and M-PCR. *Panel A:* Southern blot results of *NotI* restriction fragment alterations according to hybridisation assay. *Panel B:* PCR results of genomic DNA of mutant clones in which a wild-type pattern of exons (WT), partial deletions (PD) and total deletions (TD) of HPRT 1-9 exons are screened.

and intragenic) deletions. According to these results, ionizing radiation-treatment of 82-6 hTERT-immortalised human fibroblasts produced a spectrum of mutations significantly different from the spectrum for spontaneous mutations. The major difference lies in the portion of total deletions. Between 5 and 42% of X-ray-induced mutant clones analysed showed a total loss of the HPRT gene locus (see Table 4.10 and Figure 4.17B), whereas no total deletions in PCR analysis were found in spontaneous and 0.6-Gy mutant clones. Multiplex PCR results further suggested the general finding that the majority of the X-ray-induced mutant clones were not the deletions that could be screened by M-PCR analysis. Of 44 X-ray-induced mutant clones (without 5-specific mutant clones that were excluded from data set) examined, 20% (9/44) were total-deletion-mutant clones and 14% (6/44) showed either intragenic or terminal deletions at 5' end (centromeric) or 3' end (telomeric) of the HPRT gene locus respectively. All nine exons were synthesized from the rest of the mutant clones (66%) according to M-PCR analysis without undergoing major alterations. The spectrum of total deletions appeared to be dependent on the dose in X-ray-induced mutations at the HPRT gene locus; mutant clones with "total deletion" made up 5 (1/18) or 42% (8/19) of mutant clones isolated after irradiation with 0 or 6-Gy of X-rays respectively. The frequency of partial deletions including at least 636-2267 bp terminal-deletions in the HPRT gene also appeared to be higher for the mutant clones isolated with 0.6-Gy (29%) than from those irradiated with 6-Gy (5%).

5 Discussion

In the present study, radiation-induced mutagenesis was examined in order to gain closer insight into the relation between the erroneous rejoining of DNA double-strand breaks and any resulting mutation. Two sources of human male cells were used in this study: 82-6 hTERT, telomerase-immortalised primary fibroblasts (Yannone et al. 2001) and MGH-U1, a long known tumour cell line isolated from a bladder carcinoma (Edwards et al. 1997; Kato et al. 1978; Lin et al. 1985; Lobrich 1999). The hypoxanthine guanine phosphoribosyl transferase (HPRT) gene locus was used to detect mutations in this investigation because of the relative ease by which mutants in this X-linked, hemizygous, non-essential gene can be isolated in the presence of the purine analogue 6-thioguanine (6-TG) (Stout & Caskey 1985). General characteristics of this gene are comparable to those of hamster, mouse and man (Schmidt & Kiefer 1998; Yamada et al. 1996). Size alterations of a 2 Mbp-*NotI* restriction fragment containing the HPRT gene locus of mutant clones were made using hybridisation assay together with several other standard techniques currently used in molecular biology and cytogenetics.

5.1 Molecular Mechanisms in HPRT Gene Mutations

The presumable molecular mechanisms in the formation of *NotI* fragment alterations of mutant clones are jointly described in following paragraphs. A few of the specific mutations are separately described in the discussion of their molecular patterns in the corresponding sections.

The mutation investigated in this study should essentially be within the HPRT gene boundaries (Park et al. 1995; Yamada et al. 1996), because both spontaneous and radiation-induced mutant clones were isolated aiming at the inactivation of the selectable HPRT gene locus. Each deletion occurring in the DXS1327 probe binding site of the 2 Mbp fragment should be accompanied by point mutations or deletions within the gene as already documented by Lobrich (1999). Formation of unaltered *NotI* restriction fragments (Figure 4.3) in the presence of all HPRT exons (Tables 4.2 & 4.5) can be due to point mutations or small deletions spanning a few base pairs in the coding sequence of the HPRT gene (Lobrich 1999; Phillips et al. 1995; Sankaranarayanan 1991). An alternative interpretation for HPRT gene inactivation with presence of all exons could be its inaccessibility to transcription events. An explanation model for this could be the translocation of the entire *NotI* restriction fragment

containing the HPRT gene into hetero chromatic chromatin regions. Although the gene remained intact, cells could still survive as HPRT mutant clones because of dysfunctions in the gene.

Altered formation of a *NotI* restriction fragment (Figures 4.2, 4.3 & 4.7) is due to genomic rearrangements that may have occurred in the genomes of the cells either spontaneously or after being exposed to ionizing radiation (Lobrich 1999). Although such rearrangements make up a small percentage of HPRT somatic mutations or germinal Lesch-Nyhan mutations (Jinnah et al. 2000), these can rise to 60% of *in vitro* irradiated cells or in radiation-exposed individuals (Albertini et al. 1997; Nicklas et al. 1990). Mutant clones of the present study containing all HPRT exons (WT pattern) but showing a small *NotI* fragment could be due to deletions in the regulatory regions of the gene. To demonstrate this point: a deletion in the promotor region together with neighbouring gene sequences spanning at least a hundred kilo base pairs (resolution of pulse field gel electrophoresis is 100 kbp) could lead to the formation of a small restriction fragment as two restriction cutting sites get nearer than in a wild type gene sequence (Lobrich 1999). Another explanation model can be genomic rearrangements associated with complex molecular mechanisms because fragments obtained in the current study were measured as rearrangements of several hundred kilo base pairs.

RT-PCR results obtained in the present work showed that most of the genomic rearrangements cause the scattering of HPRT coding segments of mutant DNA because the majority of mutant clones with the presence of all exons could not give HPRT-mRNA transcripts. All WT mutant clones with unaltered restriction fragments gave RT-PCR products (see Results section Table 4.5). These results suggest that all exonic segments of these mutant clones are located on a continuous gene sequence as in the wild type gene sequence. This further supports the presumption that small deletions spanning a few base pairs or point mutations in coding segments are the reasons for the inactivation of the HPRT gene of the WT mutant clones with unaltered restriction fragments. On the other hand, the WT mutant clones with *NotI* aberrant fragments may be due to genomic rearrangements with one break point within an intronic segment of the HPRT gene as no RT-PCR products could be obtained. However, a smaller number of mutant clones with aberrant Southern bands nevertheless gave RT-PCR products (see Table 4.11). One credible explanation could be configurations of complex mutations with deletions outside of the HPRT gene and point mutations in exonic segments at the same time that leads to the synthesis of non-functional protein. In a previous study reported by Lobrich (1999), in which HPRT exons 1-9 of the mutant clones were investigated for its location, revealed that they were scattered on two

different restriction fragments. This particular study was based on X-ray-induced HPRT mutant clones derived from MGH-U1 cells and the conditions held for experimental procedures were comparable to that of the current study (see Table 4.2). These data are in consistence with the results obtained by RT-PCR analysis in the present work.

In addition, inversions of segments containing one restriction-cutting site together with parts of the HPRT gene sequences could contribute to the formation of aberrant restriction bands. Evidently, such genomic rearrangements can encompass all exons, or the exonic sequences could be scattered on another part of the chromosome. The latter explanation can be appropriate for the formation of large restriction fragments, although comprehensive molecular mechanisms of such rearrangements can only be elucidated by studying the break point regions of mutant DNA at sequence levels (Morris & Thacker 1993). Furthermore, inserted sequences of a hundred kilo base pairs to the junction regions in either regulatory or intronic regions could presumably shift neighbouring restriction cutting sites outwards thus allowing the formation of aberrant fragments. Such an interpretation can be appropriate in explaining the occurrence of large fragments with the presence of all exons.

Aberrant restriction fragments of partial deletion (PD) mutant clones are the results of genomic rearrangements. Among the PDs examined in the study, there were intragenic and end exon-deletions. End exon-deletions occurring in cells exposed to X-rays can encompass a hundred kilo base pairs creating large deletions. Although the latter event is mostly related to the formation of a small restriction fragment, a small number of mutant clones gave no signals on the Southern blots (see spontaneous and 6-Gy-induced mutants in Table 4.2). End deletion at the 3' end (telomeric end) of the gene extending beyond the DXS1327 probe-binding site should be the cause for the lack of hybridisation signals. In this category of mutants, the deletion should be at least 200 kbp. Furthermore, deletions at the 5' end (centromeric end) were observed as small restriction fragments. Genomic rearrangements of mutant clones with intragenic PDs could be explained by inversions. Such inversions, whose sequences locate within a restriction-cutting site containing the DXS1327 binding site, result in aberrant fragments. Also, insertions at breakpoint sites (when compared with non-mutant DNA) may give aberrant fragments.

Results obtained in the current study, in which an X-chromosomal probe was used to investigate the cytogenetically visible aberrations with FISH, showed that a high proportion of the examined mutant clones remained intact on the X-chromosome (Tables 4.2 & 4.5). This data suggests that translocations between X-chromosome and the autosomes (inter-chromosomal translocations) are a rare event under the conditions used. Mutant clones with

PD pattern that failed to give inter-chromosomal translocations were also reported by Lobrich (1999). In the small number of mutant clones in which inter-chromosomal translocations were found, there were mutant clones with PD pattern in the coding regions and also some with a WT pattern. All except one WT mutant clone (a MGH-U1 mutant clone with unaltered fragment, see Results Figure 4.5) had an aberrant restriction fragment. In contrast, it was shown previously that translocations containing the HPRT chromosomal region were identified only in mutant clones with a total deletion in the HPRT gene ranging up to megabase pairs (Simpson et al. 1993). Therefore, the PD mutation in this study that gave translocations is associated with relatively large genetic changes (>1 Mbp). The particular mutant clone with an unaltered restriction fragment, which nevertheless displayed a translocation (a 6-Gy-X-ray-induced HPRT mutant clone in MGH-U1 cells) is a rarer one and may not be related to ionizing radiation. However, none of the mutant clones with TD pattern exhibited translocations in the examined mutant clones in the present study. This is most likely due to the small sample size. Although the junction sites of translocations were not examined in detail, the results were consistent with the molecular characteristics in these mutant clones.

It can therefore be concluded that the deletions following radiation-exposure are mostly invisible on the cytogenetic level. The observations, that a higher proportion of mutant clones remained intact on the X-chromosome (83 and 94% of hTERT clones and MGH-U1 clones, respectively), support the premise that the intra-chromosomal exchanges (including inversions) are the main observations following radiation exposure in mutant clones. This is consistent with a previous report showing a significant contribution of intra-chromosomal rearrangements to DSB misrejoining (Lobrich et al. 2000). A majority of the examined WT pattern mutant clones was accompanied by an aberrant fragment (due to sequential change of a minimum size of 100 kbp). These data and previously published results (Lobrich 1999; Simpson et al. 1993), suggest that the failure to give cytogenetically visible inter-chromosomal translocations may be associated with genetic changes less than 1 Mbp.

Each mutant clone that gave no signal in Southern analysis is represented through a minimum deletion of 200-250 kbp spanning from exon 1 of the HPRT gene to the DXS1327 probe binding site. In addition, it was observed that a few mutant clones (HPRT-hTERT mutant clones 2/11e, 6/9d and 6/6b) of this study with such deletions had lost cell vitality in *in vitro* culture after a period of four weeks. Therefore the initial DNA damages might also affect neighbouring essential genes for cell survival, which are found on Xq26. In fact, previous studies based on a human B-lymphoblastoid cell line have suggested that the highest

probability for the location of essential cellular genes may be within ~ 540-800 kbp from the telomeric end of the HPRT gene (Nelson et al. 1995). Further, detection of HPRT deletions is limited to a size of about 3.5 Mbp, because deletions spanning to either side of neighbouring essential genes can not allow cells to remain vital (Frankenberg-Schwager et al. 2002; Lippert et al. 1997).

5.2 Acute Dose Irradiation in MGH-U1 Cells

48 HPRT mutant clones isolated from MGH-U1 confluent cell cultures were considered for the final assessment of the study (see Table 4.2). In the final data set of MGH-U1 mutant clones, there were 26 mutant clones that had arisen spontaneously and the remaining 22 mutant clones resulted from X-irradiations with and without wortmannin. Genomic DNA of these mutant clones was examined by hybridisation assay and multiplex PCR screening. Fluorescence *in situ* hybridisation was furthermore used to investigate chromosomal aberrations of the mutant clones isolated from Experiment II. 10 mutant clones whose genomic DNA showed double bands in the Southern analysis were excluded from the initial data set. These mutants with double-restriction bands (i.e. large /large or large /small) were most likely the result of two different sub clones, though isolation of 6-thioguanine resistant clones were performed very carefully to avoid mixing up with neighbouring clones (see Figure 4.8). In addition, previous studies have shown that duplications of sequences containing the hybridisation probe gave two bands with varying sizes (Lobrich 1999). The mutants that gave no signal on Southern blots and missed all exons according to multiplex PCR screening most likely have a minimum deletion size of 200-250 kbp in the HPRT gene region.

5.2.1 6-Gy X-ray-induced Mutant Clones

Fifteen of the 6-Gy X-ray-induced mutant clones were used for the final assessments of HPRT mutation spectra. Of these 15 clones 9 retained a WT pattern PCR analysis. The data seems to be unexpected, since the fraction of WT patterns is virtually comparable to those of the spontaneous mutation spectra (9/15 or 60% of 6-Gy). These WT pattern mutant clones included 25 and 29% in comparable studies performed by Schwartz et al.(1994) and Lobrich (1999) respectively. Small sampling of mutant clones may be responsible for the inverse tendencies of the current results. Only one out of 10 of X-ray-induced mutants may be of spontaneous origin and this proves that a higher proportion of mutants isolated in 6-Gy

cultures should most likely be radiation-induced (see Table 4.1). Apart from that, although it is not assumed that the selection procedures here will guarantee the independence of individual mutant clones, it should be noted that only accurate information about junction sites at the nucleotide sequence level will provide such assurance. In any case, strategies employed in isolating mutant clones in this study are comparable with previous reports (Park et al. 1995; Singleton et al. 2002; Yamada et al. 1996) and likely to ensure independence of the mutant clones.

Of nine mutant clones with presence of all of exons, 7 revealed altered restriction fragments (7/15 or 47%), while two mutant clones had unaltered fragment sizes indicating point mutations. Genomic rearrangements in intronic segments of the gene could be the cause for the formation of such altered fragments. In the fluorescence *in situ* hybridisation analysis, two cytogenetically visible translocations (see Results Table 4.2) were found in two distinguished mutant clones with WT patterns (see Figure 4.5). 31 mutant clones were subjected to this cytogenetic screening and so the percentage of mutant clones with translocations was ~7% (or 2/31). One of these mutant clones with translocations (D16) had a normal Southern band size while the other had a large restriction fragment. In the mutant clone with a normal restriction band a point mutation within the HPRT locus in addition to the chromosomal rearrangement may have occurred. The genomic rearrangement of the other mutant clone involved cytogenetic band Xq26 (containing the HPRT gene) and is therefore associated with large genetic changes (>1 Mbp) (Giver et al. 1995; Simpson et al. 1993). This translocation was unbalanced (non-reciprocal) between the X-chromosome and one of the autosomes. This is consistent with data documented in a previous report (Lobrich 1999).

One of the two PD mutant clones that gave aberrant fragments had an intragenic deletion spanning exons 2-3, whereas the other gave two varied intragenic deletions in exons 2-3 and 7-8. The latter mutation with two skipped (non-contiguous) deletions may be explained by small deletions that occurred in the primer annealing sequences of the mutant DNA. The other can be counted as a single- or multiple- partial deletion which is comparable to the partial deletions as described before. Similar small-scale mutations were also proposed in a previous report (Lobrich 1999). Exons 7-8 were always co-amplified as a single PCR. However, there were also spontaneous mutant clones that retained exonic 2-3 deletions. Therefore, the mutation (partial deletions in exons 2-3) may belong to the spontaneous category rather than to radiation-induced mutant clones. In any case, the molecular mechanisms that have taken place in forming genomic rearrangements to give large restriction fragments can be associated with the explanations given in previous paragraphs.

The PD mutant clones that gave no signals in Southern analysis had two various types of exon-deletions. One of them has a single deletion including exon 1 and the other missing exons 3, 7 and 8. The first single partial deletion mutant could be explained with a small deletion in one of the primer annealing sequences of exon 1 together with the loss of DXS1327 probe binding site. This mutant clone may have spontaneously arisen because the particular pattern (both Southern analysis and PCR screening) is found among the spontaneous mutant clones in the subset (see Table 4.2). The mutation of the mutant clone that missed exons 3, 7 and 8 and at the same time gave no signal for a restriction fragment is apparently an uncommon pattern among the X-ray-induced HPRT mutant clones. Reoccurring small deletions in the primer annealing sequences of all 3 exons are very unlikely. The mutant clone most likely has a pre-existing mutation, since exon 3 deletions are found in the category of spontaneous mutant clones and is later mutated by a small deletion in one of the primer binding sites for the co-amplification of exons 7-8. In order to be in accordance with a hybridisation signal, there should be a deletion in the probe binding site of DXS1327 and the deletion must be restricted to a few hundred base pairs. Similar radiation-induced mutations have been reported following high (Linear Energy Transfer) LET radiations previously. In recent experiments Schmidt et al. (1998) revealed non-contiguous mutation spectra in hamster CHO cells where HPRT mutant clones were induced by alpha particle radiation. In addition, a previous group also reported non-contiguous mutations of HPRT clones derived from CHO cells that were exposed to acute doses of X-rays and subjected to a second dose (Romney et al. 2001). To discriminate between these types of mutations, however, it is necessary to investigate a statistically relevant number of mutant clones. There also existed two mutants with absence of all HPRT exons and had no restriction bands on respective Southern blots. A deletion of at least 200-250 kbp cover the mutation of the two mutant clones in inactivating the gene.

5.2.2 2-Gy + Wortmannin (WM) Mutant Clones

Results obtained in this part of the study in which both irradiations were conducted with acute doses of X-rays at identical conditions, are in agreement with previous reports demonstrating an radio-sensitizing effect of wortmannin (Ortiz et al. 2004; Rosenzweig et al. 1997). Surprisingly, significant reduction in the HPRT mutagenicity was observed in the WM + 2-Gy cells compared to the cells which were irradiated with 6-Gy of X-rays but in the absence of WM. In other words, dysfunctions in NHEJ may have caused a reducing effect in the HPRT mutation in the cells at equal levels of cell survival.

Effects of wortmannin were reported for CHO cells previously. As reported in Chernikova et al. (2001), mutation induction frequencies in the HPRT gene in the presence of WM, with the same acute doses of X-rays, increased whereas the corresponding cell survival is observed to be decreased. A credible explanation for the increase in mutation-induction of those CHO cells in the presence of wortmannin may be due to the mutation induction frequencies which are generally defined as the number of mutant clones per surviving cell. Furthermore, previous reports in which repair incubation of DSBs following low LET radiation was investigated, have documented that the absence of NHEJ increases levels of misrejoining and chromosomal exchanges at radiation doses of a few Gy (Rothkamm et al. 2001). The results obtained here were inconclusive and it is therefore necessary to conduct more experiments in order to draw useful conclusions about the HPRT mutation in the absence of the NHEJ. Alternatively, it should be noted, that there may be a significant difference between radiation-induced mutation studies based on HPRT gene locus and the DSB misrejoining fidelities following repair incubation. However, the spontaneous mutation induction frequencies (with and without WM) of the present examinations yielded were almost the same (see Table 4.1) for both groups of cells with and without pre-treatment of WM (with WM + 0-Gy and without WM + 0-Gy). This suggests no significant effect of WM on the HPRT mutation in the absence of IR. Further, the effect on cell survival in the present study is concordant with previous data in which human cells were tested in WM-pre-treated X-irradiation cultures (Okayasu et al. 1998) and CHO cells investigated to find the cell cycle-dependent effects (Chernikova et al. 2001).

Based on the results obtained in the present study, the following suggestions can be made: since genomic rearrangements are believed to occur from misrejoining of DNA DSBs (Rothkamm et al. 2001), the absence of a NHEJ pathway seems to have induced a relatively low number of DSB misrejoining and this has resulted in a low number of HPRT mutant phenotypes. Although the mechanisms and enzymatic nature of alternative DSB repair pathways are unknown to date, previous reports suggest that such an alternative pathway is presumed to be suppressed in the presence of functional NHEJ (Rothkamm et al. 2001). Thus, when only a few breaks occur, as is in the current experiment (40 DSBs occur per Gy in a cell; (Foray et al. 1999; Goodhead 1994)), one can also suggest that the diminished mutation frequency in HPRT may be connected with the latter hypothesis.

All seven mutant clones gave aberrant restriction fragments (see Table 4.2), suggesting that their formation is associated with genomic rearrangements. Of the five WT mutant clones, 4 had large restriction fragments and the remaining mutant clone possessed a small

restriction fragment. The remaining two mutant clones with partial deletions both lacked exons 7-8. One of these two clones showed a large fragment while the other had a small restriction fragment. All 7 mutant clones have inactivated the HPRT gene through genomic rearrangements. No HPRT mutant clones with point mutations or small deletions were observed among them. This is in contrast to the radiation-induced HPRT mutation spectra obtained from NHEJ proficient X-ray-induced cultures with genomic rearrangements, point mutations, exonic deletions and large deletions were observed. It is tempting to speculate that if NHEJ had an effect on the formation of rearrangements as was documented previously (Rothkamm et al. 2001), that such large rearrangements should have accelerated in the irradiated cells when the NHEJ pathway was inhibited. Mutation induction frequencies of 2-Gy induced mutant clones were generally 2.5 times above the corresponding background mutation level. Thus, the net number of X-irradiated mutant clones is between four and five of the 7 mutant clones that were subjected to analysis in the current study. However, to come to a definite conclusion about the molecular spectra of HPRT mutations in wortmannin-pre-treated cells, extensive research studies based on a statistically relevant numbers of mutant clones are necessary.

5.2.3 Spontaneous Mutant Clones

The multiplex PCR results of the spontaneously arising mutant clones were as follows: 62% of WT; 34% of PD; and 4% of TD. Similar percentages have been previously reported for the spontaneous mutation patterns in 6-Gy-gamma-irradiated CHO-K1 cells with corresponding values of 77%, 20% and 3% for WT, PD and TD mutant clones respectively (Schwartz et al. 1994). In addition, several other authors have reported values with larger variations, being comparable with the results obtained in the present study for the fraction with WT pattern (Jostes et al. 1994; Zhu et al. 1996). Consistent with previous reports, genomic rearrangements make up a small percentage of spontaneous HPRT mutations in normal cells (Jinnah et al. 2000; Nicklas et al. 1989) with the exception of HPRT mutant clones which are derived from malignant cell lines (Lobrich 1999). Since certain patterns of mutant clones are considered dependent, one cannot conclude the presence of hotspots among these mutant clones.

Despite the fact that a majority of spontaneous mutant clones (13/26 or 50%) (see Table 4.2) have retained WT patterns with altered fragments, mutant clones isolated from immortalised human cells have shown a significantly smaller number of WT mutant clones with altered *NotI* restriction fragment. Previously, cytogenetic studies have shown that

malignant cells generally have chromosomal rearrangements such as translocations, inversions, insertions, and large deletions (Williams et al. 2002). Remarkably, size alterations in mutant clones with WT pattern were almost exclusively large restriction fragments thus suggesting inversions to be the cause.

Six of 9 PD mutant clones retained altered restriction fragments in hybridisation analysis, an indication that the mutation was the result of genomic rearrangements in breakable regions of the gene. It can be postulated that these aberrations may also be related to inversions, since five of the clones produced large fragments. Three mutant clones with deletions in exon 1 failed to exhibit hybridisation signals and can be expected to be dependent. Point mutations in the primer binding sites may have caused a failure to form PCR products. The mutant clone with an end deletion in exons 7-9 produced a small fragment, indicating the deletion extended beyond the terminus of the gene without including the binding site of the Southern probe. The latter mutant clone has consequently formed a small fragment with a deletion of at least 100 kbp. There was only one mutant clone with a complete deletion in PCR analysis and without a signal in the Southern analysis. This particular mutant had a minimum deletion of 200-250 kbp.

5.3 Acute Dose Irradiation in hTERT-Immortalised Human Fibroblasts

Data based on the molecular characterisation of a total of 47 (18 spontaneously arising and 29 X-ray-induced HPRT mutant clones) was considered for the final evaluation. These hTERT-immortalised HPRT mutant clones were isolated from three independently conducted mutation induction experiments. Among the 29 radiation-induced mutant clones, there were 25 mutant clones that had undergone a comparative study with hybridisation assay, Multiplex PCR, RT-PCR and fluorescence *in situ* hybridisation. More specifically, a significant proportion (64% or 7/11; two small restriction fragments of 4 mutant clones which were examined only by hybridisation assay were excluded) of X-ray-induced mutant clones that gave an altered restriction fragment, retained all HPRT exons and presented the WT pattern according to PCR analysis. This indicates that the formation of rearrangements in the HPRT gene after cells were exposed to X-rays is related to molecular rearrangements occurring in intronic segments or regulatory regions of the gene rather than in exonic regions. This data is consistent with a previous report (Lobrich 1999) and also data discussed for MGH-U1 mutant clones in this study. All except one mutant clone with total deletions in the HPRT gene according to PCR analysis gave no signal with the HPRT region specific DXS1327 probe indicating a minimum deletion of 250 kbp.

Only five spontaneous mutant clones were examined by comparative study, since the spontaneous mutation frequency of the early passage 82-6 hTERT cells was low (Mutation frequencies (Mfs) were 0.12 to 1.25×10^{-6} for Experiment I and II respectively). Difficulties to isolate spontaneous HPRT mutant clones has been reported previously in similar studies in which mutations were examined in human fibroblasts (Park et al. 1995; Yamada et al. 1996). The 13 remaining clones were added to the set from the last mutation induction experiment (Experiment III) (Mf for this was 19.5×10^{-6})(Table 4.3) and were exclusively investigated by hybridisation assay. Spontaneous mutant clones bearing WT patterns retained unaltered restriction bands confirming the association of the mutation with point mutations or small deletions in exonic segments of the HPRT gene (Park et al. 1995; Yamada et al. 1996). A comparison of obtained results of this part of study is given in Table 4.5.

5.3.1 X-ray-induced Mutant Clones

The observed mutation frequencies of X-ray-induced mutations in hTERT-immortalised cells (Table 4.3) were nearly comparable to the results reported previously for X-irradiated human fibroblasts (Park et al. 1995; Yamada et al. 1996). Results in this part of the study support the general observation that the majority of ionizing-radiation-induced mutations at the HPRT gene locus are large deletions and due to rearrangements in the HPRT gene locus; the frequency of direct large deletions (as total deletions or /and no signals) was 28% (8/29) and that of genomic rearrangements (aberrant restriction fragments) 45% (13/29). Compared to the mutation spectra of spontaneous mutant clones which predominantly resulted from point mutations or small deletions, these data are characteristic for radiation-induced mutants (Bao et al. 1995; Nelson et al. 1994; Phillips et al. 1997). Several authors have documented that the frequency of gene deletions in radiation-induced mutants is higher than the frequency in spontaneous mutants (Fusco et al. 1992; Jostes et al. 1994; Morris et al. 1993; Park et al. 1995). Further, a previous report revealed that X-ray irradiation can cause HPRT mutations that involve deletions as large as 2 Mbp (Denault & Liber 1993). Furthermore, these large deletions extended to varying degrees into the upstream and downstream regions beyond the HPRT gene locus and deletions up to at least 2.7 Mbp were observed in recent studies based on human fibroblasts (Yamada et al. 1996). Although genomic rearrangements of the HPRT mutant clones identified in this study don't deliver direct information about the exact sizes of each deletion or insertion, such rearrangements encompass at least 100 kbp. Also considering that the inversions may most likely be related to the formation of large fragments, one can speculate that the small fragments can be due to the deletions. Restriction fragment size

alterations and PCR patterns obtained for all 30 mutant clones (see Table 4.5) derived from hTERT-immortalised fibroblasts are given in Figure 4.9. By increasing the acute doses of X-rays, the generation of an unaltered *NotI* restriction fragment decreases, whereas deletions and genomic rearrangements increase (Figure 4.9 Panel A). As can be seen in Panel B, proportions of WT patterns only restricted to HPRT gene exon-screening (~50 kbp) are significantly higher than the proportion of total and PD patterns (6-Gy mutant clones). Further, a substantial fraction of mutant clones with aberrant restriction fragments whose genomic DNA retain the WT pattern according to multiplex PCR analysis are related to genomic rearrangements. Previous studies in which radiation-induced mutation was examined, have shown that large deletions are the predominant lesions after cell exposure to comparable doses of X-rays (Bao et al. 1995; Morris et al. 1993; Nelson et al. 1994). Although Panel A and Panel B of Figure 4.9 show distinguished patterns, mutant clones from 2-Gy fraction do not render a significant difference between PCR results and the results obtained from Southern blots. In the 2-Gy fraction, both show relatively similar proportions with PD and TD patterns.

However, the results obtained in this part of the study suggest that total loss of hybridisation signals is not significantly dependent on the dose. In the results obtained here, mutant clones with “no signal” comprised 27% (3/11) or 28% (5/18) of clones isolated after irradiation of hTERT-immortalised fibroblasts with acute doses of 2 or 6-Gy of X-rays respectively. Similar results have been documented by several authors previously (Schmidt & Kiefer 1998; Schwartz et al. 1994) suggesting that cell types and individual procedures of the experiments may cause these effects. Potential explanation for the marked decrease with increasing doses is a sample size of radiation-induced mutant clones. The X-ray-induced mutant clones considered in the final set of mutant clones are free from pre-existing spontaneous clones (background mutant clones were removed). The proportions of partial deletions 27% (3/11) and 14% (2/14) for 2 and 6-Gy of X-rays respectively demonstrate dose dependencies in this part of the study. These deletions are in agreement with a previous report (Yamada et al. 1996) and also with our data obtained for fractionated experiments (see further Section 5.4). Taken together, both deletions and formation of aberrant restriction fragments through genomic rearrangements increased with an increase of doses (Figure 4.9 Panel A). However, Yamada et al. (1996) suggested that there was little difference between the results obtained from Southern blot and multiplex PCR analyses. This difference may be due to the specificity of the hybridisation assay compared to conventional Southern blot methods that have previously been used in the mutation analysis (Yamada et al. 1996).

The last experiment contained significantly elevated levels of spontaneous mutations. The reason for higher spontaneous mutations is associated with a significantly elevated plating efficiency of the sub cell line of 82-6 hTERT cells (at least 50% of plating efficiency). Similar data had been documented in previous reports. Such mutational events may have arisen during the early expansion of a culture to produce a significant fraction of spontaneously arising mutants. These were commonly termed as “*Jackpots*” (Asteris & Sarkar 1996; Brown & Thacker 1984; Okinaka et al. 1993).

In the mutant fraction of 6-Gy X-ray-induced clones, there were 10 mutant clones present with all exons (WT mutant clones). Three of these mutants gave unaltered restriction fragments and the remaining seven contained altered fragments. Previous studies suggest that the kinds of point mutations and the frequency of small deletions induced by IR may differ when compared to spontaneous mutations (Nelson et al. 1994; Okinaka et al. 1993) and most of these were found in exonic segments of the gene (Manjanatha et al. 1994). Interestingly, one of the mutant clones (6/10e) with unaltered restriction fragment contained a point mutation according to the data obtained by DNA sequencing. This intron- exon junction mutation was a transversion from T to G (T:A → G:C) and found in intronic sequences, 13 base pairs upstream from exon 8. Since this is found in the 15-nucleotide (nt) 3' splice site consensus, the mutation is likely to be related to a splicing mutation (Sun & Chasin 2000). HPRT gene inactivation of 6/10e may most likely be due to an anomaly in the formation of the protein. Similar mutations of single base pair substitutions have been previously reported (Andersson et al. 1992; Bao et al. 1995). Two mutant clones in the same fraction showed a reciprocal and a non-reciprocal translocation (Figure 4.13). The reciprocal translocation (between X and 2 chromosomes)(6/12d) was of a mutant clone that had a large restriction *NotI* fragment with a wild type pattern of HPRT exons, while the non-reciprocal translocation was a mutant clone (6/6dI) with a small restriction fragment. RT-PCR analysis of these two mutant clones with translocations gave no products. Most likely, the translocation junctions lie within intronic regions of the gene. According to previous results obtained from molecular analyses for similar mutant clones, these translocations may be associated with the HPRT gene specific region of chromosome X (Lobrich 1999; Simpson et al. 1993).

Among the two mutant clones with partial deletions (PD mutant clones) in the gene, one (6/3b) had an end-deletion in exons 7-9 of the genomic DNA giving no signal with the DXS1327 probe. This particular mutant has a minimum deletion of 200 kbp. The remaining mutant clone showed a small restriction fragment with loss of exon 3 according to PCR analysis. The latter mutant clone (6/7aI) exhibited a non-reciprocal translocation (see Results

section Figure 4.13) between X and one of the autosomes. In extensive PCR studies, carried out to determine the approximate break point regions relative to the wild type gene sequence revealed that the break point of this translocation should be located between 16252 to 16872 bp (620 bp) on the HPRT gene (Gene bank sequence) (see Results 4.2.4.1). As also described in the previous paragraph, this mutation is likely to be associated with a deletion of mega base pairs, since such cytogenetically visible rearrangements are most probably due to larger deletions (Simpson et al. 1993). The two 6-Gy-induced mutant clones with total deletions in the gene gave no signals suggesting a deletion of minimum 250 kbp spanning from the gene to the DXS1327 probe binding site. From four 6-Gy X-ray-induced mutant clones whose mutation was only investigated by hybridisation assay, two gave no signals but the other two had small restriction fragments. The nature of the mutation in the two mutants without hybridisation signals could be associated with a minimum deletion of 250 kbp, because most of the mutant clones with no signals had lost the entire HPRT gene. In the other two mutant clones, genomic rearrangements may be the reasons for inactivation of the gene, when one considers the results of similar mutant clones of this study.

In the fraction of 2-Gy X-ray-induced mutant clones, there were four mutant clones with WT pattern, three PDs and four TDs. All mutant clones with the presence of a complete set of exons remained unaltered in the *NotI* restriction fragment indicating that the mutation is related to point mutations or small deletions in the coding segments of the gene. This was also consistent with the RT-PCR results. DNA sequencing of all 4 mutant clones with unaltered restriction fragments revealed that two of them had base pair substitutions in exonic segments. Mutant clone, 2/11d of Experiment I had a transversion from A to C (A: T → C: G) and it was found in exon 9 whereas the other mutant clone (2/15b) had a transition from C to T (C: G → T: A) in exon 6 (see DNA sequencing 4.2.6). Altered gene products may most likely have results in the HPRT gene inactivation of these two mutant clones. Transitions of base pairs such as found in 2/15b have been reported by Bao et al. (1995) in the spontaneous mutant clones derived from human lymphoblastoid cell line. Further, previous reports have revealed that point mutations acquired by X-ray exposure were very diverse including all types of transitions and transversions, tandem base substitutions, frameshifts, small deletions. Compared to spontaneous data, radiation-induced mutations displayed a reduced number of transitions and an increased number of small deletions (Nelson et al. 1994). Due to the fact that a relatively small number of point mutations were found by DNA sequencing in the current study and only 3 X-ray-induced mutant clones revealed the mutation, one can not draw useful conclusions. However, the point mutations found among the smaller number of

mutant clones are in agreement with previous reports (Bao et al. 1995; Leonhardt et al. 2000). In four X-ray-induced and two spontaneous mutant clones, the base pair changes could not be found. Small-scale mutations occurring in exon-intron junctions may be the cause of the inactivation of the gene in those mutant clones (Andersson et al. 1992). In addition, it had been reported previously that certain regions of the HPRT gene locus appear to be especially sensitive to radiation-induced mutations (deletions) and that these deletions may be dependent on the LET (Schwartz et al. 1994). The preferential localizations of such deletion break points were reported at or towards the 3' end of the human HPRT gene (Albertini et al. 1990c; Park et al. 1995; Thacker et al. 1990). A previous report revealed that the majority of point mutations sequenced in their studies occurred at the 3' end of the HPRT gene (Mullis & Faloona 1987).

Two of the PD mutant clones had two different contiguous end deletions in exons 1-5 and 1-2 with their restriction bands being small: The other mutant clones missed exons 7-8. The mutant clone missing exons 1-5 most likely had a deletion of a minimum size of 100 kbp from the 5' end of the HPRT gene. The mutant clone, 2/11d* from Experiment II with a deletion in exons 1-2 displayed a translocation between the X-chromosome and one of the autosomes indicating its mutation may be due to a larger deletion spanning to mega base pairs (Simpson et al. 1993). The mutant clone gave no product in RT-PCR analysis. The remaining mutant clone (2/10d) that had an intragenic contiguous deletion in exons 7-8 with its restriction fragment being a larger one also had a non-reciprocal translocation between X and one of the autosomes. The mutant clone gave no product in RT-PCR analysis indicating that most mutant clones with translocations can not synthesize HPRT-mRNA transcripts (Schmidt & Kiefer 1998). The genomic DNA of the latter mutant clone was examined thoroughly by means of PCR analysis with primers designed to amplify inner PCR products of previously targeted sequences (1533bp) to find out the approximate break point regions relative to wild type HPRT gene sequence. These results revealed that the junction point of the translocation of the mutant clone 2/10d should be within 39106 and 39723bp on the HPRT gene (Gene Bank sequence; M26434) (see Results Figure 4.11). Three mutant clones with a total deletion in HPRT gene gave no signal in the HPRT region with the specific probe; an indication of a minimum of 250 kbp deletion. The other remaining mutant clone had a normal restriction band although PCR results were negative for all coding segments along the entire gene indicating a total deletion. This particular mutant clone (2/5cI) is unique in its pattern and the size of the mutation is presumably between 50 kbp to 100 kbp, since differences below 100 kbp are not detectable in the Southern blot analysis.

5.3.2 Spontaneous Mutant clones

Spontaneously arising mutations are reported to be associated with point mutations or small-scale deletions (Giver et al. 1993; Park et al. 1995; Yamada et al. 1996). Data obtained in this part of the study is therefore in agreement with previous reports because a high proportion of mutant clones are the results of point mutations or small deletions. A total of 18 spontaneous mutant clones was collected from all three experiments. Similar to the current study, low spontaneous mutation rates at the HPRT gene locus in human fibroblasts were documented by previous reports (Park et al. 1995; Yamada et al. 1996). A total of five mutant clones was subjected to comparative study while the remaining 13 mutant clones that were isolated from Experiment III were examined only by hybridisation assay. Of these five mutant clones, 4 had unaltered restriction fragments while the remaining one retained a terminal deletion in exons 1-3. Mutant clones with unaltered fragments contained all exons. The inactivation of the HPRT gene of these 4 mutant clones may be associated with point mutations or small deletions spanning to a few base pairs in the coding segments. All except one mutant clone (K/20c) (see Table 8.1) gave RT-PCR products indicating the mutation of the HPRT mutant clones was due to point mutations or small deletions in exons that nevertheless resulted in an HPRT transcript. Two of these mutant clones were analysed by DNA sequencing (K/40f and K/28a) but no detectable point mutations or deletions based on cDNA were observed. An explanation for this may be that point mutations lie on the sequences. Mutant clone (K/20c) with a partial deletion retained a large restriction fragment suggesting that the mutation is related to genomic rearrangements following partial deletions in exons 1-3 of the gene. Cytogenetic studies failed to give indications for the presence of inter-chromosomal translocation in the mutant cells; pointing to an intra-chromosomal aberration. A similar mutant clone was previously reported to have an intragenic deletion missing exons 2-5 (Park et al. 1995). Furthermore, a spontaneous mutant clone derived from a human lymphoblastoid cell line also missed exons 2-5 but retained a mRNA transcript (Bao et al. 1995). However, an explanation could not be found. The mechanisms for such a phenomenon remain unclear. No spontaneous mutant clones with total deletions or “no signals” in hybridisation analysis which are the direct indications for large deletions were detected in the present study. In contrast, Park et al. (1995) reported 1 out of 23 HPRT mutant clones exhibited “total deletion”.

Overall data obtained in the present study can suggest that the predominant proportion of spontaneously arising mutant clones (13 mutant clones that were exclusively examined by hybridisation assay) may be due to the point mutations or small-scale deletions in the HPRT

coding segment. This is in agreement with several previous reports (Bao et al. 1995; Park et al. 1995).

5.4 Fractionated Irradiation in hTERT-Immortalised Fibroblasts

In this section, the mutagenic effects of dose fractionation versus acute dose irradiation in immortalised human primary fibroblasts were studied. In retrospect, Low Dose Rate (LDR) irradiation was considered to be an extended fraction wise induced mutation experiment, as documented in previous reports, although there existed an infinite number of irradiation intervals (Colussi & Lohman 1997; Colussi et al. 1998). In such studies, it has been shown that lethal and mutagenic effects of LDR gamma rays were lower when compared to irradiation events at higher doses (Evans et al. 1985; Nagasawa et al. 1992). In addition, some authors have reported the opposite effect; indicating LDR increased the mutation in CHO and murine lymphoma cells compared with high dose irradiations (Crompton et al. 1990; Evans et al. 1990). In both induction experiments examined in the present study, parallel acute irradiations were performed in order to provide a comparison. The results obtained from 78 independent mutant clones (including 44 mutant clones analysed by comparative study and 34 mutant clones examined only with hybridisation assay) show that mutation induction frequencies for fractionated irradiations were remarkably lower than the corresponding frequencies obtained for acute irradiations. The reason for a marked reduction in the HPRT mutation frequencies can be found in the rejoining of DSBs; with each serial irradiation cells are faced with a relatively low number of DSBs. Before the next serial irradiation occurred, a significant number of these DSBs appear to have rejoined correctly. Nelson et al. (1996) has suggested that these mutation events are the result of an incremental accumulation of mutations induced by individual 0.2-Gy gamma-ray exposures of TK6 human lymphoblasts.

5.4.1 Dose Fractionation vs. Acute Dose Mutant Clones

In the fraction of 0.6-Gy, seven of 10 mutant clones produced restriction fragment alterations suggesting the gene inactivation was related to genomic rearrangements rather than point mutations or small deletions within the gene. Furthermore, among four WT mutant clones, 3 had aberrant restriction fragments that showed a similar pattern as found in acute- dose mutant clones. In agreement with this some authors have suggested, that the mutation signatures of fractionated low doses could be similar to those of spontaneously arising mutant clones (Nelson et al. 1996).

Mutation frequencies of fractionated irradiations with a total dose of 6-Gy (0.2-Gy x 30) and its corresponding spontaneous mutations were 6.2×10^{-6} and 5×10^{-6} respectively (see Table 4.6). The HPRT mutation frequency significantly decreased in fractionated irradiations compared with corresponding frequencies for acute irradiations. Only three mutant clones in the fraction of 0.6-Gy mutant clones retained unaltered restriction fragments indicating point mutations or small deletions in coding segments of the gene. Since only six mutant clones were subjected to a comparative study, the presence and absence of exons in the remaining four mutant clones can not directly be assessed. In comparison to the overall data obtained in the study, one can assume that these four mutant clones probably consist of either PD or WT patterns. Deletions spanning the entire HPRT gene were observed exclusively at higher doses. Two 0.6-Gy mutant clones with WT patterns synthesized RT-PCR products even though the restriction fragments of these two clones were shown to be aberrant. Previously, only mutant clones with WT patterns bearing unaltered restriction fragments gave corresponding RT-PCR products; an indication that all nine exons lie on a *NotI* restriction fragment as visualised in Southern blots. The inconsistencies of the two mutant clones can be related to chromosomal changes in which the gene and its neighbouring regions, including the hybridisation probe binding site, may have translocated either within the chromosome or into other autosomes. Two mutant clones with continuous end deletions missing exons 1-3 retained unaltered restriction fragments. One of these mutant clones gave a RT-PCR product and the other failed, suggesting that the mutants are different from one another. The mutant clones with no RT-PCR product may have resulted from point mutations or small deletions in exon-intron regions of the coding segments of the gene. Figure 4.17 illustrates the mutation spectra with a total number of 44 clones. The diagram shows when increasing doses are employed, deletions of the entire HPRT gene, including neighbouring sequences increase an amount to ~50% in 6-Gy mutant clones while the wild type pattern of mutant clones decreases. Panel A of Figure 4.17 clearly shows the decrease in the formation of unaltered fragments is related to the increase in the dose. These results are in agreement with the data previously reported by several authors (Aghamohammadi et al. 1992; Bao et al. 1995; Jostes et al. 1994; Yamada et al. 1996). However, one 6-Gy induced mutant clone with a partial deletion in exon 1 gave a RT-PCR product. This suggests that the mutation was related to a deletion in a small sequence within this exon that did not affect transcription. This is further supported by the presence of an unaltered restriction fragment in the mutant DNA. Similarly, two WT mutant clones which did not produce RT-PCR products can be explained by the presence of point mutations; i.e in exon-intron junctions. Six of the 9 mutant clones

that were examined (all nine were analysed only by hybridisation assay) gave no signals on Southern blots. Considering the mutation spectra of the other experiments in this study, it is most likely that the mutant clones missed the entire HPRT gene. Three mutant clones contained small restriction fragments, suggesting the inactivation of the gene may be associated with partial deletions in the coding segments or with break points in the intronic regions of the gene. Mutant clones with aberrant restriction fragments throughout the entire study were mainly related to WT patterns in M-PCR: an indication that rearrangements should have occurred in either intronic or regulatory regions of the HPRT gene.

Results obtained for PD mutant clones which were 6 and 23% for 6-Gy and 2-Gy mutant clones, respectively are consistent with a previous report (Yamada et al. 1996). Although percentages of WT mutant clones with aberrant restriction fragments showed to be nearly the same for both acute irradiations, one 2-Gy mutant failed to generate a RT-PCR product, suggesting splicing errors or point mutations in exon-intron junctions to be the reason. Two different 2-Gy induced mutant clones synthesized RT-PCR products even though their genomic DNA displayed altered restriction fragments. One of these two mutant clones had a WT pattern while the other missed exon 1. Further, a 2-Gy mutant clone with a partial deletion in exon 1 (< 50 kbp) but bearing an unaltered restriction fragment also gave a RT-PCR product suggesting the deletion in coding regions of the mutant DNA. Since acute dose mutant clones with aberrant fragments also gave RT-PCR products, one can not assume that this behaviour is typical to fractionated mutant clones, rather this seems to be related specifically to the cell type. All 29 spontaneously arising mutant clones produced an unaltered restriction fragment which indicates that the mutation is most likely associated with point mutations or small deletions in the coding segments of the gene. This is further supported by the RT-PCR results of eight mutant clones which all produced amplification products.

6 References

1. Aghamohammadi SZ, Morris T, Stevens DL, Thacker J (1992) Rapid screening for deletion mutations in the HPRT gene using the polymerase chain reaction: X-ray and alpha-particle mutant spectra. *Mutat Res* 269: 1-7
2. Agrawal S, Marquet J, Delfau-Larue MH, Copie-Bergman C, Jouault H, Reyes F, Bensussan A, Farcet JP (1998) CD3 hyporesponsiveness and *in vitro* apoptosis are features of T cells from both malignant and nonmalignant secondary lymphoid organs. *J Clin Invest* 102: 1715-1723
3. Albertini RJ (2001) HPRT mutations in humans: biomarkers for mechanistic studies. *Mutat Res* 489: 1-16
4. Albertini RJ, Ardell SK, Judice SA, Jacobson S, Allegretta M (2000) Hypoxanthine-guanine phosphoribosyltransferase reporter gene mutation for analysis of *in vivo* clonal amplification in patients with HTLV type 1-associated Myelopathy /Tropical spastic paraparesis. *AIDS Res Hum Retroviruses* 16: 1747-1752
5. Albertini RJ, Clark LS, Nicklas JA, O'Neill JP, Hui TE, Jostes R (1997) Radiation quality affects the efficiency of induction and the molecular spectrum of HPRT mutations in human T cells. *Radiat Res* 148: 76-86
6. Albertini RJ, Nicklas JA, O'Neill JP (1990a) Studies of DNA alterations in *in vivo* somatic cell mutations in humans. *Basic Life Sci* 53: 315-328
7. Albertini RJ, Nicklas JA, O'Neill JP, Robison SH (1990b) *In vivo* somatic mutations in humans: measurement and analysis. *Ann Rev Genet* 24: 305-326
8. Albertini RJ, O'Neill JP, Nicklas JA, Recio L, Skopek TR (1990c) HPRT mutations *in vivo* in human T-lymphocytes: frequencies, spectra and clonality. *Prog Clin Biol Res* 340: 15-24
9. Allen C, Halbrook J, Nickoloff JA (2003) Interactive competition between homologous recombination and non-homologous end joining. *Mol Cancer Res* 1: 913-920
10. Amundson SA, Chen DJ (1996) Ionizing radiation-induced mutation of human cells with different DNA repair capacities. *Adv Space Res* 18: 119-126
11. Amundson SA, Chen DJ, Okinaka RT (1996) Alpha particle mutagenesis of human lymphoblastoid cell lines. *Int J Radiat Biol* 70: 219-226
12. Amundson SA, Fortunato JE, Liber HL (1992) Heritable alterations at the adenine phosphoribosyltransferase (APRT) locus in human lymphoblastoid cell lines. *Mutat Res* 284: 287-295
13. Amundson SA, Patterson A, Do KT, Fornace AJ Jr. (2002) A nucleotide excision repair master-switch: p53 regulated coordinate induction of global genomic repair genes. *Cancer Biol Ther* 1: 145-149
14. An J, Xu QZ, Sui JL, Bai B, Zhou PK (2005) Downregulation of c-myc protein by siRNA-mediated silencing of DNA-PKcs in HeLa cells. *Int J Cancer* 117: 531-537

6 REFERENCES

15. Anderson CW, Carter TH (1996) The DNA-activated protein kinase - DNA-PK. *Curr Top Microbiol Immunol* 217: 91-111
16. Anderson RA, Eliason SL (1986) Recombination of homologous DNA fragments transfected into mammalian cells occurs predominantly by terminal pairing. *Mol Cell Biol* 6: 3246-3252
17. Andersson B, Hou SM, Lambert B (1992) Mutations causing defective splicing in the human HPRT gene. *Environ Mol Mutagen* 20: 89-95
18. Applegate LA, Lautier D, Frenk E, Tyrrell RM (1992) Endogenous glutathione levels modulate the frequency of both spontaneous and long wavelength ultraviolet induced mutations in human cells. *Carcinogenesis* 13: 1557-1560
19. Asteris G, Sarkar S (1996) Bayesian procedures for the estimation of mutation rates from fluctuation experiments. *Genetics* 142: 313-326
20. Badie C, Iliakis G, Foray N, Alsbeih G, Cedervall B, Chavaudra N, Pantelias G, Arlett C, Malaise EP (1995) Induction and rejoining of DNA double-strand breaks and interphase chromosome breaks after exposure to X-rays in one normal and two hypersensitive human fibroblast cell lines. *Radiat Res* 144: 26-35
21. Bailey SM, Cornforth MN, Ullrich RL, Goodwin EH (2004) Dysfunctional mammalian telomeres join with DNA double-strand breaks. *DNA Repair (Amst)* 3: 349-357
22. Bakkenist CJ, Kastan MB (2003) DNA damage activates ATM through intermolecular autophosphorylation and dimer dissociation. *Nature* 421: 499-506
23. Ballarini F, Ottolenghi A (2003) Chromosome aberrations as biomarkers of radiation exposure: modelling basic mechanisms. *Adv Space Res* 31: 1557-1568
24. Bao CY, Ma AH, Evans HH, Horng MF, Mencl J, Hui TE, Sedwick WD (1995) Molecular analysis of hypoxanthine phosphoribosyltransferase gene deletions induced by alpha- and X-radiation in human lymphoblastoid cells. *Mutat Res* 326: 1-15
25. Bauchinger M, Schmid E (1997) Is there reliable experimental evidence for a chromosomal "fingerprint" of exposure to densely ionizing radiation? *Radiat Res* 147: 506-510
26. Bennett CB, Westmoreland TJ, Snipe JR, Resnick MA (1996) A double-strand break within a yeast artificial chromosome (YAC) containing human DNA can result in YAC loss, deletion or cell lethality. *Mol Cell Biol* 16: 4414-4425
27. Biedermann KA, Sun JR, Giaccia AJ, Tosto LM, Brown JM (1991) SCID mutation in mice confers hypersensitivity to ionizing radiation and a deficiency in DNA double-strand break repair. *Proc Natl Acad Sci USA* 88: 1394-1397
28. Bodnar AG, Ouellette M, Frolkis M, Holt SE, Chiu CP, Morin GB, Harley CB, Shay JW, Lichsteiner S, Wright WE (1998) Extension of life-span by introduction of telomerase into normal human cells. *Science* 279: 349-352
29. Boei JJ, Natarajan AT (1998) Combined use of chromosome painting and telomere detection to analyse radiation-induced chromosomal aberrations in mouse splenocytes. *Int J Radiat Biol* 73: 125-133

6 REFERENCES

30. Brendel M, Bonatto D, Strauss M, Revers LF, Pungartnik C, Saffi J, Henriques JA (2003) Role of PSO genes in repair of DNA damage of *Saccharomyces cerevisiae*. *Mutat Res* 544: 179-193
31. Brenner DJ (1996) Direct biological evidence for a significant neutron dose to survivors of the Hiroshima atomic bomb. *Radiat Res* 145: 501-507
32. Brown R, Stretch A, Thacker J (1986) The nature of mutants induced by ionizing radiation in cultured hamster cells. II. Antigenic response and reverse mutation of HPRT-deficient mutants induced by gamma-rays or ethyl methanesulphonate. *Mutat Res* 160: 111-120
33. Brown R, Thacker J (1984) The nature of mutants induced by ionizing radiation in cultured hamster cells. I. Isolation and initial characterisation of spontaneous, ionizing radiation-induced, and ethyl methanesulphonate-induced mutants resistant to 6-thioguanine. *Mutat Res* 129: 269-281
34. Brownie J, Shawcross S, Theaker J, Whitcombe D, Ferrie R, Newton C, Little S (1997) The elimination of primer-dimer accumulation in PCR. *Nucleic Acids Res* 25: 3235-3241
35. Brunn GJ, Williams J, Sabers C, Wiederrecht G, Lawrence JCJ, Abraham RT (1996) Direct inhibition of the signaling functions of the mammalian target of rapamycin by the phosphoinositide 3-kinase inhibitors, wortmannin and LY294002. *Embo J* 15: 5256-5267
36. Bryant PE (2004) Repair and chromosomal damage. *Radiother Oncol* 72: 251-256
37. Cameron JS, Moro F, Simmonds HA (1993) Gout, uric acid and purine metabolism in paediatric nephrology. *Pediatr Nephrol* 7: 105-118
38. Canman CE, Lim DS (1998) The role of ATM in DNA damage responses and cancer. *Oncogene* 17: 3301-3308
39. Carney JP, Maser RS, Oliveres H, Davis E, Le Beau M, Yates JR, Hays L, Morgan WF, Petrini JH (1998) The hMRE11/hRAD50 protein complex and Nimegen Breakage Syndrome: linkage of double-strand break repair to the cellular DNA damage response. *Cell* 93: 477-486
40. Caspari T (2000) How to activate p53. *Curr Biol* 10: 315-317
41. Cha RS, Thilly WG (1993) Specificity, efficiency, and fidelity of PCR. *PCR Methods Appl* 3: 18-29
42. Chamberlain JS, Chamberlain JR (1994) Optimization of multiplex PCRs. In: Mullis KB, Ferre F, Gibbs RA (eds) *The polymerase chain reaction*. Birkhauser, Boston, pp 38-46
43. Chen CF, Chen PL, Zhong Q, Sharp ZD, Lee WH (1999) Expression of BRC repeats in breast cancer cells disrupts the BRCA2-RAD51 complex and leads to radiation hypersensitivity and loss of G(2)/M checkpoint control. *J Biol Chem* 274: 32931-32935
44. Chernikova SB, Lindquist KL, Elkind MM (2001) Cell cycle-dependent effects of wortmannin on radiation survival and mutation. *Radiat Res* 155: 826-831
45. Chu G (1989) Pulsed field electrophoresis in contour-clamped homogeneous electric fields for the resolution of DNA by size or topology. *Electrophoresis* 10: 290-295

46. Chun HH, Gatti RA (2004) Ataxia-telangiectasia, an evolving phenotype. *DNA Repair (Amst)* 3: 1187-1196
47. Ciampi R, Knauf JA, Kerler R, Gandhi M, Zhu Z, Nikiforova MN, Rabes HM, Fagin JA, Nikiforov YE (2005) Oncogenic AKAP9-BRAF fusion is a novel mechanism of MAPK pathway activation in thyroid cancer. *J Clin Invest* 115: 94-101
48. Cirigliano V, Ejarque M, Canadas MP, Lloveras E, Plaja A, Perez MM, Fuster C, Egozcue J (2001) Clinical application of multiplex quantitative fluorescent polymerase chain reaction (QF-PCR) for the rapid prenatal detection of common chromosome aneuploidies. *Mol Hum Reprod* 7: 1001-1006
49. Cliby WA, Roberts CJ, Cimprich KA, Stringer CM, Lamb JR, Schreiber SL, Friend SH (1998) Overexpression of a kinase-inactive ATR protein causes sensitivity to DNA-damaging agents and defects in cell cycle checkpoints. *Embo J* 17: 159-169
50. Cohen SM, Brylawski BP, Cordeiro-Stone M, Kaufman DG (2002) Mapping of an origin of DNA replication near the transcriptional promoter of the human HPRT gene. *J Cell Biochem* 85: 346-356
51. Collis SJ, DeWeese TL, Jeggo PA, Parker AR (2005) The life and death of DNA-PK. *Oncogene* 24: 949-961
52. Colussi N, Lohman PH (1997) Low dose-rate X-irradiation induces larger deletions at the human HPRT locus than high dose rate X-irradiation. *Int J Radiat Biol* 72: 531-536
53. Colussi N, Van Leeuwen X, Lohman PH (1998) Similar mutational spectra in the HPRT gene of human and hamster cell lines after exposure to either low dose rate or high dose rate X-rays. *Mutat Res* 401: 89-97
54. Crompton NE, Barth B, Kiefer J (1990) Inverse dose-rate effect for the induction of 6-thioguanine-resistant mutants in Chinese hamster V79-S cells by ⁶⁰Co gamma rays. *Radiat Res* 124: 300-308
55. Crompton NE, Shi YQ, Wuergler F, Blattmann H (2002) A single low dose of X-rays induces high frequencies of genetic instability (aneuploidy) and heritable damage (apoptosis), dependent on cell type and p53 status. *Mutat Res* 517: 173-186
56. da Cruz AD, Glickman BW (1997) Nature of mutation in the human HPRT gene following *in vivo* exposure to ionizing radiation of cesium-137. *Environ Mol Mutagen* 30: 385-395
57. Dahle J, Kvam E (2003) Induction of delayed mutations and chromosomal instability in fibroblasts after UVA-, UVB-, and X-radiation. *Cancer Res* 63: 1464-1469
58. Dai Y, Kysela B, Hanakahi LA, Manolis K, Riballo E, Stumm M, Harville TO, West SC, Oettinger MA, Jeggo PA (2003) Non-homologous end-joining and V(D)J recombination require an additional factor. *Proc Natl Acad Sci USA* 100: 2462-2467
59. de Klein A, Muijtjens M, van Os R, Verhoeven Y, Smit B, Carr AM, Lehmann AR, Hoeijmakers JH (2000) Targeted disruption of the cell-cycle checkpoint gene ATR leads to early embryonic lethality in mice. *Curr Biol* 10: 479-482

60. Delacote F, Han M, Stamato TD, Jasin M, Lopez BS (2002) An XRCC4 defect or wortmannin stimulates homologous recombination specifically induced by double-strand breaks in mammalian cells. *Nucleic Acids Res* 30: 3454-3463
61. Den Dunnen JT, Grootsholten PM, Bakker E, Blonden LA, Ginjaar HB, Wapenaar MC, van Paassen HM, van Broeckhoven C, Pearson PL, van Ommen GJ (1989) Topography of the Duchenne muscular dystrophy (DMD) gene: FIGE and cDNA analysis of 194 cases reveals 115 deletions and 13 duplications. *Am J Hum Genet* 45: 835-847
62. Denault CM, Liber HL (1993) The effects of hypoxia and cysteamine on X-ray mutagenesis in human cells. I. Dose response and Southern blot analysis of induced mutants. *Radiat Res* 135: 98-107
63. Dobrovolsky VN, Shaddock JG, Heflich RH (2005) Analysis of *in vivo* mutation in the HPRT and TK genes of mouse lymphocytes. *Methods Mol Biol* 291: 133-144
64. Donoho G, Brenneman MA, Cui TX, Donoviel D, Vogel H, Goodwin EH, Chen DJ, Hasty P (2003) Deletion of BRCA2 exon 27 causes hypersensitivity to DNA crosslinks, chromosomal instability, and reduced life span in mice. *Genes Chromosomes Cancer* 36: 317-331
65. Drobetsky EA, Sage E (1993) UV-induced G:C-->A:T transitions at the APRT locus of Chinese hamster ovary cells cluster at frequently damaged 5'-TCC-3' sequences. *Mutat Res* 289: 131-138
66. Edelmann L, Spiteri E, Koeren K, Pulijaal V, Bialer MG, Shanske A, Goldberg R, Morrow BE (2001) AT- rich palindromes mediate the constitutional t(11;22) translocation. *Am J Hum Genet* 68: 1-13
67. Edwards A, Voss H, Rice P, Civitello A, Stegemann J, Schwager C, Zimmermann J, Erfle H, Caskey CT, Ansorge W (1990) Automated DNA sequencing of the human HPRT locus. *Genomics* 6: 593-608
68. Edwards AA (1997) The use of chromosomal aberrations in human lymphocytes for biological dosimetry. *Radiat Res* 148: 39-44
69. Edwards MC, Gibbs RA (1994) Multiplex PCR: advantages, development, and applications. *PCR Methods Appl* 3: 65-75
70. Edwards SM, Kent CR, McMillan TJ, Steel GG (1997) HPRT- mutation spectrum in a closely related pair of human bladder tumour cell lines after gamma-irradiation at different dose-rates. *Int J Radiat Biol* 71: 177-184
71. Ege M, Ma Y, Manfras B, Kalwak K, Lu H, Lieber MR, Schwarz K, Pannicke U (2005) Omenn syndrome due to Artemis mutations. *Blood* 105: 4179-4186
72. El-Khamisy SF, Saifi GM, Weinfeld M, Johansson F, Helleday T, Lupski JR, Caldecott KW (2005) Defective DNA single-strand break repair in spinocerebellar ataxia with axonal neuropathy-1. *Nature* 434: 108-113
73. Essers J, Hendriks RW, Wesoly J, Beerens CE, Smit B, Hoeijmakers JH, Wyman C, Dronkert ML, Kanaar R (2002) Analysis of mouse RAD54 expression and its implications for homologous recombination. *DNA Repair (Amst)* 1: 779-793

74. Evans HH, Horng MF, Mencl J, Glazier KG, Beer JZ (1985) The influence of dose rate on the lethal and mutagenic effects of X-rays in proliferating L5178Y cells differing in radiation sensitivity. *Int J Radiat Biol Relat Stud Phys Chem Med* 47: 553-562
75. Evans HH, Nielsen M, Mencl J, Horng MF, Ricanati M (1990) The effect of dose rate on X-radiation-induced mutant frequency and the nature of DNA lesions in mouse lymphoma L5178Y cells. *Radiat Res* 122: 316-325
76. Fearon ER, Vogelstein B (1990) A genetic model for colorectal tumorigenesis. *Cell* 61: 759-767
77. Fernandez-Capetillo O, Chen HT, Celeste A, Ward I, Romanienko PJ, Morales JC, Naka K, Xia Z, Camerini-Otero RD, Motoyama N, Carpenter PB, Bonner WM, Chen J, Nussenzweig A (2002) DNA damage-induced G2-M checkpoint activation by histone H2AX and 53BP1. *Nat Cell Biol* 4: 993-997
78. Finette BA, Poseno T, Albertini RJ (1996) V(D)J recombinase-mediated HPRT mutations in peripheral blood lymphocytes of normal children. *Cancer Res* 56: 1405-1412
79. Foray N, Arlett CF, Malaise EP (1999) Underestimation of the small residual damage when measuring DNA double-strand breaks (DSB): is the repair of radiation-induced DSB complete? *Int J Radiat Biol* 75: 1589-1595
80. Foray N, Marot D, Gabriel A, Randrianarison V, Carr AM, Perricaudet M, Ashworth A, Jeggo P (2003) A subset of ATM- and ATR-dependent phosphorylation events requires the BRCA1 protein. *Embo J* 22: 2860-2871
81. Frankenberg D, Kelnhofer K, Garg I, Bar K, Frankenberg-Schwager M (2002) Enhanced mutation and neoplastic transformation in human cells by 29 kVp relative to 200 kVp X rays indicating a strong dependence of RBE on photon energy. *Radiat Prot Dosimetry* 99: 261-264
82. Frankenberg-Schwager M, Garg I, Fran-Kenberg D, Greve B, Severin E, Uthe D, Gohde W (2002) Mutagenicity of low-filtered 30 kVp X-rays, mammography X-rays and conventional X-rays in cultured mammalian cells. *Int J Radiat Biol* 78: 781-789
83. Fujimori A, Tachibana A, Tatsumi K (1992) Allelic losses in mutations at the APRT locus of human lymphoblastoid cells. *Mutat Res* 269: 55-62
84. Fuscoe JC, Zimmerman LJ, Fekete A, Setzer RW, Rossiter BJ (1992) Analysis of X-ray-induced HPRT mutations in CHO cells: insertion and deletions. *Mutat Res* 269: 171-183
85. Galloway SM (1994) Chromosome aberrations induced *in vitro*: mechanisms, delayed expression and intriguing questions. *Environ Mol Mutagen* 23: 44-53
86. Gardiner K, Horisberger M, Kraus J, Tantravahi U, Korenberg J, Rao V, Ready S, Patterson D (1990) Analysis of human chromosome 21: correlation of physical and cytogenetic maps; gene CpG island distributions. *Embo J* 9: 25-34
87. Gatei M, Scott SP, Filippovitch I, Soronika N, Lavin MF, Weber B, Khanna KK (2000) Role for ATM in DNA damage-induced phosphorylation of BRCA1. *Cancer Res* 60: 3299-3304

88. Gisselsson D, Pettersson L, Hoglund M, Heidenblad M, Gorunova L, Wiegant J, Mertens F, Dal Cin P, Mitelman F, Mandahl N (2000) Chromosomal breakage-fusion-bridge events cause genetic intratumor heterogeneity. *Proc Natl Acad Sci USA* 97: 5357-5362
89. Giver CR, Nelson SL, Grosovsky AJ (1993) Spectrum of spontaneous HPRT- mutations in TK6 human lymphoblasts. *Environ Mol Mutagen* 22: 138-146
90. Giver CR, Nelson SLJ, Cha MY, Pongsaensook P, Grosovsky AJ (1995) Mutational spectrum of X-ray induced TK- human cell mutants. *Carcinogenesis* 16: 267-275
91. Goi K, Takagi M, Iwata S, Delia D, Asada M, Donghi R, Tsunematsu Y, Nakazawa S, Yamamoto H, Yokota J, Tamura K, Saeki Y, Utsunomiya J, Takahashi T, Ueda R, Ishioka C, Eguchi M, Kamata N, Mizutani S (1997) DNA damage-associated dysregulation of the cell cycle and apoptosis control in cells with germ-line p53 mutation. *Cancer Res* 57: 1895-1902
92. Goodhead DT (1994) Initial events in the cellular effects of ionizing radiations: Clustered damage in DNA. *Int J Radiat Biol* 65: 7-17
93. Goodship J, Gill H, Carter J, Jackson A, Splitt M, Wright M (2000) Autozygosity mapping of a seckel syndrome locus to chromosome 3q22. 1-q24. *Am J Hum Genet* 67: 498-503
94. Grawunder U, Wilm M, Wu X, Kulesza P, Wilson TE, Mann M, Lieber MR (1997) Activity of DNA ligase IV stimulated by complex formation with XRCC4 protein in mammalian cells. *Nature* 388: 492-495
95. Griffin CS, Thacker J (2004) The role of homologous recombination repair in the formation of chromosome aberrations. *Cytogenet Genome Res* 104: 21-27
96. Griffiths SD, Clarke AR, Healy LE, Ross G, Ford AM, Hooper ML, Wyllie AH, Greaves M (1997) Absence of p53 permits propagation of mutant cells following genotoxic damage. *Oncogene* 14: 523-531
97. Grosovsky AJ, Parks KK, Giver CR, Nelson SL (1996) Clonal analysis of delayed karyotypic abnormalities and gene mutations in radiation-induced genetic instability. *Mol Cell Biol* 16: 6252-6262
98. Hall EJ (2000) *Radiology for the Radiologists*. 5th ed. Lippincott Williams & Wilkins, Philadelphia
99. Hall EJ, Astor M, Bedford J, Borek C, Curtis SB, Fry M, Geard C, Hei T, Mitchell J, Oleinick N (1988) Basic radiobiology. *Am J Clin Oncol* 11: 220-252
100. Hammarsten O, Chu G (1998) DNA-dependent protein kinase: DNA binding and activation in the absence of Ku. *Proc Natl Acad Sci USA* 95: 525-530
101. Hartley KO, Gell D, Smith GC, Zhang H, Divecha N, Connelly MA, Admon A, Lees-Miller SP, Anderson CW, Jackson SP (1995) DNA-dependent protein kinase catalytic subunit: A relative of phosphatidylinositol 3-kinase and the ataxia telangiectasia gene product. *Cell* 82: 849-856
102. Harvey AC, Jackson SP, Downs JA (2005) *Saccharomyces cerevisiae* histone H2A Ser122 facilitates DNA repair. *Genetics* 170: 543-553

103. Harvey AN, Costa ND, Savage JR, Thacker J (1997) Chromosomal aberrations induced by defined DNA double-strand breaks: the origin of achromatic lesions. *Somat Cell Mol Genet* 23: 211-219
104. Hashimoto M, Rao S, Tokuno O, Yamamoto K, Takata M, Takeda S, Utsumi H (2003) DNA-PK: the major target for wortmannin-mediated radiosensitization by the inhibition of DSB repair via NHEJ pathway. *J Radiat Res (Tokyo)* 44: 151-159
105. Heidenreich WF, Paretzke HG (2004) Interpretation by modelling of observations in radon radiation carcinogenesis. *Radiat Prot Dosimetry* 112: 501-507
106. Helbig R, Gerland E, Speit G (1994) The molecular nature of mutations induced by adriamycin at the HPRT locus of V79 cells. *Mutagenesis* 9: 113-116
107. Helt CE, Cliby WA, Keng PC, Bambara RA, O'Reilly MA (2005) Ataxia telangiectasia mutated (ATM) and ATM and Rad3-related protein exhibit selective target specificities in response to different forms of DNA damage. *J Biol Chem* 280: 1186-1192
108. Hendrickson EA, Qin XQ, Bump EA, Schatz DG, Oettinger M, Weaver DT (1991) A link between double-strand break-related repair and V(D)J recombination: the SCID mutation. *Proc Natl Acad Sci USA* 88: 4061-4065
109. Hlatky LR, Sachs RK, Hahnfeldt P (1992) The ratio of dicentrics to centric rings produced in human lymphocytes by acute low-LET radiation. *Radiat Res* 129: 304-308
110. Horikawa K, Kawaguchi T, Ishihara S, Nagakura S, Hidaka M, Kagimoto T, Mitsuya H, Nakakuma H (2002) Frequent detection of T cells with mutations of the hypoxanthine-guanine phosphoribosyl transferase gene in patients with paroxysmal nocturnal hemoglobinuria. *Blood* 99: 24-29
111. Hou SM (1994) Novel types of mutation identified at the HPRT locus of human T-lymphocytes. *Mutat Res* 308: 23-31
112. Hu X, Ray PN, Worton RG (1991) Mechanisms of tandem duplication in the Duchenne muscular dystrophy gene include both homologous and non-homologous intra-chromosomal recombination. *Embo J* 10: 2471-2477
113. Hunter TC, Melancon SB, Dallaire L, Taft S, Skopek TR, Albertini RJ, O'Neill JP (1996) Germinal HPRT splice donor site mutation results in multiple RNA splicing products in T-lymphocyte cultures. *Somat Cell Mol Genet* 22: 145-150
114. Hutchinson F (1995) Analysis of deletions induced in the genome of mammalian cells by ionizing radiation. *J Mol Biol* 254: 372-380
115. Ichikawa H, Schimizu K, Saito A, Wang DN, Oliva R, Kobayashi H, Kaneko Y, Miyoshi H, Smith CL, Cantor CR (1992) Long-distance restriction mapping of the proximal long arm of human 21 with *NotI* linking clones. *Proc Natl Acad Sci USA* 89: 23-27
116. Jackson SP (2002) Sensing and repairing DNA double-strand breaks. *Carcinogenesis* 23: 687-696
117. Jayanth VR, Bayne MT, Varnes ME (1994) Effects of extracellular and intracellular pH on repair of potentially lethal damage, chromosome aberrations and DNA double-strand breaks in irradiated plateau-phase A549 cells. *Radiat Res* 139: 152-162

118. Jeggo PA (1998) Identification of genes involved in repair of DNA double-strand breaks in mammalian cells. *Radiat Res* 150: 80-91
119. Jeggo PA, Lobrich M (2005) Artemis links ATM to double strand break rejoining. *Cell Cycle* 4: 359-362
120. Jin L, Richards A, Brown DWG (1996) Development of a dual target-PCR for detection and characterisation of measles virus in clinical specimens. *Mol Cell Probes* 10: 191-200
121. Jinnah HA, De Gregorio L, Harris JC, Nyhan WL, O'Neill JP (2000) The spectrum of inherited mutations causing HPRT deficiency: 75 new cases and a review of 196 previously reported cases. *Mutat Res* 463: 309-326
122. Jolly DJ (1986) The role of the HPRT gene in human disease. *Horiz Biochem Biophys* 8: 123-168
123. Jolly DJ, Okayama H, Berg P, Esty AC, Filpula D, Bohlen P, Johnson GG, Shively JE, Hunkapillar T, Friedmann T (1983) Isolation and characterisation of a full-length expressible cDNA for human hypoxanthine phosphoribosyl transferase. *Proc Natl Acad Sci USA* 80: 477-481
124. Jostes RF (1996) Genetic, cytogenetic, and carcinogenic effects of radon: a review. *Mutat Res* 340: 125-139
125. Jostes RF, Fleck EW, Morgan TL, Stiegler GL, Cross FT (1994) Southern blot and polymerase chain reaction exon analyses of HPRT- mutations induced by radon and radon progeny. *Radiat Res* 137: 371-379
126. Kadhim MA, Lorimore SA, Townsend KM, Goodhead DT, Buckle VJ, Wright EG (1995) Radiation-induced genomic instability: delayed cytogenetic aberrations and apoptosis in primary human bone marrow cells. *Int J Radiat Biol* 67: 287-293
127. Karanjawala ZE, Adachi N, Irvine RA, Oh EK, Shibata D, Schwarz K, Hsieh CL, Lieber MR (2002) The embryonic lethality in DNA ligase IV-deficient mice is rescued by deletion of Ku: implications for unifying the heterogeneous phenotypes of NHEJ mutants. *DNA Repair (Amst)* 1: 1017-1026
128. Karanjawala ZE, Hinton DR, Oh E, Hsieh CL, Lieber MR (2003) Developmental retinal apoptosis in Ku86-/- mice. *DNA Repair (Amst)* 2: 1429-1434
129. Kastan MB, Onyekwere O, Sidransky D, Vogelstein B, Craig RW (1991) Participation of p53 protein in the cellular response to DNA damage. *Cancer Res* 51: 6304-6311
130. Kato T, Ishikawa K, Nemoto R, Senoo A, Amano Y (1978) Morphological characterisation of two established cell lines. *Tohoku J Exp Med* 124: 339-349
131. Khanna KK, Jackson SP (2001) DNA double-strand breaks: signaling, repair and the cancer connection. *Nat Genet* 27: 247-254
132. Khanna KK, Lavin MF, Jackson SP, Mulhern TD (2001) ATM, a central controller of cellular responses to DNA damage. *Cell Death Differ* 8: 1052-1065
133. Kim SH, Moores JC, David D, Respass JG, Jolly DJ, Friedmann T (1986) The organization of the human HPRT gene. *Nucleic Acids Res* 14: 3103-3118

134. Kinashi Y, Masunaga S, Suzuki M, Nagata K, Ono K (2003) The biological effect of the phosphatidylinositol 3-kinase wortmannin following thermal neutron irradiation. *Nippon Igaku Hoshasen Gakkai Zasshi* 63: 405-408
135. Kinashi Y, Okayasu R, Iliakis GE, Nagasawa H, Little JB (1995) Induction of DNA double-strand breaks by restriction enzymes in X-ray-sensitive mutant Chinese hamster ovary cells measured by pulsed-field gel electrophoresis. *Radiat Res* 141: 153-159
136. Koch CA, Agyei R, Galicia S, Metalnikov P, O'Donnell P, Starostine A, Weinfeld M, Durocher D (2004) XRCC4 physically links DNA end processing by polynucleotide kinase to DNA ligation by DNA ligase IV. *Embo J* 23: 3874-3885
137. Kudsk KA, Tranbaugh RF, Sheldon GF (1981) Acute surgical illness in patients with sickle cell anemia. *Am J Surg* 142: 113-117
138. Kuhne M, Riballo E, Rief N, Rothkamm K, Jeggo PA, Lobrich M (2004) A double-strand break repair defect in ATM-deficient cells contributes to radiosensitivity. *Cancer Res* 64: 500-508
139. Lee JH, Paull TT (2004) Direct activation of the ATM protein kinase by the MRE11/RAD50/NBS1 complex. *Science* 304: 93-96
140. Lee JH, Paull TT (2005) ATM activation by DNA double-strand breaks through the MRE11/RAD50/NBS1 complex. *Science* 308: 551-554
141. Leonhardt EA, Trinh M, Chu K, Dewey WC (2000) Mutations induced in the HPRT gene by X-irradiation during G1 or S: analysis of base pair alterations, small deletions, and splice errors. *Mutat Res* 471: 7-19
142. Lesch M, Nyhan WL (1964) A Familial Disorder of Uric Acid Metabolism and Central Nervous System Function. *Am J Med* 36: 561-570
143. Li CY, Yandell DW, Little JB (1992) Molecular mechanisms of spontaneous and induced loss of heterozygosity in human cell *in vivo*. *Somatic Cell Genet* 8: 77-87
144. Li Z, Otevrel T, Gao Y, Cheng HL, Seed B, Stamato TD, Taccioli GE, Alt FW (1995) The XRCC4 gene encodes a novel protein involved in DNA double-strand break repair and V(D)J recombination. *Cell* 83: 1079-1089
145. Liang L, Shao C, Deng L, Mendonca MS, Stambrook PJ, Tischfield JA (2002) Radiation-induced genetic instability *in vivo* depends on p53 status. *Mutat Res* 502: 69-80
146. Liber HL, LeMotte PK, Little JB (1983) Toxicity and mutagenicity of X-rays and [¹²⁵I]dUrd or [³H]TdR incorporated in the DNA of human lymphoblast cells. *Mutat Res* 111: 387-404
147. Liber HL, Yandell DW, Little JB (1989) A comparison of mutation induction at the TK and HPRT loci in human lymphoblastoid cells; quantitative differences are due to an additional class of mutations at the autosomal TK locus. *Mutat Res* 216: 9-17
148. Lieber MR, Grawunder U, Wu X, Yaneva M (1997) Tying loose ends: roles of Ku and DNA-dependent protein kinase in the repair of double-strand breaks. *Curr Opin Genet Dev* 7: 99-104

149. Lieber MR, Ma Y, Pannicke U, Schwarz K (2003) Mechanism and regulation of human non-homologous DNA end-joining. *Nat Rev Mol Cell Biol* 4: 712-720
150. Lin CW, Lin JC, Prout GR Jr. (1985) Establishment and characterisation of four human bladder tumor cell lines and sublines with different degrees of malignancy. *Cancer Res* 45: 5070-5079
151. Lippert MJ, Albertini RJ, Nicklas JA (1995) Physical mapping of the human HPRT chromosomal region (Xq26). *Mutat Res* 326: 39-49
152. Lippert MJ, Rainville IR, Nicklas JA, Albertini RJ (1997) Large deletions partially external to the human HPRT gene result in chimeric transcripts. *Mutagenesis* 12: 185-190
153. Lobrich M (1999) Untersuchung zur Fehlreparatur strahleninduzierter DNA-Doppelstrangbrüche in Säugerzellen. *Habil. Gießen*
154. Lobrich M, Cooper PK, Rydberg B (1996) Non-random distribution of DNA double-strand breaks induced by particle irradiation. *Int J Radiat Biol* 70: 493-503
155. Lobrich M, Jeggo PA (2005) Harmonising the response to DSBs: a new string in the ATM bow. *DNA Repair (Amst)* 4: 749-759
156. Lobrich M, Kuhne M, Wetzel J, Rothkamm K (2000) Joining of correct and incorrect DNA double-strand break ends in normal human and ataxia telangiectasia fibroblasts. *Genes Chromosomes Cancer* 27: 59-68
157. Lobrich M, Rief N, Kuhne M, Heckmann M, Fleckenstein J, Rube C, Uder M (2005) *In vivo* formation and repair of DNA double-strand breaks after computed tomography examinations. *Proc Natl Acad Sci USA* 102: 8984-8989
158. Lowe SW, Ruley HE, Jacks T, Housman DE (1993a) p53-dependent apoptosis modulates the cytotoxicity of anticancer agents. *Cell* 74: 957-967
159. Lowe SW, Schmitt EM, Smith SW, Osborne BA, Jacks T (1993b) p53 is required for radiation-induced apoptosis in mouse thymocytes. *Nature* 362: 847-849
160. Ma Y, Lieber MR (2002) Binding of inositol hexakisphosphate (IP6) to Ku but not to DNA-PKcs. *J Biol Chem* 277: 10756-10759
161. Manjanatha MG, Lindsey LA, Mittelstaedt RA, Heflich RH (1994) Low HPRT mRNA levels and multiple HPRT mRNA species in 6-thioguanine-resistant Chinese hamster cell mutants possessing nonsense mutations. *Mutat Res* 308: 65-75
162. Markenson AL, Chandra M, Lewy JE, Miller DR (1978) Sickel cell anemia, the nephrotic syndrome and hypoplastic crisis in a sibship. *Am J Med* 64: 719-723
163. McMillan TJ, Tobi S, Mateos S, Lemon C (2001) The use of DNA double-strand break quantification in radiotherapy. *Int J Radiat Oncol Biol Phys* 49: 373-377
164. Meek K, Gupta S, Ramsden DA, Lees-Miller SP (2004) The DNA-dependent protein kinase: the director at the end. *Immunol Rev* 200: 132-141
165. Melton DW, Konecki DS, Brennand J, Caskey CT (1984) Structure, expression and mutation of the hypoxanthine phosphoribosyltransferase gene. *Proc Natl Acad Sci USA* 81: 2147-2151

166. Mendrysa SM, McElwee MK, Michalowski J, O'Leary KA, Young KM, Perry ME (2003) mdm2 Is critical for inhibition of p53 during lymphopoiesis and the response to ionizing irradiation. *Mol Cell Biol* 23: 462-472
167. Merel P, Prieur A, Pfeiffer P, Delattre O (2002) Absence of major defects in non-homologous DNA end joining in human breast cancer cell lines. *Oncogene* 21: 5654-5659
168. Miles C, Sargent G, Phear G, Meuth M (1990) DNA sequence analysis of gamma radiation-induced deletions and insertions at the APRT locus of hamster cells. *Mol Carcinog* 3: 233-242
169. Mizuki M, Fenski R, Halfter H, Matsumura I, Schmidt R, Muller C, Gruning W, Kratz-Albers K, Serve S, Steur C, Buchner T, Kienast J, Kanakura Y, Berdel WE, Serve H (2000) Flt3 mutations from patients with acute myeloid leukemia induce transformation of 32D cells mediated by the Ras and STAT5 pathways. *Blood* 96: 3907-3914
170. Mognato M, Bortoletto E, Ferraro P, Baggio L, Cherubini R, Canova S, Russo A, Celotti L (2003) Genetic damage induced by *in vitro* irradiation of human G0 lymphocytes with low-energy protons (28 keV/microm): HPRT mutations and chromosome aberrations. *Radiat Res* 160: 52-60
171. Mohrenweiser H (1994) International commission for protection against environmental mutagens and carcinogens. Working paper no. 5. Impact of the molecular spectrum of mutational lesions on estimates of germinal gene-mutation rates. *Mutat Res* 304: 119-137
172. Mondello C, Faravelli M, Pipitone L, Rollier A, Di Leonardo A, Giulotto E (2001) Gene amplification in fibroblasts from ataxia telangiectasia (A-T) patients and in X-ray hypersensitive AT-like Chinese hamster mutants. *Carcinogenesis* 22: 141-145
173. Morales CP, Holt SE, Ouellette M, Kaur KJ, Yan Y, Wilson KS, White MA, Wright WE, Shay JW (1999) Absence of cancer associated changes in human fibroblasts immortalised with telomerase. *Nat Genet* 21: 115-118
174. Morris T, Masson W, Singleton B, Thacker J (1993) Analysis of large deletions in the HPRT gene of primary human fibroblasts using the polymerase chain reaction. *Somat Cell Mol Genet* 19: 9-19
175. Morris T, Thacker J (1993) Formation of large deletions by illegitimate recombination in the HPRT gene of primary human fibroblasts. *Proc Natl Acad Sci USA* 90: 1392-1396
176. Morrison C, Sonoda E, Takao N, Shinohara A, Yamamoto K, Takeda S (2000) The controlling role of ATM in homologous recombinational repair of DNA damage. *Embo J* 19: 463-471
177. Moshous D, Callebaut I, de Chasseval R, Corneo B, Cavazzana-Calvo M, Le Deist F, Tezcan I, Sanal O, Bertrand Y, Philippe N, Fischer A, de Villartay JP (2001) Artemis, a novel DNA double-strand break repair/V(D)J recombination protein, is mutated in human severe combined immune deficiency. *Cell* 105: 177-186
178. Moshous D, Pannetier C, Chasseval RR, Deist FI F, Cavazzana-Calvo M, Romana S, Macintyre E, Canioni D, Brousse N, Fischer A, Casanova JL, Villartay JP (2003) Partial T and B lymphocyte immunodeficiency and predisposition to lymphoma in patients with hypomorphic mutations in Artemis. *J Clin Invest* 111: 381-387

179. Mosmann T (1983) Rapid colorimetric assay for cellular growth and survival: Application to proliferation and cytotoxicity assays. *J Immunol Methods* 65: 55-63
180. Mullis KB, Faloona FA (1987) Specific synthesis of DNA *in vitro* via a polymerase - catalysed chain reaction. *Methods in Enzymol* 155: 335-350
181. Nagasawa H, Huo L, Little JB (2003) Increased bystander mutagenic effect in DNA double-strand break repair-deficient mammalian cells. *Int J Radiat Biol* 79: 35-41
182. Nagasawa H, Little JB, Tsang NM, Saunders E, Tesmer J, Strniste GF (1992) Effect of dose rate on the survival of irradiated human skin fibroblasts. *Radiat Res* 132: 375-379
183. Natarajan AT, Balajee AS, Boei JJ, Chatterjee S, Darroudi F, Grigorova M, Noditi M, Oh HJ, Slijepcevic P, Vermeulen S (1994) Recent developments in the assessment of chromosomal damage. *Int J Radiat Biol* 66: 615-623
184. Nelson SL, Giver CR, Grosovsky AJ (1994) Spectrum of X-ray-induced mutations in the human HPRT gene. *Carcinogenesis* 15: 495-502
185. Nelson SL, Jones IM, Fuscoe JC, Burkhardt-Schultz K, Grosovsky AJ (1995) Mapping the end points of large deletions affecting the HPRT locus in human peripheral blood cells and cell lines. *Radiat Res* 141: 2-10
186. Nelson SL, Parks KK, Grosovsky AJ (1996) Ionizing radiation signature mutations in human cell mutants induced by low-dose exposures. *Mutagenesis* 11: 275-279
187. Nghiem P, Park PK, Kim Y, Vaziri C, Schreiber SL (2001) ATR inhibition selectively sensitizes G1 checkpoint-deficient cells to lethal premature chromatin condensation. *Proc Natl Acad Sci USA* 98: 9092-9097
188. Nias AHW (1998) *An introduction to Radiobiology*. 2nd ed. John Wiley & Sons, Chichester
189. Nicholls RD, Fischel-Ghodsian N, Higgs DR (1987) Recombination at the human alpha-globin gene cluster: sequence features and topological constraints. *Cell* 49: 369-378
190. Nicklas JA, Falta MT, Hunter TC, O'Neill JP, Jacobson-Kram D, Williams JR, Albertini RJ (1990) Molecular analysis of *in vivo* HPRT mutations in human T lymphocytes. V. Effects of total body irradiation secondary to radioimmunoglobulin therapy (RIT). *Mutagenesis* 5: 461-468
191. Nicklas JA, Hunter TC, O'Neill JP, Albertini RJ (1989) Molecular analyses of *in vivo* HPRT mutations in human T-lymphocytes. III. Longitudinal study of HPRT gene structural alterations and T-cell clonal origins. *Mutat Res* 215: 147-160
192. Niimi N, Sugo N, Aratani Y, Koyama H (2005) Genetic interaction between DNA polymerase beta and DNA-PKcs in embryogenesis and neurogenesis. *Cell Death Differ* 12: 184-191
193. Nissani M, Carlson E (1975) Letter: The role of Hermann J. Muller in the Drosophila Group. *Genetics* 81: 222a-222d
194. Nitta Y, Hoshi M (2003) Relationship between oocyte apoptosis and ovarian tumours induced by high and low LET radiations in mice. *Int J Radiat Biol* 79: 241-250

195. Nyhan WL (2005) Lesch-Nyhan Disease. *J Hist Neurosci* 14: 1-10
196. O'Driscoll M, Ruiz-Perez V, Woods CG, Jeggo PA, Goodship JA (2003) A splicing mutation affecting expression of ataxia-telangiectasia and Rad3-related protein (ATR) results in Seckel syndrome. *Nat Genet* 33: 497-501
197. Oguchi K, Takagi M, Tsuchida R, Taya Y, Ito E, Isoyama K, Ishii E, Zannini L, Delia D, Mizutani S (2003) Missense mutation and defective function of ATM in a childhood acute leukemia patient with MLL gene rearrangement. *Blood* 101: 3622-3627
198. Ohashi A, Zdzienicka MZ, Chen J, Couch FJ (2005) Fanconi anemia complementation group D2 (FANCD2) functions independently of BRCA2- and RAD51-associated homologous recombination in response to DNA damage. *J Biol Chem* 280: 14877-14883
199. Okano H, Saito Y, Miyazawa T, Shinbo T, Chou D, Kosugi S, Takahashi Y, Odani S, Niwa O, Kominami R (1999) Homozygous deletions and point mutations of the Ikaros gene in gamma-ray-induced mouse thymic lymphomas. *Oncogene* 18: 6677-6683
200. Okayasu R, Suetomi K, Ullrich RL (1998) Wortmannin inhibits repair of DNA double-strand breaks in irradiated normal human cells. *Radiat Res* 149: 440-445
201. Okinaka RT, Anzick SL, Oller A, Thilly WG (1993) Analysis of large X-ray-induced mutant populations by denaturing gradient gel electrophoresis. *Radiat Res* 135: 212-221
202. O'Neill JP, Finette BA (1998) Transition mutations at CpG dinucleotides are the most frequent *in vivo* spontaneous single-based substitution mutation in the human HPRT gene. *Environ Mol Mutagen* 32: 188-191
203. O'Neill JP, Rogan PK, Cariello N, Nicklas JA (1998) Mutations that alter RNA splicing of the human HPRT gene: a review of the spectrum. *Mutat Res* 411: 179-214
204. O'Neill JP, Sullivan LM, Hunter TC, Nicklas JA (1991) Cytosine arabinoside enhancement of gamma irradiation induced mutations in human T-lymphocytes. *Environ Mol Mutagen* 17: 231-237
205. Ortiz T, Lopez S, Burguillos MA, Edreira A, Pinero J (2004) Radiosensitizer effect of wortmannin in radioresistant bladder tumoral cell lines. *Int J Oncol* 24: 169-175
206. Paeratakul U, Taylor MW (1986) Isolation and characterisation of mutants at the APRT locus in the L-5178Y TK⁺/TK⁻ mouse lymphoma cell line. *Mutat Res* 160: 61-69
207. Pandita TK, Lieberman HB, Lim DS, Dhar S, Zheng W, Taya Y, Kastan MB (2000) Ionizing radiation activates the ATM kinase throughout the cell cycle. *Oncogene* 19: 1386-1391
208. Park MS, Hanks T, Jaberaboansari A, Chen DJ (1995) Molecular analysis of gamma-ray-induced mutations at the HPRT locus in primary human skin fibroblasts by multiplex polymerase chain reaction. *Radiat Res* 141: 11-18
209. Pastwa E, Blasiak J (2003) Non-homologous DNA end-joining. *Acta Biochim Pol* 50: 891-908
210. Patel PI, Framson PE, Caskey CT, Chinault AC (1986) Fine structure of the human hypoxanthine phosphoribosyltransferase gene. *Mol Cell Biol* 6: 393-403

- 211. Peng Y, Zhang Q, Nagasawa H, Okayasu R, Liber HL, Bedford JS (2002) Silencing expression of the catalytic subunit of DNA-dependent protein kinase by small interfering RNA sensitizes human cells for radiation-induced chromosome damage, cell killing and mutation. *Cancer Res* 62: 6400-6404
- 212. Pfeiffer P, Goedecke W, Kuhfittig-Kulle S, Obe G (2004) Pathways of DNA double-strand break repair and their impact on the prevention and formation of chromosomal aberrations. *Cytogenet Genome Res* 104: 7-13
- 213. Phillips EN, Gebow D, Liber HL (1997) Spectra of X-ray-induced and spontaneous intragenic HPRT mutations in closely related human cells differentially expressing the p53 tumor suppressor gene. *Radiat Res* 147: 138-147
- 214. Phillips EN, Xia F, Kelsey KT, Liber HL (1995) Spectra of spontaneous and X-ray-induced mutations at the HPRT locus in related human lymphoblast cell lines that express wild-type or mutant p53. *Radiat Res* 143: 255-262
- 215. Pirzio LM, Freulet-Marriere MA, Bai Y, Fouladi B, Murnane JP, Sabatier L, Desmaze C (2004) Human fibroblasts expressing hTERT show remarkable karyotype stability even after exposure to ionizing radiation. *Cytogenet Genome Res* 104: 87-94
- 216. Platzer M, Rotman G, Bauer D, Uziel T, Savitsky K, Bar-Shira A, Gilad S, Shiloh Y, Rosenthal A (1997) Ataxia-telangiectasia locus: sequence analysis of 184 kb of human genomic DNA containing the entire ATM gene. *Genome Res* 7: 592-605
- 217. Pluth JM, Fried LM, Kirchgessner CU (2001) Severe combined immunodeficient cells expressing mutant hRAD54 exhibit a marked DNA double-strand break repair and error-prone chromosome repair defect. *Cancer Res* 61: 2649-2655
- 218. Podlutzky A, Osterholm AM, Hou SM, Hofmaier A, Lambert B (1998) Spectrum of point mutations in the coding region of the hypoxanthine-guanine phosphoribosyltransferase (HPRT) gene in human T-lymphocytes *in vivo*. *Carcinogenesis* 19: 557-566
- 219. Preisler HD, Kotelnikov VM, LaFollette S, Taylor St, Mundle S, Wood N, Coon JSt, Hutchinson J, Panje W, Caldarelli DD, Griem K (1996) Continued malignant cell proliferation in head and neck tumors during cytotoxic therapy. *Clin Cancer Res* 2: 1453-1460
- 220. Preston RJ (1990) Mechanisms of induction of specific chromosomal alterations. *Basic Life Sci* 53: 329-336
- 221. Price BD, Youmell MB (1996) The phosphatidylinositol 3-kinase inhibitor wortmannin sensitizes murine fibroblasts and human tumor cells to radiation and blocks induction of p53 following DNA Damage. *Cancer Res* 56: 246-250
- 222. Rainville IR, Albertini R, O'Neill JP, Nicklas J (1995) Breakpoints and junctional regions of intragenic deletions in the HPRT gene in human T-cells. *Somatic Cell Mol Genet* 21: 309-326
- 223. Rapp A, Greulich KO (2004) After double-strand break induction by UV-A, homologous recombination and non-homologous end-joining cooperate at the same DSB if both systems are available. *J Cell Sci* 117: 4935-4945

- 224. Recio L, Cochrane J, Simpson D, Skopek TR, O'Neill JP, Nicklas JA, Albertini RJ (1990) DNA sequence analysis of *in vivo* HPRT mutation in human T lymphocytes. *Mutagenesis* 5: 505-510
- 225. Riballo E, Kuhne M, Rief N, Doherty A, Smith GC, Recio MJ, Reis C, Dahm K, Fricke A, Krempler A, Parker AR, Jackson SP, Gennery A, Jeggo PA, Lobrich M (2004) A pathway of double-strand break rejoining dependent upon ATM, Artemis, and proteins locating to gamma-H2AX foci. *Mol Cell* 16: 715-724
- 226. Richardson C, Jasin M (2000) Coupled homologous and non-homologous repair of a double-strand break preserves genomic integrity in mammalian cells. *Mol Cell Biol* 20: 9068-9075
- 227. Robertson JM, Walsh-Weller J (1998) An introduction to PCR primer design and optimisation of amplification reactions. *Methods Mol Biol* 98: 121-154
- 228. Rogakou EP, Pilch DR, Orr AH, Ivanova VS, Bonner WM (1998) DNA double-stranded breaks induce histone H2AX phosphorylation on serine 139. *J Biol Chem* 273: 5858-5868
- 229. Romney CA, Paulauskis JD, Nagasawa H, Little JB (2001) Multiple manifestations of X-ray-induced genomic instability in Chinese hamster ovary (CHO) cells. *Mol Carcinog* 32: 118-127
- 230. Rooney S, Alt FW, Sekiguchi J, Manis JP (2005) Artemis-independent functions of DNA-dependent protein kinase in Ig heavy chain class switch recombination and development. *Proc Natl Acad Sci USA* 102: 2471-2475
- 231. Roques CN, Boyer JC, Farber RA (2001) Microsatellite Mutation Rates Are Equivalent in Normal and Telomerase-immortalised Human Fibroblasts. *Cancer Res* 61: 8405-8407
- 232. Rosenzweig KE, Youmell MB, Palayoor ST, Price BD (1997) Radiosensitization of human tumor cells by the phosphatidylinositol 3-kinase inhibitors wortmannin and LY294002 correlates with inhibition of DNA-dependent protein kinase and prolonged G2-M delay. *Clin Cancer Res* 3: 1149-1156
- 233. Rothkamm K, Kuhne M, Jeggo PA, Lobrich M (2001) Radiation-induced genomic rearrangements formed by non-homologous end-joining of DNA double-strand breaks. *Cancer Res* 61: 3886-3893
- 234. Rothkamm K, Lobrich M (1999) Misrejoining of DNA double-strand breaks in primary and transformed human and rodent cells: a comparison between the HPRT region and other genomic locations. *Mutat Res* 433: 193-205
- 235. Rothkamm K, Lobrich M (2003) Evidence for a lack of DNA double-strand break repair in human cells exposed to very low x-ray doses. *Proc Natl Acad Sci USA* 100: 5057-5062
- 236. Rydberg B, Lobrich M, Cooper PK (1994) DNA double-strand breaks induced by high-energy neon and iron ions in human fibroblasts. I. Pulsed-field gel electrophoresis method. *Radiat Res* 139: 133-141
- 237. Sachs RK, Levy D, Hahnfeldt P, Hlatky L (2004) Quantitative analysis of radiation-induced chromosome aberrations. *Cytogenet Genome Res* 104: 142-148

- 238. Saffi J, Feldmann H, Winnacker EL, Henriques JA (2001) Interaction of the yeast Pso5/Rad16 and Sgs1 proteins: influences on DNA repair and aging. *Mutat Res* 486: 195-206
- 239. Sankaranarayanan K (1991) Ionizing radiation and genetic risks. III. Nature of spontaneous and radiation-induced mutations in mammalian *in vitro* systems and mechanisms of induction of mutations by radiation. *Mutat Res* 258: 75-97
- 240. Sasaki MS, Ejima Y, Tachibana A, Yamada T, Ishizaki K, Shimizu T, Nomura T (2002) DNA damage response pathway in radioadaptive response. *Mutat Res* 504: 101-118
- 241. Schecker JA, Reynolds RJ (1995) Radiation, Cell Cycle, and Cancer. *Los Alamos Science* 23: 51-89
- 242. Schmidt P (1999) Mutationsauslösung durch verschiedene Strahlenarten in Nager- und Humanzellen: Induktion und molekulare Analyse. Diss. Gießen
- 243. Schmidt P, Kiefer J (1998) Deletion-pattern analysis of alpha-particle and X-ray induced mutations at the HPRT locus of V79 Chinese hamster cells. *Mutat Res* 421: 149-161
- 244. Schwartz JL, Rotmensch J, Sun J, An J, Xu Z, Yu Y, Hsie AW (1994) Multiplex polymerase chain reaction-based deletion analysis of spontaneous, gamma ray- and alpha-induced HPRT mutants of CHO-K1 cells. *Mutagenesis* 9: 537-540
- 245. Scully R, Xie A (2005) In my end is my beginning: control of end resection and DSBR pathway 'choice' by cyclin-dependent kinases. *Oncogene* 24: 2871-2876
- 246. Seegmiller JE, Rosenbloom FM, Kelley WN (1967) Enzyme defect associated with a sex-linked human neurological disorder and excessive purine synthesis. *Science* 155: 1682-1684
- 247. Shao C, Deng L, Henegariu O, Liang L, Stambrook PJ, Tischfield JA (2000) Chromosome instability contributes to loss of heterozygosity in mice lacking p53. *Proc Natl Acad Sci USA* 97: 7405-7410
- 248. Shiloh Y (2003) ATM and related protein kinases: safeguarding genome integrity. *Nat Rev Cancer* 3: 155-168
- 249. Shuber AP, Skoletsky J, Stern R, Handelin BL (1993) Efficient 12-mutation testing in the CFTR gene: a general model for complex mutation analysis. *Hum Mol Genet* 2: 153-158
- 250. Silva MJ, Costa P, Dias A, Valente M, Louro H, Boavida MG (2005) Comparative analysis of the mutagenic activity of oxaliplatin and cisplatin in the HPRT gene of CHO cells. *Environ Mol Mutagen* 46: 104-115
- 251. Simpson P, Morris T, Savage J, Thacker J (1993) High-resolution cytogenetic analysis of X-ray induced mutations of the HPRT gene of primary human fibroblasts. *Cytogenet Cell Genet* 64: 39-45
- 252. Singleton BK, Griffin CS, Thacker J (2002) Clustered DNA damage leads to complex genetic changes in irradiated human cells. *Cancer Res* 62: 6263-6269
- 253. Slupphaug G, Kavli B, Krokan HE (2003) The interacting pathways for prevention and repair of oxidative DNA damage. *Mutat Res* 531: 231-251

254. Snouwaert JN, Gowen LC, Latour AM, Mohn AR, Xiao A, DiBiase L, Koller BH (1999) BRCA1 deficient embryonic stem cells display a decreased homologous recombination frequency and an increased frequency of non-homologous recombination that is corrected by expression of a BRCA1 transgene. *Oncogene* 18: 7900-7907
255. Steel GG (1996) From targets to genes : a brief history of radiosensitivity. *Phys Med Biol* 41: 205-222
256. Stewart GS, Maser RS, Stankovic T, Bressan DA, Kaplan MI, Jaspers NG, Raams A, Byrd PJ, Petrini JH, Taylor AM (1999) The DNA double-strand break repair gene hMRE11 is mutated in individuals with an ataxia-telangiectasia-like disorder. *Cell* 99: 577-587
257. Stiff T, O'Driscoll M, Rief N, Iwabuchi K, Lobrich M, Jeggo PA (2004) ATM and DNA-PK function redundantly to phosphorylate H2AX after exposure to ionizing radiation. *Cancer Res* 64: 2390-2396
258. Stiff T, Reis C, Alderton GK, Woodbine L, O'Driscoll M, Jeggo PA (2005) NBS1 is required for ATR-dependent phosphorylation events. *Embo J* 24: 199-208
259. Stout JT, Caskey CT (1985) HPRT: Gene structure, expression and mutation. *Ann Rev Genet* 19: 127-148
260. Sun H, Chasin LA (2000) Multiple splicing defects in an intronic false exon. *Mol Cell Biol* 20: 6414-6425
261. Takata M, Sasaki MS, Sonoda E, Morrison C, Hashimoto M, Utsumi H, Yamaguchi-Iwai Y, Shinohara A, Takeda S (1998) Homologous recombination and non-homologous end-joining pathways of DNA double-strand break repair have overlapping roles in the maintenance of chromosomal integrity in vertebrate cells. *Embo J* 17: 5497-5508
262. Tatsumi K, Tachibana A, Fujimori A (1992) Molecular bases for hereditary cancer-prone diseases. *J Dermatol* 19: 684-689
263. Teo SH, Jackson SP (2000) LifIp targets the DNA ligase Lig4p to sites of DNA double-strand breaks. *Curr Biol* 10: 165-168
264. Thacker J (2005) The RAD51 gene family, genetic instability and cancer. *Cancer Lett* 219: 125-135
265. Thacker J, Fleck EW, Morris T, Rossiter BJ, Morgan TL (1990) Localization of deletion breakpoints in radiation-induced mutants of the HPRT gene in hamster cells. *Mutat Res* 232: 163-170
266. Thacker J, Zdzienicka MZ (2004) The XRCC genes: expanding roles in DNA double-strand break repair. *DNA Repair (Amst)* 3: 1081-1090
267. Thilly WG, Liu VF, Brown BJ, Cariello NF, Kat AG, Keohavong P (1989) Direct measurement of mutational spectra in humans. *Genome* 31: 590-593
268. Trosko JE (1996) Role of low-level ionizing radiation in multi-step carcinogenic process. *Health Phys* 70: 812-822

269. Tutt A, Bertwistle D, Valentine J, Gabriel A, Swift S, Ross G, Griffin C, Thacker J, Ashworth A (2001) Mutation in BRCA2 stimulates error-prone homology-directed repair of DNA double-strand breaks occurring between repeated sequences. *Embo J* 20: 4704-4716
270. Van Dyck E, Stasiak A, Stasiak AZ, West SC (1999) Binding of double-strand breaks in DNA by human RAD52 protein. *Nature* 398: 728-731
271. Van Raamsdonk CD, Fitch KR, Fuchs H, de Angelis MH, Barsh GS (2004) Effects of G-protein mutations on skin color. *Nat Genet* 36: 961-968
272. Van Steeg H, Mullenders LH, Vijg J (2000) Mutagenesis and carcinogenesis in nucleotide excision repair-deficient XPA knock out mice. *Mutat Res* 450: 167-180
273. Van Zeeland AA, Simons JW (1975) Ploidy level and mutation to hypoxanthine-guanine-phosphoribosyl-transferase (HGPRT) deficiency in Chinese hamster cells. *Mutat Res* 28: 239-250
274. Varon R, Vissinga C, Platzer M, Cerosaletti KM, Chrzanowska KH, Saar K, Beckmann G, Seemanova E, Cooper PR, Nowak NJ, Stumm M, Weemaes CM, Gatti RA, Wilson RK, Digweed M, Rosenthal A, Sperling K, Concannon P, Reis A (1998) Nibrin, a novel DNA double-strand break repair protein, is mutated in Nijmegen breakage syndrome. *Cell* 93: 467-476
275. Vilenchik MM, Knudson AG (2003) Endogenous DNA double-strand breaks: production, fidelity of repair, and induction of cancer. *Proc Natl Acad Sci USA* 100: 12871-12876
276. Vilenchik MM, Knudson AG Jr. (2000) Inverse radiation dose-rate effects on somatic and germ-line mutations and DNA damage rates. *Proc Natl Acad Sci USA* 97: 5381-5386
277. Virsik-Kopp P, Rave-Frank M, Hofman-Huther H, Schmidberger H (2004) Role of DNA-dependent protein kinase in the process of radiation-induced aberration formation. *Int J Radiat Biol* 80: 125-133
278. Vrieling H, Van Rooijen ML, Groen NA, Zdzienicka MZ, Simons JW, Lohman PH, van Zeeland AA (1989) DNA strand specificity for UV-induced mutations in mammalian cells. *Mol Cell Biol* 9: 1277-1283
279. Wang J, Pluth JM, Cooper PK, Cowan MJ, Chen DJ, Yannone SM (2005) Artemis deficiency confers a DNA double-strand break repair defect and Artemis phosphorylation status is altered by DNA damage and cell cycle progression. *DNA Repair (Amst)* 4: 556-570
280. Wang L, Cui Y, Lord BI, Roberts SA, Potten CS, Hendry JH, Scott D (1996) Gamma-ray-induced cell killing and chromosome abnormalities in the bone marrow of p53-deficient mice. *Radiat Res* 146: 259-266
281. Watkins PC, Tanzi RE, Gibbons KT, Tricoli JV, Landes G, Eddy R, Shows TB, Gusella JF (1985) Isolation of polymorphic DNA segments from human chromosome 21. *Nucleic Acids Res* 13: 6075-6088
282. Wiese C, Gauny SS, Liu WC, Cherbonnel-Lasserre CL, Kronenberg A (2001) Different mechanisms of radiation-induced loss of heterozygosity in two human lymphoid cell lines from a single donor. *Cancer Res* 61: 1129-1137

283. Williams M, Rainville IR, Nicklas JA (2002) Use of inverse PCR to amplify and sequence breakpoints of HPRT deletion and translocation mutations. *Environ Mol Mutagen* 39: 22-32
284. Wilson TE, Grawunder U, Lieber MR (1997) Yeast DNA ligase IV mediates non-homologous DNA end joining. *Nature* 388: 495-498
285. Winton DJ, Gooderham NJ, Boobis AR, Davies DS, Ponder BA (1990) Mutagenesis of mouse intestine *in vivo* using the Dlb-I specific locus test: Studies with 1,2-dimethylhydrazine, dimethyl-nitrosamine, and the dietary mutagen 2-amino-2,8-dimethylimidazo (4,5-f) quinoxaline. *Cancer Res* 50: 7992-7996
286. Wood LD, Halvorsen TL, Dhar S, Baur JA, Pandita RK, Wright WE, Hande MP, Calaf G, Hei TK, Levine F, Shay J, Wang JJ, Pandita TK (2001) Characterisation of ataxia telangiectasia fibroblasts with extended life-span through telomerase expression. *Oncogene* 20: 278-288
287. Wymann MP, Bulgarelli-Leva G, Zvelebil MJ, Pirola L, Vanhaesebroeck B, Waterfield MD, Panayotou G (1996) Wortmannin inactivates phosphoinositide 3-kinase by covalent modification of Lys-802, a residue involved in the phosphate transfer reaction. *Mol Cell Biol* 16: 1722-1733
288. Yamada Y, Park MS, Okinaka RT, Chen DJ (1996) Molecular analysis and comparison of radiation-induced large deletions of the HPRT locus in primary human skin fibroblasts. *Radiat Res* 145: 481-490
289. Yamaguchi-Iwai Y, Sonoda E, Sasaki MS, Morrison C, Haraguchi T, Hiraoka Y, Yamashita YM, Yagi T, Takata M, Price C, Kakazu N, Takeda S (1999) MRE11 is essential for the maintenance of chromosomal DNA in vertebrate cells. *Embo J* 18: 6619-6629
290. Yamamoto K, Hirano S, Ishiai M, Morishima K, Kitao H, Namikoshi K, Kimura M, Matsushita N, Arakawa H, Buerstedde JM, Komatsu K, Thompson LH, Takata M (2005) Fanconi anemia protein FANCD2 promotes immunoglobulin gene conversion and DNA repair through a mechanism related to homologous recombination. *Mol Cell Biol* 25: 34-43
291. Yaneva M, Kowalewski T, Lieber MR (1997) Interaction of DNA-dependent protein kinase with DNA and with Ku: biochemical and atomic-force microscopy studies. *Embo J* 16: 5098-5112
292. Yang TP, Stout JT, Konecki DS, Patel PI, Alford RL, Caskey CT (1988) Spontaneous reversion of novel Lesch-Nyhan mutation by HPRT gene rearrangement. *Somat Cell Mol Genet* 14: 293-303
293. Yannone SM, Roy S, Chan DW, Murphy MB, Huang S, Campisi J, Chen DJ (2001) Werner syndrome protein is regulated and phosphorylated by DNA-dependent protein kinase. *J Biol Chem* 276: 38242-38248
294. Yen PH, Li XM, Tsai SP, Johnson C, Mohandas T, Shapiro LJ (1990) Frequent deletions of the human X chromosome distal short arm result from recombination between low copy repetitive elements. *Cell* 61: 603-610
295. Yoshioka M, O'Neill JP, Vacek PM, Finette BA (2001) Gestational age and gender-specific in utero V(D)J recombinase-mediated deletions. *Cancer Res* 61: 3432-3438

- 296. Young DA, Prout GR Jr, Lin CW (1985) Production and characterisation of mouse monoclonal antibodies to human bladder tumor-associated antigens. *Cancer Res* 45: 4439-4446
- 297. Young LC, Peters AC, Maeda T, Edelmann W, Kucherlapati R, Andrew SE, Tron VA (2003) DNA mismatch repair protein Msh6 is required for optimal levels of ultraviolet-B-induced apoptosis in primary mouse fibroblasts. *J Invest Dermatol* 121: 876-880
- 298. Zhang Y, Lim CU, Williams ES, Zhou J, Zhang Q, Fox MH, Bailey SM, Liber HL (2005) NBS1 knockdown by small interfering RNA increases ionizing radiation mutagenesis and telomere association in human cells. *Cancer Res* 65: 5544-5553
- 299. Zhu LX, Waldren CA, Vannias D, Hei TK (1996) Cellular and molecular analysis of mutagenesis induced by charged particles of defined linear energy transfer. *Radiat Res* 145: 251-259
- 300. Zou L, Elledge SJ (2003) Sensing DNA damage through ATRIP recognition of RPA-ssDNA complexes. *Science* 300: 1542-1548
- 301. Zou L, Liu D, Elledge SJ (2003) Replication protein A-mediated recruitment and activation of Rad17 complexes. *Proc Natl Acad Sci USA* 100: 13827-13832

7 Acknowledgements

First of all, I would like to emphasize how grateful I am to my project supervisor and promotor Prof. Markus Löbrich for his scientific guidance and for all his advice, and to thank him for allowing me to perform time-consuming mutation induction experiments and current analysis in his laboratory. Secondly, Prof. Mathias Montenarh has also earned my thanks for his contribution as the second reviewer of my thesis.

Special thanks to Dr. Kai Rothkamm for his assistance in the lab and productive discussions, and I also wish to thank Dr. Andrea Krempler for her help in finalising my work.

It is important that I thank Dr. Martin Kühne for his assistance in planning the last part of my experiments.

For his assistance, in FISH analysis, I owe a great deal of thanks to Dr. Salam A. Warda, and no less do I owe to Dr. Ines Krüger for sharing methodological protocols and guidance for the surviving experiments.

My thanks to Andreas Fricke for his assistance in relevant computational software, but I also wish to express my gratitude to all other colleagues in our team for their persevering cooperation in the laboratory.

My gratitude is also extended to the secretary of the department, Ms. Anne Lore Malter, but not forgetting Mr. Elmar Arend for coming to my aid with technical know-how, and Ms. Roswitha Schepp for all the related lab work.

Very special thanks to Prof. Samuel Samnick and my indispensable friends, Birgit Vordestemann, Dr. Uenal Coskun, Rolf Lehmann and Sirikumara Ukwatte for their inimitable support during all the work I undertook who gave me all the courage and strength that was necessary after the tragic loss of relatives and friends in one of the world's worst natural catastrophes - namely, the Tsunami of December, 2004.

And last but not least, to my wife, Neelanthie for her love, patience and support - and my sister, Ranjanie Gunasekara, as well as my parents for giving me the courage to carry on working up to the very end.

8 **Appendix**

Table 8.1 Summarised data of HPRT mutant clones in hTERT-immortalised primary fibroblasts of three independent mutation induction experiments following acute dose irradiation..... 136

Table 8.2 Summarised data of HPRT mutant clones of hTERT-immortalised isolated from two independent mutation induction experiments based on fractionated irradiation 137

Publications 139

CV 140

Table 8.1. Summarised data of HPRT mutant clones in hTERT-immortalised primary fibroblasts of three independent mutation induction experiments (Exp I, II and III). Mutation induction was conducted here using acute dose irradiations.

Dose	Mutant ¹ Naming	Restriction ² Analysis	RT-PCR (Presence + /Absence -)	M-PCR (failed exons)	FISH (+t/-t)
0-Gy (5)	K/28a K/40f K/16aI* K/18b* K/20c*	normal normal normal normal large	+ + + + -	none none none none exons 1-3	- - - - -
(13)	K/fII** K/2fI** K/2hI** K/1hI** K/1cI** K/1aI** K/2eII** K/2aI** K/1dII** K/2jII** K/1II** K/1bI** K/2g**	large normal normal normal normal normal normal large normal normal normal normal normal	analysed only with hybridisation assay		
2-Gy ³ (6)	2/10d 2/11d 2/11e 2/14eI 2/15b 2/16cII	large normal no signal normal normal normal	- + - + + +	exons 7-8 none exons 1-9 none none none	+ - - - - -
(5)	2/2c* 2/4d* 2/5cI* 2/7cI* 2/11d*	no signal small normal no signal small	- - - - -	exons1-9 exons1-5 exons1-9 exons1-9 exons1-2	- - - - +
6-Gy ³ (14)	6/3b 6/4d 6/6dI 6/6dII 6/5dI 6/6b 6/7aI 6/9d 6/10e 6/12c 6/12d 6/20cI 6/20cII 6/20e	no signal large small normal small no signal small no signal normal large large small normal large	- - - + - - - - + - - - + -	exons 7-9 none none none none exons 1-9 exon 3 exons 1-9 none none none none none	- - + - - - + - - - + - - -
(4)	6/2fI** 6/1g** 6/2e** 6/1cII**	no signal small no signal small	analysed only with hybridisation assay		

¹ Mutant clones were named after an arbitrary nomenclature starting from irradiated (2 and 6-Gy) doses and unirradiated controls (K), the number of the flask in which cell monolayers initially contained /irradiated (i.e. 1, 2, 3 etc.), the naming of the mutants from which plate they were isolated such as from a, b, c etc (Cells in flasks were seeded into several petri dishes for 6 -TG selections) and if mutant clones are those isolated from the same

Contd.

dish, their designation is suffixed by roman numerals (i.e. I, II, III etc.). Those underlined are the mutant colonies isolated from the same plate and to be distinguished by the designation of each mutant.

² Genomic DNA of mutant clones were digested with *NotI* restriction endonuclease and subjected to PFGE /Southern hybridisation analysis. Depending on the radioactive signals, mutant clones were grouped into normal, large, small. and no signal. type clones.

³ Number of induced mutants given here are corrected for background mutants, subtracting the existing background mutant fraction from initially collected /analysed mutant clones.

Mutant clones that are in bold have shown inter-chromosomal translocations between X- chromosome and the autosomes. Clones that were not designated by asterisk are derived from Experiment I.

* HPRT mutant clones collected from Experiment II
 ** HPRT mutant clones collected from Experiment III analysed only with Southern hybridisation
 normal = 2 Mbp
 large > 2 Mbp
 small < 2 Mbp
 none all the exons presence
 +t / -t presence and absences of translocations

Table 8.2. Summarised data of HPRT mutant clones of hTERT-immortalised human fibroblasts by hybridisation assay (Restriction fragment analysis), cDNA analysis and multiplex PCR. Mutant clones were isolated from two independent mutation induction experiments based on fractionated irradiation.

Dose (X-ray)	Mutant Naming ¹	Restriction ² Analysis	RT-PCR product (Presence + / Absence -)	M-PCR Failed Exons
0-Gy (8)	K/6aII	normal	+	none
	K/3aII	normal	+	none
	K/5b	normal	+	none
	K/1aII	normal	+	none
	K/6d	normal	+	none
	K/1b	normal	+	none
	K/1j	normal	+	none
	K/3f	normal	+	none
<hr/>				
(21)	K/2j*	normal] analysed only with hybridisation assay	
	K/2g*	normal		
	K/1e*	normal		
	K/3e*	normal		
	K/1i*	normal		
	K/2h*	normal		
	K/1f*	normal		
	K/3i*	normal		
	K/3g*	normal		
	K/2e*	normal		
	K/2a*	normal		
	K/1c*	normal		
	K/1a*	normal		
	K/1b*	normal		
	K/1d*	normal		
	K/2b*	normal		
	K/2f*	normal		
	K/2i*	normal		
	K/3b*	normal		
	K/3d*	normal		
K/3f*	normal			
<hr/>				
0.6-Gy (6)	0.6/1h	large	-	none
	0.6/4fI	normal	+	1-3 exons
	0.6/4fII	normal	-	1-3 exons
	0.6/3g	normal	-	none
	0.6/4g	small	+	none
	0.6/6d	large	+	none

Contd.

(4)	0.6/1c*	small	}	analysed only with hybridisation assay
	0.6/1e*	small		
	0.6/1i1*	small		
	0.6/2dV*	small		
<hr/>				
2-Gy (13)	2/3eI	small	+	exon 1
	2/3eII	small	+	none
	2/3dI	small	-	none
	2/3bI	small	-	none
	2/3hI	no signal	-	1-9 exons
	2/3hII	small	-	exon 1
	2/3fI	normal	-	none
	2/3fII	small	-	none
	2/3gII	small	-	none
	2/3aI	small	-	none
	2/1I	small	-	none
	2/3c	small	-	none
	2/2c	normal	+	exon 1
<hr/>				
6-Gy (17)	6/3aII	no signal	-	1-9 exons
	6/2fII	small	-	1-9 exons
	6/2cI	no signal	-	1-9 exons
	6/3e	small	-	none
	6/1f	normal	-	none
	6/2hI	normal	+	exon 1
	6/2hII	no signal	-	1-9 exons
	6/3bI	no signal	-	1-9 exons
	6/1cI	small	-	none
	6/3I	no signal	-	1-9 exons
	6/2aI	no signal	-	1-9 exons
	6/1aI	small	-	none
	6/1j	no signal	-	1-9 exons
	6/3c	small	-	none
	6/3d	large	-	none
	6/3f	large	-	none
	6/1d	normal	-	none
<hr/>				
(9)	6/aI*	small	}	analysed only with hybridisation assay
	6/bI*	no signal		
	6/cII*	no signal		
	6/dII*	no signal		
	6/eI*	small		
	6/fII*	no signal		
	6/gI*	small		
	6/hI*	no signal		
	6/II*	no signal		

¹ Mutants were named after an arbitrary nomenclature starting from irradiated (0.6, 2 and 6-Gy) doses and unirradiated controls (K), number of the flask in which cell monolayers initially contained /irradiated (i.e. 1, 2, 3 etc.), the naming of the mutants from which plate they were isolated such as from a, b, c etc (Cell contents in flasks were seeded into several petri dishes for 6-TG selections) and if the mutant clones are those isolated from the same dish, their designation is suffixed by roman numerals (i.e. I, II, III, IV and V).

² Genomic DNA of mutant clones were digested with a rarely cutting restriction endonuclease *NotI* and subjected to PFGE /Southern hybridisation analysis. Depending on the migration lengths of radioactive signals, the specific mutants were grouped into normal, large, small and no signal. type clones.

normal = 2 Mbp; large > 2 Mbp; small < 2 Mbp; none = all the exons presence

Mutant clones isolated from Experiment I are designated by asterisk (*), whereas clones that are not designated by asterisk are derived from Experiment II

Following paper publications are in progress:

- Radiation-induced mutations resulting from misrejoined DNA double-strand breaks
- Molecular characterisation of HPRT mutant clones following fractionated irradiations

Curriculum vitae

Personal details:

Name: Karumpullige Udaya Thilaka Gunasekara

Date of Birth: 21.11.1965

Place of Birth: Imaduwa, Sri Lanka

Education:

2000 - present Doctoral training /Research associate at the Department of
Biophysics, University of the Saarland

1994 - 2000 Diploma undergraduate studies in Food chemistry
/Environmental toxicology, University of Kaiserslautern

1990 - 1994 Medical research associate (Ayurvedic products), Sri Lanka

1986 - 1989 Agriculture Science (B.Sc special) undergraduate course,
University of Peradeniya, Sri Lanka

